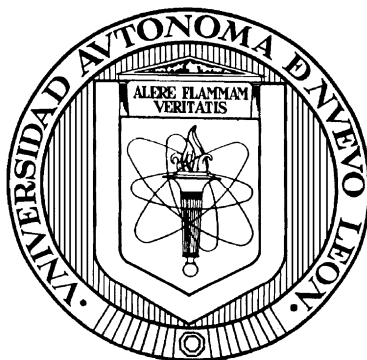


**UNIVERSIDAD AUTÓNOMA DE NUEVO LEÓN**

**FACULTAD DE CIENCIAS QUÍMICAS**



**SYNTHESIS, CHARACTERIZATION, DETERMINATION  
OF LUMINESCENT PROPERTIES OF TETRACOORDINATE  
ORGANOBORON COMPOUNDS DERIVATIVES FROM ORGANIC  
TRIDENTATE LIGANDS, AND THEIR POTENTIAL  
APPLICATION IN OLEDs.**

**By**

**RODRIGO ALONSO CHAN NAVARRO**

**In partial fulfillment of the requirements for the Degree of  
Doctor of Science with Orientation in Materials Chemistry**

**AUGUST 2014**

## SUMMARY

M. en C. Rodrigo Alonso Chan Navarro

Graduation Date: August 2014

Universidad Autónoma de Nuevo León

Facultad de Ciencias Químicas

**Study Title: Synthesis, characterization, determination of luminescent properties of tetracoordinate organoboron compounds derivatives from organic tridentate ligands, and their potential application in OLEDs.**

Page numbers: 120

Candidate for the degree of  
Doctorate of Sciences with  
Orientation in Materials Chemistry.

Study area: Materials Chemistry

### **Purpose and study method:**

Coordination complexes with main group elements offer an interesting alternative for the preparation of molecular materials with luminescent properties. These materials compared with their inorganic analogues, and organic polymers offer the versatility and reproducibility of the synthetic process. It is important to notice that have been reported organic compounds boron mostly derivatives of bidentate ligands with interesting photo, and electroluminescent properties. However studies of boron compounds derived from tridentate ligands have been scarcely explored. Based on the above this work research were synthesized six new compounds derived from tridentate ligands with potential application as emitter material, and an electron transport layer in the assembly of electroluminescent devices type OLED.

### **Conclusions and contributions:**

In this work research was reported five new structures of tridentate ligands and boron compounds, which were characterized by spectroscopic and spectrometric techniques and x-ray diffraction. The same way the photophysical parameters, thermal and non linear properties of all materials were studied. In some cases it was possible to carry out theoretical studies in order to analyze in depth the luminescent response. Electroluminescent devices type OLED were fabricated with the boron compounds **9a** and **10a** obtained as a results current-voltage curves, indicating that these materials have capable a poor electroluminescent performance.

### ASSESSOR SIGNATURE

---

Ph.D. Víctor M. Jiménez Pérez

This thesis was realized at laboratory of materials III into the postgraduate area of Facultad de Ciencias Químicas from Universidad Autónoma de Nuevo León under the management of Ph.D. Víctor M. Jiménez Pérez.

This project was carried out with the financial support from **CONACYT** (grant: 156450) and **PAICYT-UANL** (grant: CN886-11) as well as **CONACYT** scholarship, and it was complemented with two short stays with the collaboration of Ph.D. Gabriel Ramos-Ortíz and Ph.D.s Ivana Moggio and Eduardo Arias.

## **DIVULGATION PROYECT AND STAYS PERFORMED**

The study realized in this thesis has been divulged in a national and international meetings and it has been generated two publications:

Rodrigo A. Chan, Blanca M. Muñoz Flores, Víctor M. Jiménez Pérez. Síntesis por multicomponentes de compuestos de boro derivados de salicilidenbenzoilhidrazonas. Una aproximación verde. Congreso Internacional de Química e Ingeniería Verde, Monterrey, Nuevo León, México, realizada los días 24-26 de Octubre de 2012.

Rodrigo Chan-Navarro, Víctor M. Jiménez-Pérez, Blanca M. Muñoz-Flores, aH. V. Rasika Dias, Ivana Moggio, Eduardo Arias, Gabriel Ramos-Ortíz, Rosa Santillan, ConcepciónGarcía, Maria Eugenia Ochoa, Muhammed Yousufuddin, and NoemiWaksman. Luminescent organoboron compounds derived from salicylidenebenzohydrazide: Synthesis, charaterization, structure, and Photophysical properties. 247<sup>th</sup> American Chemical Society National Meeting, Dallas, Texas, USA, realized on March 16-20, 2014.

Rodrigo Chan-Navarro, Víctor M. Jiménez-Pérez, Blanca M. Muñoz-Flores, aH. V. Rasika Dias, Ivana Moggio, Eduardo Arias, Gabriel Ramos-Ortíz, Rosa Santillan, ConcepciónGarcía, Maria Eugenia Ochoa, Muhammed Yousufuddin, and NoemiWaksman. Luminescent organoboron compounds derived from salicylidenebenzohydrazide: Synthesis, characterization, structure, and photophysical properties. *Dyes and Pigm.* 99 (2013) 1036-1043.

Rodrigo Chan-Navarro, Blanca M. Muñoz-Flores, Víctor M. Jiménez-Pérez. Gabriel Ramos-Ortíz, Ivana Moggio, Eduardo Arias, María. C. García-López, Víctor Rosas, and Mario Rodríguez. Multicomponent Microwave-assisted Synthesis of Boronates derived from Schiff Bases: Nonlinear Optical Properties, Thermal Analyses, Cyclic Voltammetry and Computational Study. Submitted, June 21<sup>st</sup>, 2014.

In addition, two short stays were performed:

March 1<sup>st</sup> to August 30<sup>th</sup>, 2013. Stay in the laboratory of materials of Centro de investigación en Óptica (CIO) León, Guanajuato, México under the management of Ph.D. Gabriel Ramos-Ortíz.

October 1<sup>st</sup> to November 31<sup>th</sup>, 2014. Stay in the laboratory of advanced materials of Centro de investigación en Química Aplicada (CIQA) Saltillo, Coahuila, México under the management of Ph.D. Ivana Moggio.

## ACKNOWLEDGEMENTS

I am indebted to Ph.D. Victor M. Jimenez-Perez for the opportunity to take part of his research group as well as shared knowledge but most of all for their trust and friendship but most of all for their trust and friendship with which you have distinguished me over the last three years.

I am also grateful to Ph.D. Blanca M. Muñoz-Flores for their trust and friendship awarded, as well as Ph.D.s Rasika Díaz, Gabriel Ramos-Ortiz, Rosa Santillan, Ivanna Moggio and Eduardo Arias for their supported and collaboration in this project.

I also thank at thesis committee, Ph.D.s Boris Ildusovich Kharisov, Sylvain Bernes Flouriot, and Perla Elizondo de Cota, for their corrections, suggestions and interest, in the review of these research work.

Finally, I greatly appreciate the support of my classmates from the laboratory of materials III, especially María C. Garcia-López, my present and future, by their patience and unconditional support for achieving this common goal.

## CONTENTS

	<b>Page</b>
Title page .....	0
Thesis approval sheet .....	0
Summary .....	0
Development project .....	i
Divulcation project and stays performed .....	ii
Acknowledgments .....	iv
List of figures .....	v
List of schemes .....	vi
List of tables.....	vii
List of abbreviations.....	viii
List of organic compounds synthesized .....	x
<b>1. Introduction.....</b>	<b>1</b>
<b>2. Background.....</b>	<b>4</b>
<b>2.1 General aspect of boron.....</b>	<b>4</b>
<b>2.2 Luminescent organoboron compounds:</b> photo- and electroluminescent properties.....	<b>6</b>
<b>3. Hypothesis.....</b>	<b>18</b>
<b>3.1 General objective.....</b>	<b>18</b>
<b>3.2 Specific objectives.....</b>	<b>19</b>
<b>4. Materials and methods.....</b>	<b>21</b>
<b>4.1 Material and equipment.....</b>	<b>21</b>
<b>4.2 X-ray data collection and structure determination.....</b>	<b>22</b>

4.3 Absorbance, emission and luminescence quantum yields.....	23
4.4 Fabrication of electroluminescent devices.....	23
4.5 Third-harmonic generation experiment.....	25
4.6 Theoretical study.....	26
4.7 Synthesis procedure of compounds <b>1a-12a</b> .....	27
4.7.1 ( <i>E</i> )-N'-(4-(diethylamino)-2-hydroxysalicylidine) benzohydrazide ( <b>1a</b> ).....	27
4.7.2 ( <i>E</i> )-N'-(4-(methoxy)-2-hydroxysalicylidine) benzohydrazide ( <b>2a</b> ).....	28
4.7.3 ( <i>E</i> )-N'-(4-(diethylamino)-2-hydroxysalicylidine)- 4-nitrobenzohydrazide ( <b>3a</b> ).....	29
4.7.4 ( <i>E</i> )-N'-(4-(methoxy)-2-hydroxysalicylidine)- 4-nitrobenzohydrazide ( <b>4a</b> ).....	29
4.7.5 ( <i>E</i> )-(2-hydroxy-1-naphthalidene) benzohydrazide ( <b>5a</b> ).....	30
4.7.6 ( <i>E</i> )-(2-hydroxy-1-naphthalidene)- 4-nitrobenzohydrazide ( <b>6a</b> ).....	31
4.7.7 ( <i>E</i> )-N'-(4-(diethylamino)-2-hydroxysalicylidine) benzohydrazidato-phenyl-boron ( <b>7a</b> ).....	
4.7.8 ( <i>E</i> )-N'-(4-(methoxy)-2-hydroxysalicylidine) benzohydrazidato-phenyl-boron ( <b>8a</b> ).....	32 33
4.7.9 ( <i>E</i> )-N'-(4-(diethylamino)-2-hydroxysalicylidine)- 4-nitrobenzohydrazidato-phenyl boron ( <b>9a</b> ).....	34
4.7.10 ( <i>E</i> )-N'-(4-(methoxy)-2-hydroxysalicylidine)- 4-nitrobenzohydrazidato-phenyl boron ( <b>10a</b> ).....	35
4.7.11 ( <i>E</i> )-(2-hydroxy-1-naphthalidene)benzohydrazidato- phenyl-boron ( <b>11a</b> ).....	36
4.7.12 ( <i>E</i> )-(2-hydroxy-1-naphthalidene)4-nitro- benzohydrazidato-phenyl-boron ( <b>12a</b> ).....	38
4.8 Synthesis under microwave irradiation.....	39
4.8.1 Method A. Synthesis under microwave irradiation using an organic solvent, exemplified with <b>7a</b> .....	39

<b>4.8.2</b> Disposal of hazardous waste.....	<b>40</b>
<b>5.</b> Results and discussion.....	<b>41</b>
<b>5.1</b> Synthesis.....	<b>41</b>
<b>5.2</b> Chemical structure elucidation.....	<b>43</b>
<b>5.3</b> X-ray analysis.....	<b>48</b>
<b>5.4</b> Optical properties.....	<b>55</b>
<b>5.5</b> Optical nonlinear properties.....	<b>61</b>
<b>5.6</b> Thermal analysis.....	<b>64</b>
<b>5.7</b> Computational study.....	<b>66</b>
<b>5.8</b> Fabrication of electroluminescent devices type OLED derived from <b>9a-10a</b> .....	<b>68</b>
<b>6.</b> Conclusion.....	<b>70</b>
<b>6.1</b> Perspectives.....	<b>73</b>
<b>7.</b> References.....	<b>74</b>
<b>8.</b> Appendix.....	<b>83</b>
<b>9.</b> Autobiographic summary.....	<b>116</b>

## LIST OF FIGURES

Figure		Page
1	Electronic structure of boron compounds: <i>electrophilic</i> (red) and <i>nucleophilic</i> (blue) behaviour.....	5
2	Structural feature of tetracoordinate organoboron compounds.....	5
3	Schematic configuration of the device of double organic layer.....	24
4	<sup>1</sup> H NMR spectrum of free ligand <b>1a</b> in dimethyl sulfoxide-d <sub>6</sub> .....	44
5	<sup>11</sup> B NMR spectrum of boron compound <b>7a</b> in DMSO-d <sub>6</sub> .....	45
6	X-ray molecular structures of <b>1a</b> and <b>2a</b> .....	50
7	X-ray molecular structures of <b>7a</b> and <b>8a</b> .....	50
8	Molecular structure of <b>12a</b> .....	50
9	UV-Vis spectra in THF of compounds <b>1-4a</b> and <b>7-10a</b> .....	56
10	Emission spectra of compounds <b>1a</b> , <b>3a</b> , and <b>7-10a</b> in THF.....	58
11	Excitation spectra of compounds <b>1a</b> , <b>3a</b> , <b>7-10a</b> in THF.....	59
12	UV-Vis spectra in chloroform of compounds <b>1a</b> , <b>11-12a</b> .....	60
13	Fluorescence spectra of Schiff base <b>5a</b> and their boro compound <b>12a</b> .....	61
14	THG Maker-fringe patterns for thin solid films doped with 30 wt% of compounds <b>1a</b> , <b>7a</b> , <b>9-10a</b> .....	62
15	TGA thermogram of Schiff bases <b>1-6a</b> .....	65
16	TGA thermograms of boron compounds <b>7-12a</b> .....	66
17	Occupied orbitals (HOMO, yellow) and virtual orbitals (LUMO, blue) for the $\pi$ - $\pi^*$ transition in compound <b>7a</b> (top) and <b>9a-NO<sub>2</sub></b> (bottom).....	68
18	Occupied orbitals (HOMO, yellow) and virtual orbitals (LUMO, blue) for the $\pi$ - $\pi^*$ transition in compound <b>8a</b> (top) and <b>10a-NO<sub>2</sub></b> (bottom).....	68
19	Current density-Voltage curves for OLEDs using <b>9a</b> and <b>10a</b> boron compounds.....	69

## LIST OF SCHEMES

Scheme		Page
1	Photoluminescent organoboron compound <b>1-2</b> .....	6
2	Organoboron compounds <b>3-6</b> used as emitter materials in OLEDs.....	8
3	Fluorescent organoboron compounds <b>7-9</b> derived from pyrazolate ligand.....	8
4	Organoboron compounds <b>10-12</b> derived from 2-pyridyl pyrrolide ligand.....	9
5	Electroluminescent organoboron compound <b>13</b> derived from 8-hydroxyquinolato ligand.....	10
6	Organoboron compound <b>14-15</b> derived from bidentate (N,N) ligand.....	10
7	Organoboron compounds <b>16-19</b> derived from phenol-pyridyl ligands.....	11
8	Luminescent organoboron compounds <b>20-22</b> derived from quinolate ligand.....	12
9	Organoboron compound <b>23</b> derived from pyridine-phenol ligand.....	12
10	Dinuclear organoboron <b>24-27</b> derived from ladder type conjugated $\pi$ system.....	13
11	Organoboron compounds <b>28-30</b> derived from oxazolyphenolate ligand.....	14
12	Organoboron compounds <b>31-32</b> derived from phenol-pyridyl ligand.....	14
13	Four-coordinate binuclear organoboron compounds <b>33-35</b> derived from 2-(N-aryl) formiminopyrrolyl ligand.....	15
14	Organoboron compounds <b>36-39</b> derived from 2- (N-arylformimino)pyrrolyl ligand.....	16

<b>15</b>	Synthesis under microwave irradiation of compounds <b>7-10</b> .....	<b>39</b>
<b>16</b>	Synthesis of Schiff bases <b>1a-6a</b> .....	<b>41</b>
<b>17</b>	Synthesis of organic compounds derived from Schiff bases <b>7a-12a</b> .....	<b>42</b>
<b>18</b>	Proposed fragmentation of boron compounds <b>7a-10a</b> .....	<b>46</b>
<b>19</b>	Proposed fragmentation of compound <b>11a</b> according to its mass spectrum.....	<b>47</b>
<b>20</b>	Deviation ( $\theta$ ) of the boron atom from the salicylideneimino/or naphthalidenimino-plane in compounds <b>7a, 8a</b> and <b>12a</b> .....	<b>50</b>
<b>21</b>	Structural modification of the boron compounds .....	<b>59</b>

## LIST OF TABLES

<b>Table</b>		<b>Pag</b>
<b>1</b>	Comparison of the time reaction and yields from different methods of compounds <b>7a-10a</b> .....	<b>42</b>
<b>2</b>	Selected <sup>1</sup> H, <sup>11</sup> B, <sup>13</sup> C NMR (ppm) and IR (cm <sup>-1</sup> ) data for compounds <b>1a-6a</b> and <b>7-12a</b> .....	<b>44</b>
<b>3</b>	Elemental analysis of compounds of free ligands <b>1a, 2a, 6a</b> and boron compounds <b>7a-12a</b> .....	<b>48</b>
<b>4</b>	Crystal data for compounds <b>1a, 2a, 7a,</b> and <b>8a</b> .....	<b>51</b>
<b>5</b>	Crystal data for compound <b>12a</b> .....	<b>52</b>
<b>6</b>	Selected bond distances (°) and angles (deg) for <b>1a-2a</b> and <b>7a-8a</b> .....	<b>53</b>
<b>7</b>	Selected bond distances (°) and angles (deg) for <b>12a</b> .....	<b>54</b>
<b>8</b>	Photophysical data of Schiff bases <b>1a-4a</b> and boron compounds <b>7a-10a</b> .....	<b>56</b>
<b>9</b>	Optical nonlinear response and thermal properties of compounds <b>1a-12a</b> .....	<b>63</b>
<b>10</b>	Calculated values of maximum absorption wavelength using TDDFT at the level B3LYP/6-311++G**//B3LYP/6-31G* and PCM solvent model.....	<b>67</b>

## LIST OF ABBREVIATIONS

OLED	organic light emitting diode	$T_{d5}$	decomposition temperature at 5%
Alq <sub>3</sub>	tris-(8-hydroxyquinolate) aluminum	Tm	melting transition process
$\Phi$	quantum yields	MHz	megahertz
UV	ultraviolet region	PS	polystyrene
nm	nanometers	mm	millimeter
cd/m <sup>2</sup>	unit of luminance	AFM	atomic force microscopy
mA/cm <sup>2</sup>	unit of current density	$\chi^{(3)}$	third order nonlinear susceptibility
S <sub>1</sub> , LE	locally excited state	OPO	optical parametric oscillator
S <sub>1</sub> , CT	charge transfer state	THG	third harmonic generation
HOMO	highest occupied molecular orbital	PCM	polarizable continuum model
LUMO	lowest unoccupied molecular orbital	TD-DFT	time dependent density functional theory
[BF <sub>3</sub> O(Et) <sub>2</sub> ]	boron trifluoride etherate	DMF	N,N-dimethyl formamide
ETL	electron transport layer	DMSO	dimethyl sulfoxide
<sup>1</sup> H	proton NMR	IR	infrared
<sup>11</sup> B	boron NMR	eV	unit of energy
<sup>13</sup> C	carbon NMR	AIE	aggregation-induced emission
DEPT	distortionless enhancement by polarization transfer	$\Delta\nu$	difference frequency
HETCOR	2-D heterocorrelation	ITO	indium tin oxide
HMBC	heteronuclear multiple bond correlation	EML	emissive materials layer
COSY	correlation spectroscopy	ETL	electronic transport layer
Eg	optical band gap	HTL	hole transport layer
THF	Tetrahydrofuran	APCI	atmospheric pressure chemical ionization
M <sup>-1</sup> cm <sup>-1</sup>	unit of molar extinction coefficient	HR-MS	high resolution mass spectrometry
NMR	nuclear magnetic resonance	$\Phi$	fluorescent quantum yield
h	Planck constant	PEDOT:PSS	poly(3,4ethylenedioxythiophene)
ppm	parts per million	AIE	aggregation-induced emission
$\delta$	Chemical shift	$\pi$ - $\pi^*$	Electronic transition
u.m.a	unit of molar mass	$\lambda_{max}$	maximum absorption peak
Å	length measurement unit	-C=N-	azomethine group
DTA	differential thermal analysis		
TGA	thermogravimetric analysis		

## LIST OF ORGANIC COMPOUNDS SYNTHESIZED

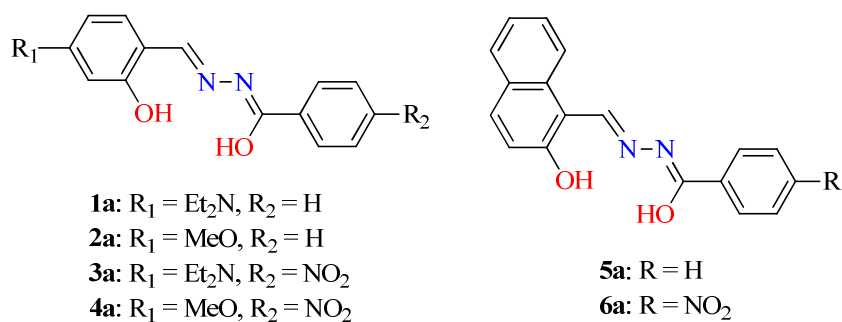


**Figure 1.** Salicylidene- **1a-4a** and naphthalidenebenzohydrazides **5a-6a**.

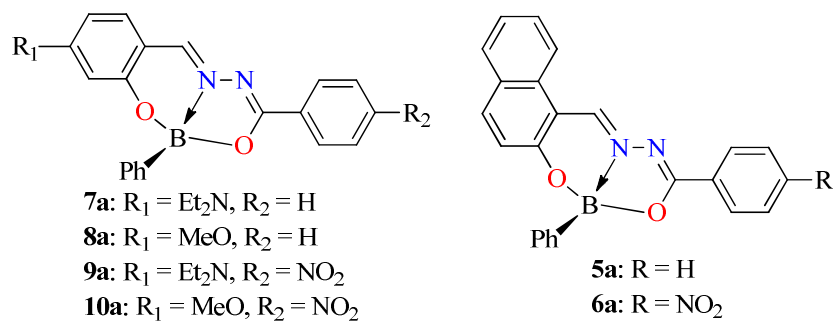


**Figure 2.** Boron compounds derivatives from salicylidenebenzohydrazides **7a-10a** and naphthalidenebenzohydrazides **11a-12a**.

# INTRODUCTION

Luminescence is a spontaneous emission of electromagnetic radiation from an electronically excited material, which is not in thermal equilibrium with the environment. Depending of the way that energy is applied, it is going to give different types of luminescent process such as fluorescence, phosphorescence, thermoluminescence, chemiluminescence, triboluminescence, radioluminescence, sonoluminescence, and electroluminescence. This concept was introduced by Eilhard Wiedemann in 1888 and it was defined as all phenomenon of light, which is not conditioned for an increase of the temperature.<sup>1</sup> In this context, organic luminescent materials have received considerable attention due to their potential use in optoelectronic applications such as emitter materials, electron-transport materials, host/hole-blocking materials for organic light emitting diodes (OLEDs), biological imaging materials, and photo-responsive materials.<sup>2</sup> Luminescent main-group coordination compounds particularly have demonstrated to be an important group of emitter materials for the assembly of OLEDs. In fact, tris-(8-hydroxyquinolate)aluminum ( $\text{Alq}_3$ ), reported by Tang and VanSlyke in 1987, was the first complex used as an emitter material in the

assembly of OLEDs.<sup>3</sup> However, it has a few shortcomings such as green emission and a poor long-term stability in electroluminescent devices.<sup>4</sup>

On the other hand, considerable effort has been invested in the design and synthesis of new boron compounds, which has improved the chemical and optical properties in comparison to aluminum derivatives such as good solubility in organic solvents, high fluorescent quantum yields ( $\Phi$ ), air-stable, low cost, and easy deposition on substrate surfaces by means of direct thermal evaporation.<sup>5</sup> In this regard, much attention has been paid to transition metal complexes due to their interesting electroluminescent properties such as highly emission and good thermal stability.<sup>6</sup> However, heavy metals such as Ir,<sup>7</sup> Pt,<sup>8</sup> and Cu<sup>9</sup> are extremely moisture- and/or oxygen-sensitive.

Organoboron compounds are also attractive functional materials due to their applications in areas such as supramolecular chemistry;<sup>10</sup> medicinal chemistry: anticancer agents in boron neutron capture therapy,<sup>11</sup> and materials chemistry as fluorescents probes<sup>12</sup> and imaging material,<sup>13</sup> laser dyes,<sup>14</sup> fluoride ion sensor,<sup>15</sup> OLEDs,<sup>16</sup> organic field-effect transistors,<sup>17</sup> photo-responsive materials<sup>18</sup> and nonlinear optics.<sup>19</sup> In particular, the interest has increased to those organoboron compounds derived from Schiff bases, due to they provide an interesting and wide variety of molecular structural conformations and in addition the electron withdrawing  $-C=N-$  group interacts with metal ions giving *push-pull* complexes with different optoelectronic properties<sup>20</sup> with potential applications.<sup>21</sup>

This research describes in detail a new study into a serie of organoboron compounds derived from Schiff bases, which has showed interesting properties that make of them potentially useful in the assembly of electroluminescent devices. This document is separated into seven chapters, which describes the design, synthesis, chemical-optical characterization, and rationalization of the photophysical properties of those new materials as well as the assembly of an electroluminescent device type OLED using an organoboron compound as emitter and electron transport material. Third order non linear optical properties of organoboron compounds derived from salicylidenbenzoylhydrazide and their free ligands were tested. In addition, the thermal properties and computational studies for someone of them are also reported.

A brief summary about of the purpose and importance into this research work is described in the first chapter. The background provides an overview of the luminescent boron compounds that have been used in the developing of electroluminescent devices type OLED. The problem approach, hypothesis and objective of this research work are exposed in the third section. All the materials, laboratory equipment, synthetic procedure, and the experimental methodology used into of this document are described in the fourth section. The fifth section offers an analysis and discussion of the most outstanding results obtained into this project. The sixth section describes the major contributions made in this research work. Finally, the last section collects the references cited in the text as well as the supplementary material.

# BACKGROUND

## 2.1 General aspect of boron

The electronic structure of boron atom and its position on the periodic table, makes those boron compounds behave as *electrophilic* molecules (Lewis Acid) with a trigonal planar molecular geometry and an isoelectronic behaviour to carbocations. Moreover, the boron atom has the ability for to form an additional bond and to generate an anionic tetravalent boron compound with a tetrahedral structure and a *nucleophilic* behavior (Lewis base).<sup>22</sup> This double behavior allow that those materials can be stable while retaining significant reactivity, which defines their unique, versatile, interconvertible, and tunable chemical properties. The organoboron compounds are considered a viable alternative for the development of luminescent materials, due to its *electrophilic* character, that allows the formation of stable dative covalent bond with distinctive reactivity, which can be exploited (**Figure 1**).

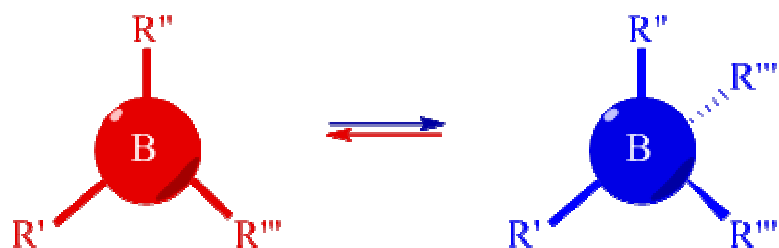


**Figure 1.** Electronic structure of boron compounds: *electrophilic* (red) and *nucleophilic* (blue) behaviour.

Thus, a great diversity of multidentate ligands have the possibility of coordination with boron compounds giving tetracoordinate organoboron compounds that allows to tune the electronic and optical properties through of the formation of the dative bond and the strategic substitution of specific functional groups into a rigid conjugated  $\pi$ - system (**Figure 2**).

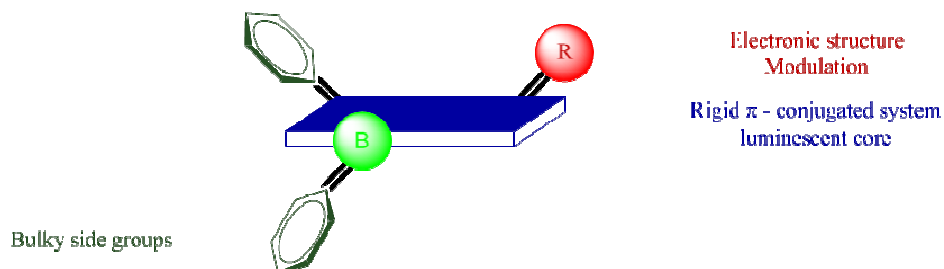
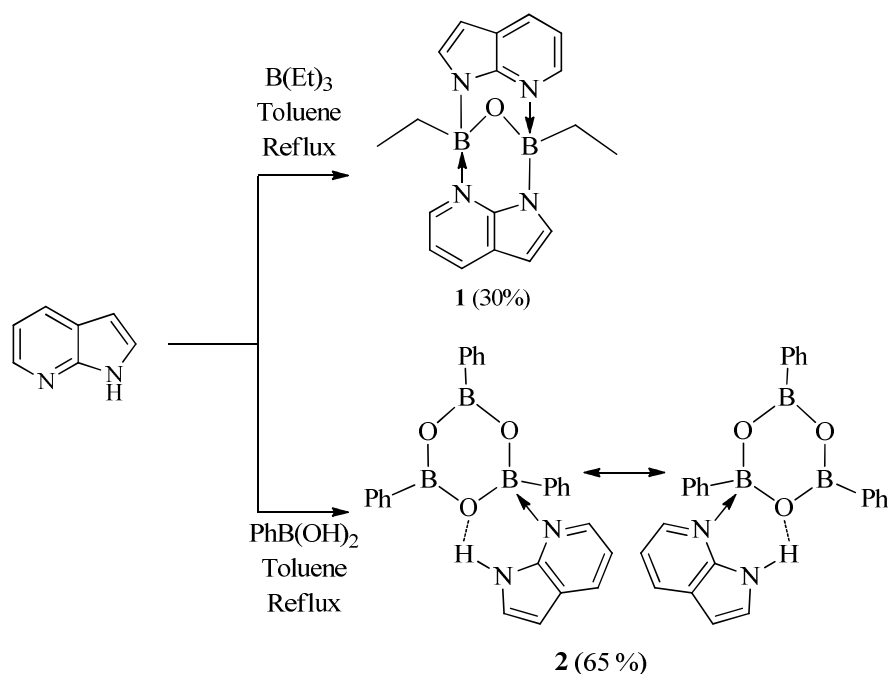


**Figure 2.** Structural feature of tetracoordinate organoboron compounds.

## 2.2 Luminescent organoboron compounds: photo- and electroluminescent properties.

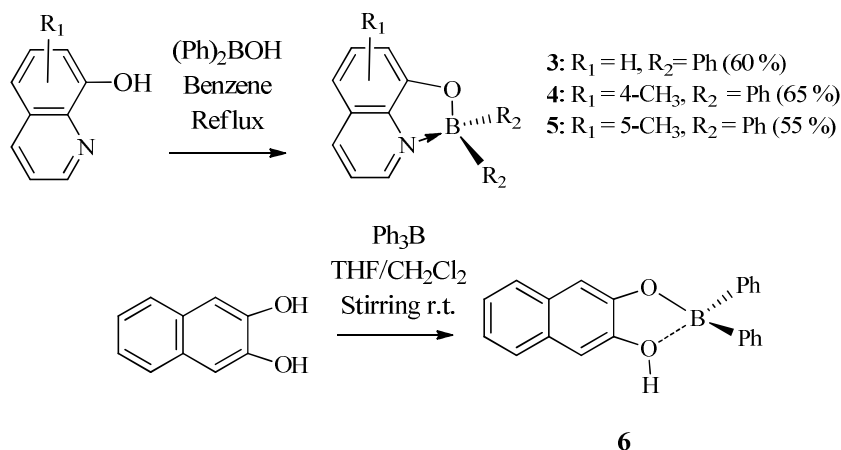
The first luminescent organoboron compound **1** was synthesized by Hassan *et al.* (Scheme 1), where and it was observed blue emission which was attributed to the formation of the N→B dative covalent bond via the donation of lone-pairs of the nitrogen atom to the boron atom changing the emission wavelength from UV to blue region.<sup>23</sup> One year later, Wu *et al.* reported the synthesis of a 7-azaindole adduct of boroxine **2**, which was obtained of the reaction between PhB(OH)<sub>2</sub> with 7-azaindole.<sup>24</sup> This molecule showed an interesting difference in the emission maximum of the solution (368 nm) and solid spectra (400 nm). This behaviour in solution was attributed an intermolecular dissociation-association process in 7-azaindole ligand (Scheme 1).



**Scheme 1.** Photoluminescent organoboron compound 1-2.

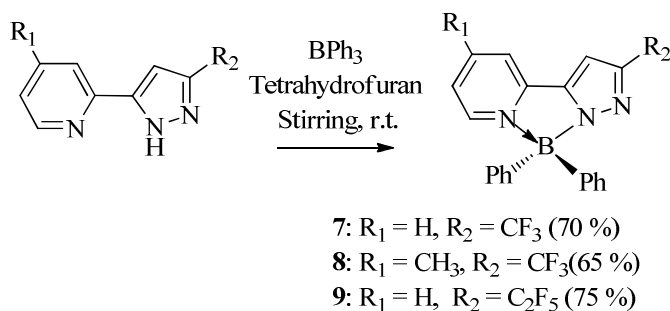
Preliminary results on electroluminescence properties of the organoboron compounds **5-7** derived from bidentate ligands were reported by Anderson *et al.* The authors showed that it is possible to achieve a subtle tuning of the absorption and emission characteristics in solution and in solid state, due to the systematic substitution with methyl groups around the periphery of the 8-hydroxyquinoline ligand in the boron compounds (**Scheme 2**).<sup>25</sup> The electroluminescent device containing the compound **5** as emitter material showed a luminance of 4000 cd/m<sup>2</sup> at a current density of 150 mA/cm<sup>2</sup> and a voltage over 15 V.

On the other hand, Min Kim *et al.* reported the photo and electroluminescent properties of an organoboron compound coordinated with an analogous molecule to the naphthalene, which shows maximum emission peak at 480 nm in the photoluminescence spectra (**Scheme 2**). The electroluminescent device containing **6** as the emitting layer showed a blue luminescence with maximum emission peak at 498 nm with a luminance of 0.80 cd/m<sup>2</sup> and a quantum efficiency of 4.89 %.<sup>26</sup> The authors suggested that some interaction occurs in the devices due to the existent displacement of 18 nm between the emission peaks.



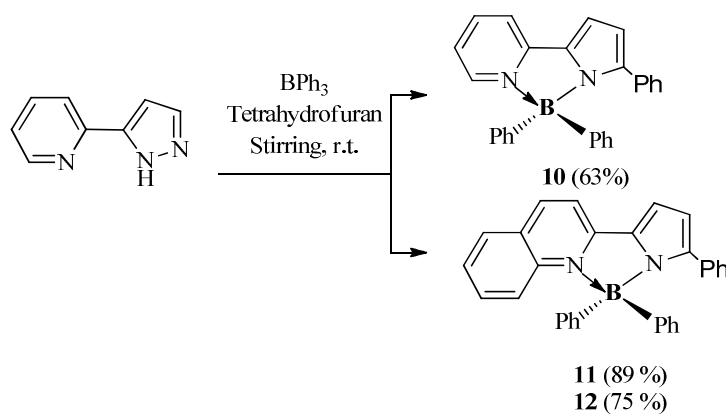
**Scheme 2.** Organoboron compounds **3-6** used as emitter materials in OLEDs.

Meanwhile, Cheng *et al.* reported the dual fluorescent behaviour of a series of organoboron compounds derived from 5-(2-pyridyl)pyrazolate ligand (**Scheme 3**). The boron compounds **7-9** showed in solution, two emission peaks at 382 (505), 360 (488) and 370 (512) nm, respectively, due to the photoinduced electro transfer process from the phenyl moiety to the pyrazolate ligand.<sup>27</sup> The author suggests that an ideal boron-ligand system for devices could exhibit both a locally excited state ( $S_1$ , LE) and a charge transfer state ( $S_1$ , CT) emissions.



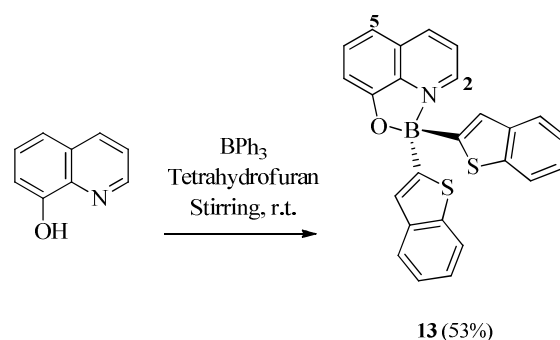
**Scheme 3.** Fluorescent organoboron compounds **7-9** derived from pyrazolate ligand.

The rational color tuning and the luminescent properties of a series of organoboron compounds derived from 2-pyridyl pyrrolide ligand were reported by Chi *et al.* The organoboron compounds **10-12** were thermally stable and showed a strong photoluminescence with emission bands at 490, 510 and 575 nm, respectively (**Scheme 4**).<sup>28</sup> The electroluminescent devices using **12** as the host-emitter produced a saturated red-orange electroluminescence with maximum emission peak at 580 nm and a luminance of 5000 cd/m<sup>2</sup> at a voltage of 15 V with an external quantum efficiency of 0.5 %.



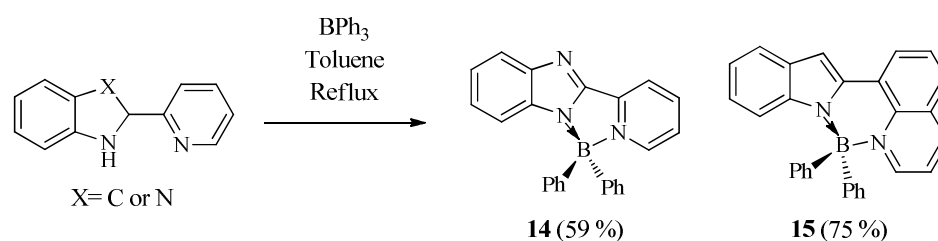
**Scheme 4.** Organoboron compounds **10-12** derived from 2-pyridyl pyrrolide ligand.

Other electroluminescent devices were fabricated by Cui *et al.* using organoboron compound **13** derived from 8-hydroxyquinolato ligand as an emitter layer (**Scheme 5**). These authors found that the substituent group at C-5 or C-2 of the ligand has a significant effect on the emission band and  $\Phi$  of the boron compound.<sup>29</sup> The device using **13** as an emitter and electron transport layer produced a broad bluish-green emission band at 501 nm with a luminance over 1050 cd/m<sup>2</sup> at a voltage around of 10 V.



**Scheme 5.** Electroluminescent organoboron compound **13** derived from 8-hydroxyquinolato ligand.

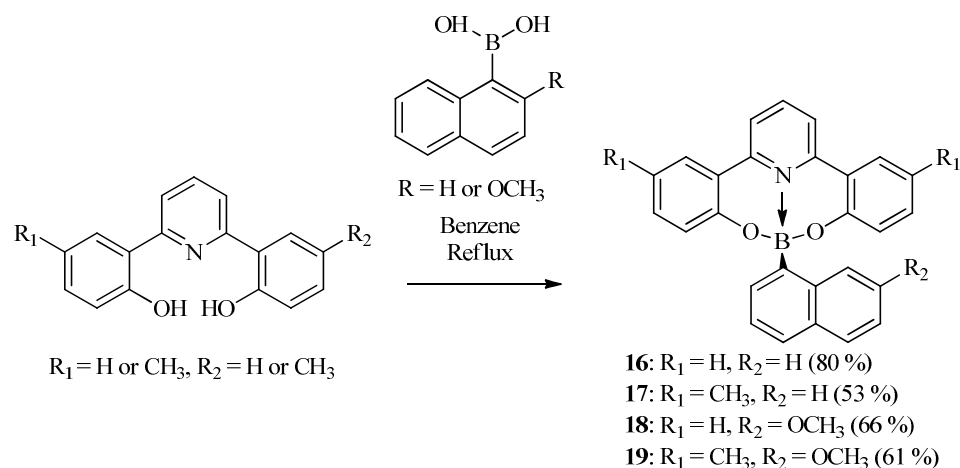
This same group research reported later, the successful assembly of blue and red electroluminescent devices using the compounds **14-15** derived from bidentate (N,N) ligand.<sup>30</sup> These materials showed to be able to function both as emitter and electron transport materials in electroluminescent devices (**Scheme 6**). The device using **14** produced a yellowish orange emission band at 501 nm with a luminance of 429 cd/m<sup>2</sup> at 24 V.



**Scheme 6.** Organoboron compound **14-15** derived from bidentate (N,N) ligand.

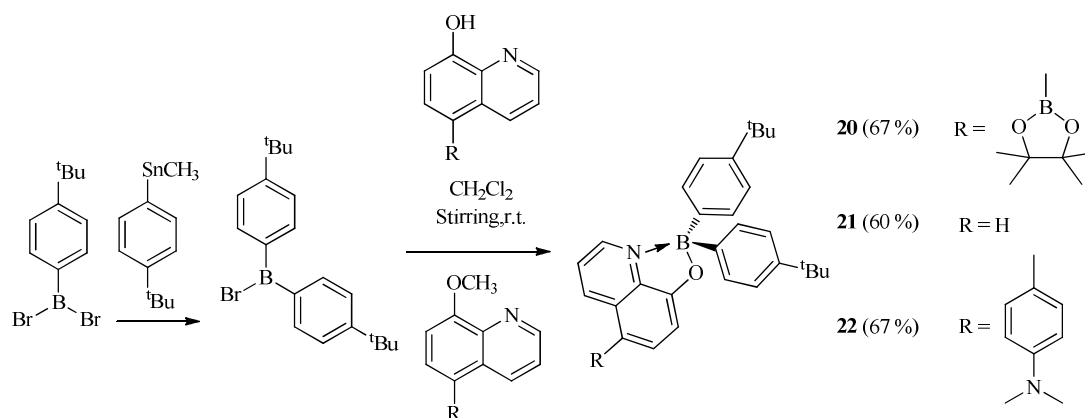
Zhang *et al.* reported the synthesis of the organoboron compounds **16-19** obtaining by the reaction between boronic acid derivatives with phenol-pyridyl ligands.<sup>31</sup> These compounds showed a blue photoluminescence with emission bands at

461 (**16**), 478 (**17**), 459 (**18**) and 479 (**19**) due to the intraligand  $\pi \rightarrow \pi^*$  electron transition of phenol-pyridyl system (**Scheme 7**). Among these materials, the compound **16** had  $\Phi$  of 30% higher than those of **17** (21%), **18** (16%), and **19** (14%). The authors attributed the low yield of **18** and **19** due to the thermal motion of the conformationally mobile methoxy group, which results in energy loss *via* nonradiative decay. The electroluminescent device using **16** as an emitter layer showed a white emission band with a maximum luminance of 1016 cd/m<sup>2</sup> at a current density of 202 mA/cm<sup>2</sup> to 14 V.



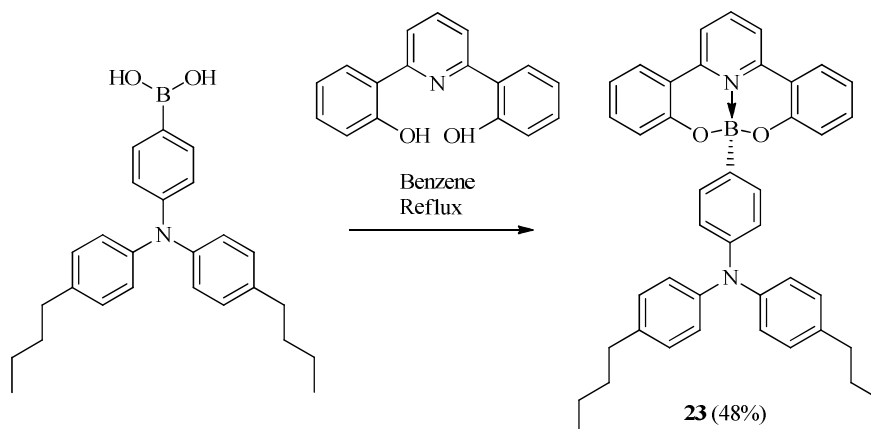
**Scheme 7.** Organoboron compounds **16-19** derived from phenol-pyridyl ligands.

The tuning of the optical properties of a series of organoboron compounds **20-22** derived from quinolate ligand were reported by Qin *et al.* (**Scheme 8**) The authors demonstrated that the modification of the 5-substituent with electro-withdrawing and electron-donating groups from quinolate ligand allows a displacement of the emission band from blue to red region due to the effect of 5-substituents on the HOMO and LUMO level.<sup>32</sup>



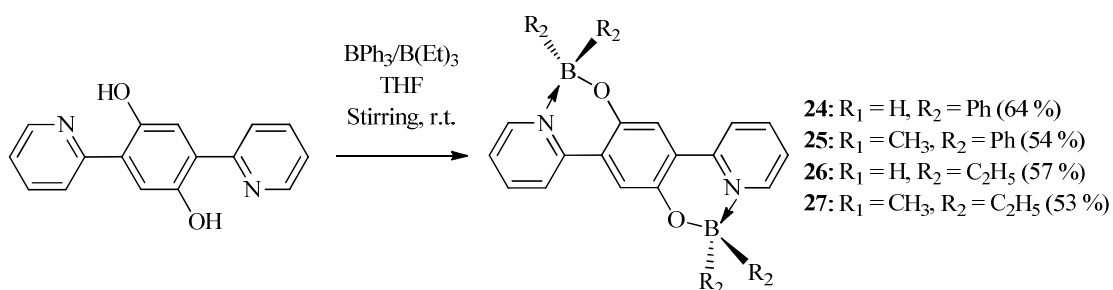
**Scheme 8.** Luminescent organoboron compounds **20-22** derived from quinolate ligand.

Taking that in consideration, Wang *et al.* reported the synthesis of a multifunctional organoboron compound **23** derived from pyridine-phenol ligand (**Scheme 9**). The authors demonstrated that this material is able of functioning as a hole-transporting layer, an electron transporting layer and emitting layer in a one molecule due to the incorporation of electron-rich and electron-deficient groups.<sup>33</sup> The electroluminescent device using **23** as emitting layer produced a yellow light emission band at 575 nm with a maximum luminance of 2654 cd/m<sup>2</sup> and a maximum efficiency of 5.2 cd/A.



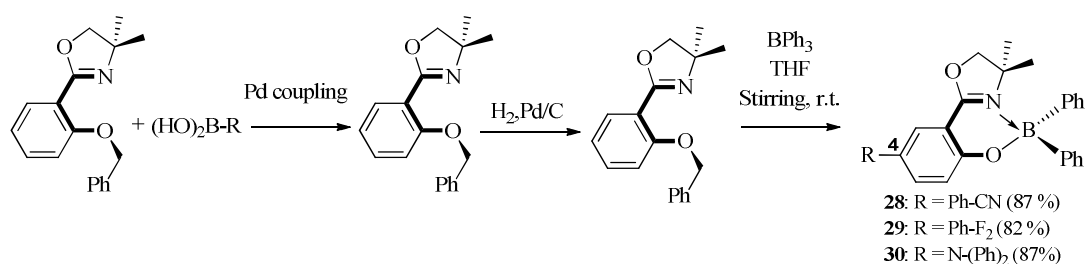
**Scheme 9.** Organoboron compound **23** derived from pyridine-phenol ligand.

An interesting kind of electroluminescent dinuclear organoboron compounds **24-27** were reported by Zhan *et al.* These molecules containing two boron atoms into ladder type conjugated  $\pi$ - system exhibited a high thermal stability and strong electron affinity due to the effect of the extended  $\pi$ -conjugation (**Scheme 10**). The electroluminescent device using **24** as emitting layer produced an orange emission band at 580 nm with a maximum luminance of 9754 cd/m<sup>2</sup> and a maximum efficiency of 4.02 cd/A with a voltage of 2.5 V.<sup>34</sup>



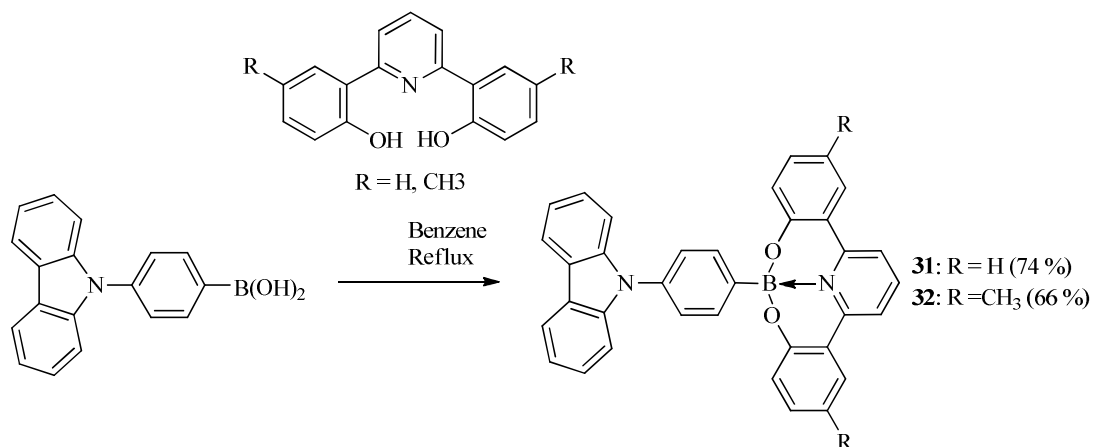
**Scheme 10.** Dinuclear organoboron **24-27** derived from ladder type conjugated  $\pi$  system.

An innovative strategy was reported by Ko *et al.* The photophysical properties of organoboron compounds **28-30** derived from oxazolyphenolate ligand were tuned from blue to green region by substitution with electron-withdrawing and donating groups at the 4-position of the phenoxide (**Scheme 11**). The organoboron compound **29** showed a bipolar character due to intramolecular charge transfer in the complex with an emission band at 422 nm and a high photoluminescence quantum yield in toluene of 34 %.<sup>35</sup> The electroluminescent device using **30** as emitter showed an emission band at 527 nm with a maximum luminance of 2905 cd/m<sup>2</sup> at a current density of 6 mA/cm<sup>2</sup> and a voltage of 4.3 V.



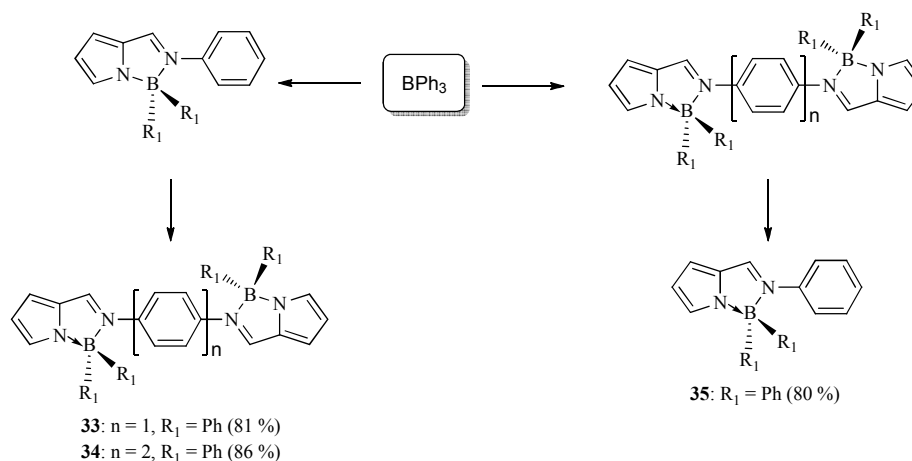
**Scheme 11.** Organoboron compounds **28-30** derived from oxazolyphenolate ligand.

In this regard, the photo and electroluminescent properties of organoboron compounds **31-32** (**Scheme 12**) derived from phenol pyridyl ligand were reported by Zhang *et al.* The electroluminescent device using **31** as emitter showed a yellowish-white emission band at 527 nm with a maximum luminance of 2383 cd/m<sup>2</sup> at a current efficiency of 1.40 cd/A and a voltage of 13 V.<sup>36</sup> The authors attributed that the high luminance obtained may could be related to the higher value of  $\Phi$  in solid state (12%).



**Scheme 12.** Organoboron compounds **31-32** derived from phenol-pyridyl ligand.

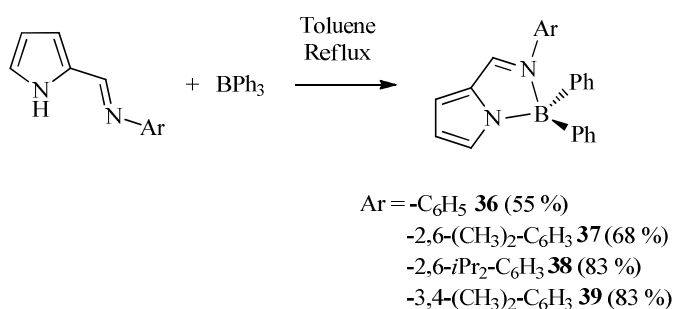
A recent study found that four-coordinate binuclear organoboron complexes **33-35** derived from 2-(N-aryl) formiminopyrrolyl ligand demonstrated to be moisture and air sensitive (**Scheme 13**). Non-doped devices prepared by spin coating using the compounds **33-34** showed maximum luminances in the order of  $10^3$  cd/m<sup>2</sup> and maximum efficiencies of 0.3/A.<sup>37</sup> The electroluminescence spectra for **33-34** showed a displacement of 20 nm with respect to photoluminescence spectra in solution. The authors attributed this behaviour to intermolecular interactions in solid state, stabilizing the excited state.



**Scheme 13.** Four-coordinate binuclear organoboron compounds **33-35** derived from 2-(N-aryl) formiminopyrrolyl ligand.

Recently this same group reported the synthesis and characterized by multiple spectroscopic methods of different tetracoordinate mononuclear organoboron compounds **36-39** containing 2-(N-arylformimino)pyrrolyl ligands with N-aryl ring substituents of different electronic and steric natures (**Scheme 14**). The best electroluminescent device was fabricated using the compound **39** showed an emission

band at 492 nm with a maximum luminance of 614 cd/cm<sup>2</sup> at a current efficiency of 0.2 cd/A and an external quantum efficiency of 7.9 %.<sup>38</sup> The author found that the electronic properties of these compounds could be varied by changing the electron-donating or electron-withdrawing character of the aniline substituents.



**Scheme 14.** Organoboron compounds **36-39** derived from 2- (N-arylformimino)pyrrolyl ligand.

The literature showed that in the last two decades of the organoboron compounds derived from bidentate ligand have been widely studied. However, with tridentate ligands has been scarce investigated. In addition, it has only been studied the optical non linear properties of a small group of them with transition metals and some main group elements. Therefore, the investigation on the luminescence properties have not been studied deeply. The analysis of the literature shows that the tuning of luminescent properties of these materials have been performed from boron trifluoride etherate [BF<sub>3</sub>O(Et)<sub>2</sub>], which is a precursor highly unstable and expensive.<sup>39</sup>

Due to that boron compounds derived from bidentate ligands have been widely used as emitting layers in the assembly of electroluminescent devices, we asking the next question. Organoboron compounds derivatives from tridentate ligands could also act as emitting materials? We propose the following hypothesis as well as a serie of objetives that are described in the next chapter.

## **HYPOTHESIS**

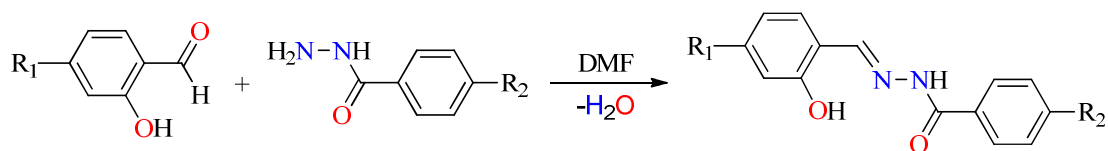
Tetracoordinate organoboron compounds derived from organic tridentate ligands exhibited luminescent properties and act as an electron transport layer (ETL), and as an emitting layer in the assembly of electroluminescent devices type OLED.

## **GENERAL OBJECTIVE**

Synthesize, characterize, determination of luminescent properties of new organoboron compounds derived from Schiff bases and the potential fabrication of an electroluminescent device type OLED.

## SPECIFIC OBJECTIVES

- To synthesize the Schiff bases **1a-6a** from a condensation reaction.

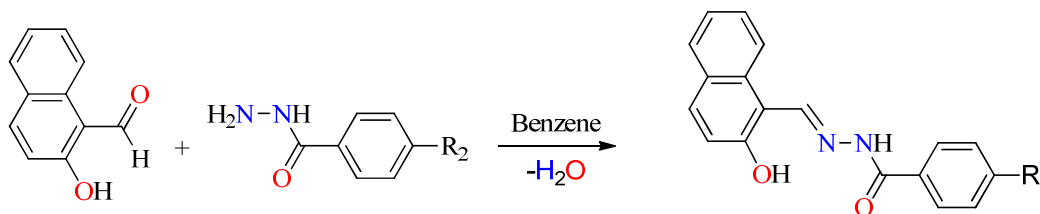


**1a:** R<sub>1</sub> = Et<sub>2</sub>N, R<sub>2</sub> = H

**2a:** R<sub>1</sub> = MeO, R<sub>2</sub> = H

**3a:** R<sub>1</sub> = Et<sub>2</sub>N, R<sub>2</sub> = NO<sub>2</sub>

**4a:** R<sub>1</sub> = MeO, R<sub>2</sub> = NO<sub>2</sub>

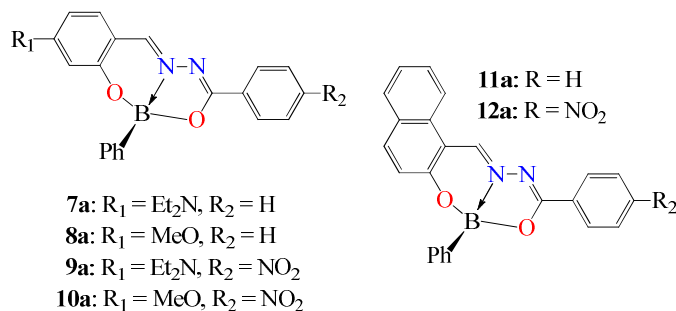


**5a:** R = H

**6a:** R = NO<sub>2</sub>

- To synthesize the organoboron compounds **7a-12a** using the free Schiff bases

**1a-6a.**



**7a:** R<sub>1</sub> = Et<sub>2</sub>N, R<sub>2</sub> = H

**8a:** R<sub>1</sub> = MeO, R<sub>2</sub> = H

**9a:** R<sub>1</sub> = Et<sub>2</sub>N, R<sub>2</sub> = NO<sub>2</sub>

**10a:** R<sub>1</sub> = MeO, R<sub>2</sub> = NO<sub>2</sub>

**11a:** R = H

**12a:** R = NO<sub>2</sub>

- To characterize the organoboron compounds by different spectroscopic and spectrometric techniques such as multinuclear magnetic resonance ( $^1\text{H}$ ,  $^{11}\text{B}$ ,  $^{13}\text{C}$ , DEPT, HETCOR, HMBC, COSY). Complementary techniques such as infrared, and ultraviolet-visible spectroscopy, elemental analysis, and high mass spectrometry are going to use too.
- To obtain the crystal structural by single crystal X-ray diffracction the organoboron compounds and Schiff bases.
- To determine the photo- and electro- luminescent properties of organic molecules synthesise previously.
- To assemble electroluminescent devices type OLED using the organoboron compounds derived from Schiff bases with those organic materials that shows the best features.

# MATERIALS AND METHODS

## 4.1. Material and equipment

All starting materials were purchased from Aldrich Chemical Company. Solvents were used without further purification. Melting points were determined on an Electrothermal Mel-Temp apparatus and are uncorrected. Infrared spectra were recorded using a Bruker Tensor 27 FT-IR spectrophotometer equipped with a Pike Miracle™ ATR accessory with a single reflection ZnSe ATR crystal. UV spectra were obtained with a Shimadzu 2401PC UV/VIS spectrophotometer and emission measurements were performed on a Perkin-Elmer LS-50B luminescence spectrometer. Multinuclear magnetic resonance experiments as  $^1\text{H}$ ,  $^{13}\text{C}$ , and  $^{11}\text{B}$ -NMR spectra were recorded on a Bruker advance DPX 400. Chemical shifts (ppm) are relative to  $(\text{CH}_3)_4\text{Si}$  for  $^1\text{H}$  and  $^{13}\text{C}$ .  $^{11}\text{B}$  NMR spectra were referenced externally to  $\text{BF}_3\cdot\text{OEt}_2$ . Mass spectra were recorded on an AB Sciex API 2000™ LC/MS/MS System. Elemental analyses were carried out on a Thermo Finnigan Flash EA 1112 elemental microanalyzer. High resolution mass spectra were acquired by LC/MSD TOF on an Agilent Technologies instrument with

APCI as ionization source. Simultaneous thermal analysis (TGA-DTA) were carried out in the temperature range 25 to 600 °C under nitrogen atmosphere at a heating rate of 10 °C min<sup>-1</sup> using a TA instruments-SDT 2960 thermal analyzer.

The photophysical measurements were carried out in spectrophotometric grade solvents (tetrahydrofuran and chloroform) freshly distilled and the solutions were studied just as prepared.<sup>40</sup>

#### **4.2. X-ray data collection and structure determination**

The data for **1**, **2**, **7**, **8**, and **12** were covered with a layer of hydrocarbon oil that was selected and mounted with paratone-N oil on a cryo-loop, and immediately placed in the low-temperature nitrogen stream at 100(2) K. The data for **1**, **2**, **7**, **8**, and **12** were recorded on a Bruker SMART APEX CCD area detector system equipped with a Oxford Cryosystems 700 Series Cryostream cooler, a graphite monochromator, and a Mo K $\alpha$  fine-focus sealed tube ( $\lambda = 0.71073 \text{ \AA}$ ). The structures were solved by direct methods using SHELXS-97<sup>41</sup> and refined against  $F^2$  on all data by full-matrix least-squares with SHELXL-97.<sup>42</sup> Absorption corrections were applied by using SADABS. The CCDC files 944174-944177 contain the supplementary crystallographic data for **1-2**, **7**, and **8**. These data can be obtained free of charge via or from the Cambridge Crystallographic Data Centre (CCDC), 12 Union Road, Cambridge, CB2 1EZ, UK. <http://www.ccdc.cam.ac.uk/conts/retrieving.html>.

### 4.3. Absorbance, emission and luminescence quantum yields

UV-Vis absorption spectra were measured on a Shimadzu 2401PC spectrophotometer. Optical band gap ( $E_g$ ) was determined from the intercept with the X axis of the tangent of the absorption spectrum drawn at absorbance of 0.1. The emission spectra have been recorded with a Perkin-Elmer LS 50B spectrofluorometer, by exciting 10 nm below the longer wavelength absorption band. Fluorescence quantum yields in solution ( $\phi$ ) were determined according to the procedure reported in literature<sup>43</sup> and using quinine sulphate in  $H_2SO_4$  0.1 M ( $\phi = 0.54$  at 310 nm) as the standard. Temperature was regulated at  $25.0 \pm 0.5$  °C with a water circulating bath. Three solutions with absorbance at the excitation wavelength lower than 0.1 were analysed for each sample and the quantum yield was averaged. Stokes' shift values were calculated from the excitation and fluorescence maximums. Fluorescence lifetimes were obtained at room temperature by the time correlated single photon counting (TCSPC) technique on a Horiba Jobin Yvon TemPro instrument with a nanoLED laser of 370 nm excitation (1 MHz repetition rate) and by using a 0.01% ultrapure water dispersion of Ludox AS40 (Aldrich) for the prompt signal. Fits were performed on the DAS6 software of the instrument.

#### 4.4. Fabrication of electroluminescent devices

Diodes were prepared in typical configuration of ITO/PEDOT:PSS/**10a**/Al (**Figure 3**). ITO substrates (Spi. Inc, 8-10  $\Omega/\text{cm}^2$ ) were first cleaned in ultrasonic bath (Branson 200) in dichloromethane for 10', hexane for 10' and methanol for 60', and then dried in an oven. Lithography was carried out in order to obtain active areas of 6  $\text{mm}^2$ . PEDOT:PSS (Clevios P by Clevios) was filtered and then deposited on the ITO slides by spin coating at 5000 rpm to give a 20 nm layer. The active layer of **10** was deposited by spin coating technique on the ITO-glass substrate. The aluminium was vacuum evaporated at a rate of 1.5 to 3  $\text{\AA}/\text{s}$  at a typical pressure of  $10^{-6}$  torr in an Intercovamex TE18P vacuum chamber; the thickness was controlled by the quartz balance monitor  $\sim 100$  nm. The electrical and luminescent characteristics of the devices were measured by using a source measurement unit (Keithley 2420) and an optical powermeter (Newport 1930-C).

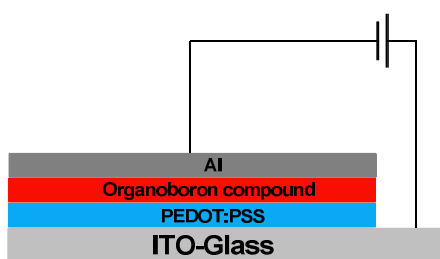


**Figure 3.** Schematic configuration of the device of double organic layer.

#### 4.5. Third-harmonic generation experiment

It is important to notice that due to structural design of the Schiff base **1-4a**, and their organoboron compounds **7-10a** were carried out the determination of the optical non linear properties with the purpose enriches the study of the photophysical properties.

The organic materials **1-4a**, and **7-10a** were studied in solid films using the guest (molecule)-host (polymer) ratios approach 70:30 wt. % of polystyrene (PS), and compounds under test were dissolved in tetrahydrofurane. The solid films were deposited on glass substrates of a 1 mm of thick by using the spin coating technique. The solid films had typical thickness between 400 and 480 nm with good optical quality. The film thickness was measured by a Nanosurf Easyscan 2 AFM at a scanning of 50  $\mu\text{m/s}$  and an applied dynamic force of 2 mg. Third-order nonlinear susceptibility in solid film  $\chi^{(3)}(-3\omega, \omega, \omega, \omega)$  were determinate according to the procedure reported in literature<sup>44</sup> by the Maker-fringes technique at the IR wavelength of 1300 nm. It consisted of Nd-YAG laser- pumped optical parametric oscillator (OPO) that delivered pulses of 7 ns at a repetition rate of 10 Hz. The idler beam of the OPO system tuned at 1300 nm was focused into the polystyrene films doped with the molecule of interest. Typical pump irradiance at sample position was about 0.5  $\text{GW/cm}^2$ . The third harmonic beam emerging from films was separated from the pump beam by using a color filter and detected with a PMT and a lock-in amplifier. The third harmonic generation (THG) measurements were performed for incidents angles in the range from  $-40^\circ$  to  $40^\circ$  with steps of  $0.27^\circ$ . Whole of the experiment was computer controlled. The Marker Fringer

technique compares the third harmonic peak intensity  $I^{3\omega}$  from the substrate-film with that produced from the glass substrate alone. The nonlinear susceptibility  $\chi^{(3)}$  in a film of thickness  $L_f$  is determinate from equation (1):

$$\chi^3 = \chi_s^3 \frac{2}{\pi} \left( \frac{L_{c,s}}{L_f} \right) \left( \frac{I_f^{3\omega}}{I_s^{3\omega}} \right) \left( \frac{I_f^{3\omega}}{I_s^{3\omega}} \right)^{1/2} \quad (1)$$

Where  $\chi_s^{(3)}$  and  $L_{c,s}$  are the nonlinear susceptibility and coherence length, respectively, for the glass substrate at the fundamental wavelength. In our calculation, we consider  $\chi_s^{(3)} = 3.1 \times 10^{-14}$  esu and  $L_{c,s} = 11 \mu\text{m}$  for the glass substrate. In any case, our samples satisfied the condition  $L_f \ll L_{c,s}$ , in which the equation (1) is valid.

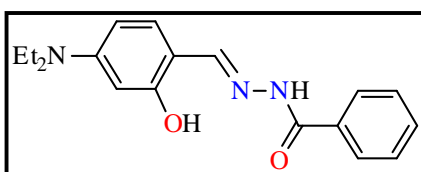
#### 4.6 Computacional study

All calculations were done with GAMESS-US version 1 MAY 2013 (R1).<sup>45</sup> All the structures were optimized at the B3LYP<sup>46</sup>/6-31G\* level of theory, both in the gas phase and with the PCM solvent model. The solvents specified by the PCM solvent model<sup>47</sup> were acetone (EPS=20.70 D), THF (EPS=7.58 D), chloroform (EPS=4.90 D) and toluene (EPS=2.38 D). The optimized structures were subjected to vibrational analysis to ensure they were stationary points on the energy hypersurface, yielding only real vibrational frequencies. The excitation energies were calculated using TDDFT single points at the B3LYP/6-311++G\*\* level on the previously optimized geometries, both in the gas phase and with PCM solvent model. The three lowest roots were

calculated in all cases. Convolution of the resulting excited energies to simulated UV-Vis spectra was done with Gabedit v. 2.4.8.<sup>48</sup>

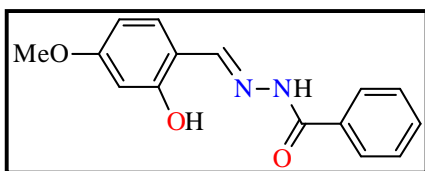
#### 4.7. Synthesis procedure of compounds 1-12a.

##### 4.7.1. (*E*)-N'-(4-(diethylamino)-2-hydroxysalicylidine) benzohydrazide (**1a**)



A solution of 4-diethylaminosalicylaldehyde 0.193 g (1.0 mmol) and benzoylhydrazide 0.136 g (1.0 mmol) in DMF were hot boiling for 5 min and then the mixture was cooled to room temperature and poured into 200 mL of crushed ice and 1 mL of concentrated sulfuric acid. The reaction mixture was slowly cooled to room temperature. The precipitated was filtrated and washed with hexane, followed by recrystallization in an ethyl acetate/hexane (1:1) mixture to give 0.26 g (0.85 mmol, 85 % yield) of **1a** as a green crystalline solid. M.P.: 219 °C. IR<sub>νmax</sub> (ATR): 3032, 3174, 1625, 1587, 1517 cm<sup>-1</sup>. UV/Vis (THF): λ<sub>abs/max</sub>, ε<sub>max</sub>\*10<sup>4</sup>: 362 nm, 6.5 M<sup>-1</sup>cm<sup>-1</sup>. Fluorescence (THF): λ<sub>fluor</sub>: 452 nm. <sup>1</sup>H NMR (400 MHz, DMSO-*d*<sub>6</sub>) δ 1.09 (6H, t, *J* = 6.8 Hz, H-16), 3.34 (4H, s, H-15), 6.14 (1H, s, H-3), 6.28 (1H, d, *J* = 8.8 Hz, H-5), 7.19 (1H, d, *J* = 8.8 Hz, H-6), 7.54 (2H, m, H-11,13), 7.58 (1H, m, H-12), 7.93 (2H, d, *J* = 8.8 Hz, H-10,14), 8.44 (1H, s, H-7), 11.52 (1H, s, NH), 12.83 (1H, s, OH) ppm. <sup>13</sup>C{<sup>1</sup>H} NMR (100 MHz, DMSO-*d*<sub>6</sub>) δ 12.5 (C-16), 43.8 (C-15), 97.5 (C-3), 103.6 (C-5), 106.4 (C-1), 127.4 (C-10,1), 128.4 (C-11,13,12), 131.6 (C-6), 133.2 (C-9), 150.0 (C-7), 150.1 (C-4), 159.8 (C-2), 162.2 (C-8) ppm. Anal. Calc. for C<sub>18</sub>H<sub>21</sub>N<sub>3</sub>O<sub>2</sub>: C; 69.43. H; 6.80. N; 13.49, Found: C; 69.44. H; 7.06. N; 13.57.

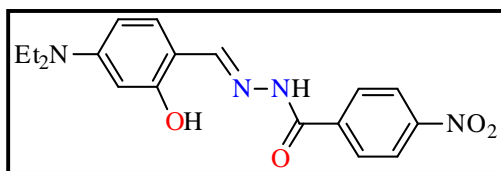
#### 4.7.2. (*E*)-*N*'-(4-(methoxy)-2-hydroxysalicylidine) benzohydrazide (**2a**)



Preparation of **2a** was accomplished like that of **1a** from 4-methoxysalicylaldehyde (0.152 g, 1.0 mmol) and benzoylhydrazide (0.136 g, 1.0 mmol). Yield:

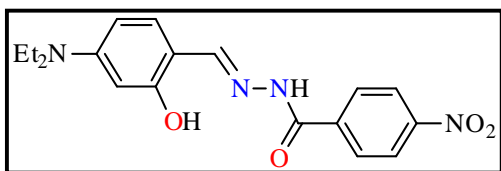
0.25 g (91 %). White solid, M.P.: 181 °C. IR<sub>max</sub> (ATR): 3527, 3050, 3180, 1624, 1601, 1506, 1284 cm<sup>-1</sup>. UV/Vis (THF): λ<sub>abs/max</sub>, ε<sub>max</sub>\*10<sup>4</sup>: 330 nm, 4.2 M<sup>-1</sup>cm<sup>-1</sup>. <sup>1</sup>H NMR (400 MHz, DMSO-*d*<sub>6</sub>) δ 3.77 (3H, s, H-15), 6.53 (1H, s, H-3), 6.54 (1H, s, H-5), 7.43 (1H, d, *J* = 8 Hz, H-6), 7.54 (2H, st, H-11,13), 7.60 (1H, st, H-12), 7.93 (2H, d, *J* = 8 Hz, H-10,14), 8.55 (1H, s, H-7), 11.65 (1H, s, NH), 12.02 (1H, s, OH) ppm. <sup>13</sup>C{<sup>1</sup>H} NMR (100 MHz, DMSO-*d*<sub>6</sub>) δ 55.3 (C-15), 101.2 (C-3), 106.5 (C-5), 111.7 (C-1), 127.6 (C-10,14), 128.5 (C-11,13), 131.2 (C-6), 131.9 (C-12), 132.9 (C-9), 148.8 (C-7), 159.4 (C-4), 162.1 (C-2), 162.6 (C-8) ppm. HETCOR correlation [δ<sub>H</sub>/δ<sub>C</sub>]: 3.77/55.3 (H-15/C-5), 6.53/101.2 (H-3/C-3), 6.54/106.5 (H-5/C-5), 7.54/128.5 (H-11,13/C-11,13), 7.60/131.9 (H-12/C-12), 7.93/127.6 (H-10,14/C-10,14), 8.55/148.8 (H-7/C-7). COSY correlation [δ<sub>H</sub>/δ<sub>H</sub>]: 7.43/6.53 (H-6/H-3), 7.43/6.54 (H-6/H-5), 7.93 (H-10,14/H-11,13). APCI-MS *m/z* (%): 270.80 (M<sup>+</sup> 1), 77.00 (73), 105.00 (63), 150.00 (50), 95.00 (44), 135.00 (21), 107.00(13). Anal. Calc. for C<sub>15</sub>H<sub>14</sub>N<sub>2</sub>O<sub>3</sub> · H<sub>2</sub>O: C; 62.49. H; 5.59. N; 9.72, Found: C; 62.69. H; 5.82. N; 9.51.

#### 4.7.3. (E)-N'-(4-(diethylamino)-2-hydroxysalicylidine)-4-nitrobenzohydrazide (**3a**)



Preparation of **3a** was accomplished like that of **1a** from 4-diethylaminosalicylaldehyde (0.193 g, 1.0 mmol) and 4-nitrobenzoylhydrazide (0.181 g, 1.0 mmol). Yield: 0.35 g (98 %), red solid. M.P.: 225 °C (lit. 230 °C).<sup>49</sup> IR<sub>vmax</sub> (ATR): 3358, 3176, 2979, 1629, 1590, 1516 cm<sup>-1</sup>. UV/Vis (THF): λ<sub>abs/max</sub>, ε<sub>max</sub>\*10<sup>4</sup>: 343 nm, 5.70 M<sup>-1</sup>cm<sup>-1</sup>. Fluorescence (THF): λ<sub>fluor</sub>: 411 nm. <sup>1</sup>H NMR (400 MHz, DMSO-*d*<sub>6</sub>) δ: 1.10 (6H, t, *J* = 6.8 Hz, H-16), 3.35 (4H, s, H-15), 6.12 (1H, s, H-3), 6.28 (1H, d, *J* = 8.8 Hz, H-5), 7.24 (1H, d, *J* = 8.8 Hz, H-6), 8.37 (2H, m, H-11,13), 8.14 (2H, d, *J* = 8.8 Hz, H-10,14), 8.45 (1H, s, H-7), 11.30 (1H, s, NH), 12.09 (1H, s, OH) ppm. <sup>13</sup>C{<sup>1</sup>H} NMR (100 MHz, DMSO-*d*<sub>6</sub>) δ: 12.5 (C-16), 43.8 (C-15), 97.4 (C-3), 103.8 (C-5), 106.3 (C-1), 123.7 (C-10,14), 129.0 (C-11,13), 131.6 (C-6), 138.9 (C-12), 149.2 (C-9), 150.4 (C-4), 150.7 (C-7) 159.8 (C-2), 160.5 (C-8) ppm.

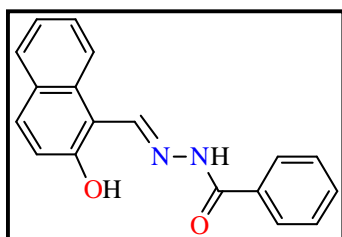
#### 4.7.4. (E)-N'-(4-(methoxy)-2-hydroxysalicylidine)-4-nitrobenzohydrazide (**4a**)



Preparation of **4a** was accomplished like that of **1a** from 4-methoxysalicylaldehyde (0.152 g, 1.0 mmol) and 4-nitrobenzoylhydrazide (0.181 g, 1.0 mmol). Yield: 0.30 g (95%). Yellow solid. M.P.: 219 °C (lit. 228 °C).<sup>50</sup> IR<sub>vmax</sub> (ATR): 3331, 3198, 2976, 1624, 1598, 1599, 1281 cm<sup>-1</sup>. UV UV/Vis (THF): λ<sub>abs/max</sub>, ε<sub>max</sub>\*10<sup>4</sup>: 345 nm, 1.80 M<sup>-1</sup>cm<sup>-1</sup>. <sup>1</sup>H NMR (400 MHz, DMSO-*d*<sub>6</sub>) δ: 3.78 (3H, s,

H-15), 6.51 (1H, s, H-3), 6.54 (1H, s, H-5), 7.48 (1H, d,  $J = 8$  Hz, H-6), 8.38 (2H, d, H-11,13), 8.16 (2H, d,  $J = 8$  Hz, H-10,14), 8.58 (1H, s, H-7), 11.45 (1H, s, NH), 12.27 (1H, s, OH) ppm.  $^{13}\text{C}\{^1\text{H}\}$  NMR (100 MHz, DMSO- $d_6$ )  $\delta$  55.3 (C-15), 101.1 (C-3), 106.2 (C-5), 111.7 (C-1), 123.7 (C-10,14), 129.1 (C-11,13), 131.0 (C-6), 149.3 (C-7), 149.5 (C-9), 159.4 (C-4), 160.9 (C-2), 162.3 (C-8) ppm.

#### 4.7.5. (*E*)-(2-hydroxy-1-naphthalidene) benzohydrazide (**5a**)

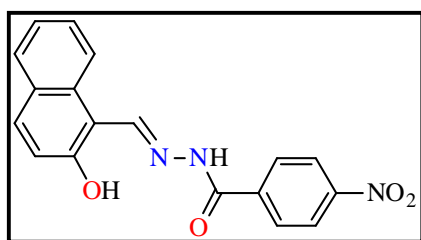


A solution of 2-hydroxy-1-naphthaldehyde (0.172 g, 1.0 mmol) and benzoylhydrazide (0.136 g, 1.0 mmol) in benzene under reflux for 24 h, using a Dean-Stark apparatus for eliminate of water by azeotropic distillation.

The reaction mixture was slowly cooled to room temperature. The precipitated was filtrated, and washed with hexane, giving 0.26 g (87% yield) of **5a** as a yellow light solid. M.P.: 214 °C (lit. 260°C).<sup>51</sup>. IR<sub>vmax</sub> (ATR): 3163, 1640, 1575 1468 cm<sup>-1</sup>. UV UV/Vis (CHCl<sub>3</sub>):  $\lambda_{\text{abs/max}}$ ,  $\epsilon_{\text{max}} \cdot 10^4$ : 364 nm, 1.30 M<sup>-1</sup>cm<sup>-1</sup>. Fluorescence (CHCl<sub>3</sub>):  $\lambda_{\text{fluor/max}}$ : 406 nm.  $^1\text{H}$  NMR (400 MHz, DMSO- $d_6$ )  $\delta$  7.25 (1H, d,  $J=9.2$  Hz, H-3), 7.42 (1H, t,  $J=7.2$  Hz, H-7), 7.60 (2H, d,  $J = 7.6$  Hz, H-15,17), 7.64 (1H, m, H-16), 7.67 (1H, m, H-8), 7.91 (1H, d,  $J = 8.0$  Hz, H-6), 7.94 (1H, d,  $J = 9.2$  Hz, H-4), 7.99 (2H, d,  $J = 7.2$  Hz, H-14, 18), 8.23 (1H, d,  $J = 8.8$  Hz, H-9), 9.49 (1H, s, H-11), 12.23 (1H, s, NH), 12.79 (1H, s, OH) ppm.  $^{13}\text{C}\{^1\text{H}\}$  NMR (100 MHz, DMSO- $d_6$ )  $\delta$  108.45 (C-1), 118.87 (C-3), 120.55 (C-9), 123.51 (C-7), 127.53 (C-14,18), 127.75 (C-16), 128.61 (C-15,17), 128.94 (C-6), 130.82 (C-5), 131.55 (C-10), 132.06 (C-8), 132.59 (C-13), 132.71 (C-4),

146.79 (C-11), 157.97 (C-2), 162.48 (C-12) ppm. HETCOR correlation [ $\delta_{\text{H}}/\delta_{\text{C}}$ ]: 7.25/118.87 (H-3/C-3), 7.42/123.51 (H-7/C-7), 7.64/127.75 (H-16/C-16), 7.60/128.61 (H-15,17/C-15,17), 7.67/132.06 (H-8/C-8), 7.91/128.94 (H-6/C-6), 7.94/132.71 (H-4/C-4), 7.99/127.53 (H-14,18/C-14,18), 8.23/120.55 (H-9/C-9), 9.49/146.79 (H-11/C-11) ppm. COSY correlation [ $\delta_{\text{H}}/\delta_{\text{H}}$ ]: 7.25/7.94 (H-3/H-4), 7.91/7.42 (H-6/H-7), 7.67/8.23 (H-8/H-9), 7.99/7.60 (H-14,18/H-15,17), 7.60/7.64 (H-15,17/H-16) ppm.

#### 4.7.6. (*E*)-(2-hydroxy-1-naphthalidene)-4-nitrobenzohydrazide (**6a**)

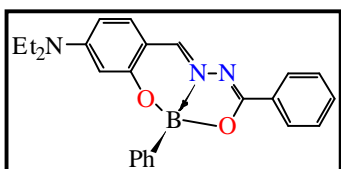


Preparation of **6a** was accomplished like that of **5a** from 2-hydroxy-1-naphthaldehyde (0.172 g, 1.0 mmol) and 4-nitrobenzoylhydrazide (0.181 g, 1.0 mmol). Yield: 0.22 g (65%). Yellow solid. M.P.:

223 °C. IR<sub>umax</sub> (ATR): 3321, 3216, 1644, 1579, 1522, 1340 cm<sup>-1</sup>. UV UV/Vis (CHCl<sub>3</sub>):  $\lambda_{\text{abs/max}}$ ,  $\epsilon_{\text{max}} \cdot 10^4$ : 379 nm, 0.74 M<sup>-1</sup>cm<sup>-1</sup>. <sup>1</sup>H NMR (400 MHz, DMSO-*d*<sub>6</sub>)  $\delta$ : 7.25 (1H, d, *J* = 8.8 Hz, H-3), 7.42 (1H, t, *J* = 7.6 Hz, H-7), 7.62 (1H, t, *J* = 7.6 Hz, H-8), 7.90 (1H, d, *J* = 8.0 Hz, H-6), 7.95 (1H, d, *J* = 9.2 Hz, H-4), 8.04 (2H, d, *J* = 8.8 Hz, H-15,17), 8.29 (2H, d, *J* = 8.4 Hz, H-14,18), 8.33 (1H, sa, H-9), 9.48 (1H, s, H-11), 12.48 (1H, s, NH), 12.57 (1H, s, OH) ppm. <sup>13</sup>C{<sup>1</sup>H} NMR (100 MHz, DMSO-*d*<sub>6</sub>)  $\delta$ : 108.48 (C-1), 118.79 (C-3), 120.89 (C-9), 123.50 (C-14,18), 123.60 (C-7), 127.81 (C-5), 127.87 (C-8), 128.39 (C-15,17), 128.96 (C-6), 130.84 (C-10), 131.55 (C-13), 133.10 (C-4), 147.86 (C-11), 148.86 (C-16), 158.14 (C-2), 160.88 (C-12) ppm. HETCOR correlation [ $\delta_{\text{H}}/\delta_{\text{C}}$ ]: 7.25/118.79 (H-3/C-3), 7.42/123.60 (H-7/C-7), 7.62/127.87 (H-8/C-8), 7.90/128.96 (H-

6/C-6), 7.95/133.10 (H-4/C-4), 8.04/128.39 (H-15,17/C-15,17), 8.29/123.50 (H-14,18/C-14,18), 9.48/147.86 (H-11/C-11) ppm. COSY correlation [ $\delta_{\text{H}}/\delta_{\text{H}}$ ]: 7.95/7.25 (H-4/H-3), 7.90/7.42 (H-6/H-7), 7.62/7.42 (H-8/H-7). 7.62/8.33 (H-8/H-9), 8.04/8.29 (H-15,17/H-14,18) ppm. Anal. Calc. for  $\text{C}_{18}\text{H}_{13}\text{N}_3\text{O}_4$ : C; 64.50. H; 3.90. N; 12.50, Found: C; 55.34. H; 4.04 . N; 17.47.

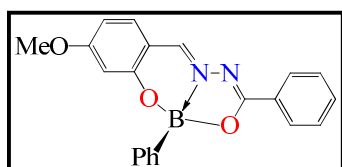
#### 4.7.7. (*E*)-*N*'-(4-(diethylamino)-2-hydroxysalicylidine)benzohydrazidato-phenylboron (**7a**)



A solution of **1a** (1.0 mmol) and phenylboronic acid (1.0 mmol) in benzene were heated under reflux for 48 h, using a Dean-Stark apparatus for the removal of water by azeotropic distillation. The reaction mixture was slowly warmed to room temperature. The precipitated was filtrated and washed with hexane, followed by recrystallization in an ethyl acetate/hexane (1:1) mixture to give 0.33 g (84 %) of **7a** as a yellow solid. M. P. 153 °C. IR<sub>vmax</sub> (ATR): 3036, 1608, 1528, 1183, 1136, 697, 613  $\text{cm}^{-1}$ . UV/Vis (THF):  $\lambda_{\text{abs/max}}$ ,  $\epsilon_{\text{max}} * 10^4$ : 394 nm, 3.80  $\text{M}^{-1}\text{cm}^{-1}$ . Fluorescence (THF):  $\lambda_{\text{fluor/max}}$ : 452 nm.  $^1\text{H}$  NMR (400 MHz,  $\text{CDCl}_3$ )  $\delta$ : 1.23 (6H, t,  $J = 7.2$  Hz, H-16), 3.43 (4H, m, H-15), 6.40 (1H, dd,  $J = 2.4, 8.8$  Hz, H-5), 6.29 (1H, d, H-3), 7.15 (1H, d,  $J = 8.8$  Hz, H-6), 7.19 (1H, da, H-12), 7.20 (1H, sa, H-m), 7.43 (2H, m, H-11,13), 7.46 (2H, m, H-o), 7.52 (1H, st, H-p), 8.11 (1H, s, H-7), 8.15 (2H, d,  $J = 8.8$  Hz, H-10,14) ppm.  $^{13}\text{C}\{^1\text{H}\}$  NMR (100 MHz,  $\text{CDCl}_3$ )  $\delta$ : 12.6 (C-16), 44.8 (C-15), 99.2 (C-3), 105.8 (C-5), 107.8 (C-1), 127.6 (C-12), 127.3 (C-m), 132.4 (C-i), 128.2 (C-10,14), 128.4 (C-o), 131.1 (C-11,13), 132.0

(C-p), 154.6 (C-9), 132.5 (C-6), 144.9 (C-7), 158.4 (C-4), 167.7 (C-2), 169.9 (C-8) ppm. HETCOR correlation [ $\delta_{\text{H}}/\delta_{\text{C}}$ ]: 1.23/12.6 (H-16/C-16), 3.43/44.8 (H-15/C-15), 6.40/105.8 (H-5/C-5), 6.29/99.2 (H-3/C-3), 7.15/132.5 (H-6/C-6), 7.19/127.6 (H-12/C-12), 7.20/127.3 (H-m/C-m), 7.43/131.1 (H-11,13/C-11,13), 7.46/128.4 (H-o/C-o), 7.52/132.0 (H-p/C-p), 8.15/128.2 (H-10,14/C-10,14), 8.11/144.9 (H-7/C-7). COSY correlation [ $\delta_{\text{H}}/\delta_{\text{H}}$ ]: 6.29/6.40 (H-3/H-5), 7.15/6.40 (H-6/H-5), 7.46/7.20 (H-o/H-m), 8.15/7.43 (H-10,14/H-11,13).  $^{11}\text{B}$  NMR (128 MHz,  $\text{CDCl}_3$ )  $\delta$ : 7.5 ppm. APCI-MS:  $m/z$  (%): 397.90 (30) [ $\text{M}^+1$ ], 320.00 (5) [ $\text{M}^+-\text{C}_6\text{H}_5$ ], 292.30 (100) [ $\text{M}^+-\text{C}_6\text{H}_5\text{N}_2$ ], 173.00 (33), 145.10 (16), 118.40 (17), 91.20 (15), 77.00 (11), 62.70 (6). Anal. Calc. for  $\text{C}_{24}\text{H}_{24}\text{BN}_3\text{O}_2$ : C; 72.56. H; 6.09. N; 10.58, Found: C; 72.57. H; 6.34. N; 10.53.

#### 4.7.8. (*E*)- $\text{N}'$ -(4-(methoxy)-2-hydroxysalicylidine)benzohydrazidato-phenyl-boron (**8a**)



Preparation of **8a** was accomplished like that of **7a** from compound **2a** (1.0 mmol) and phenylboronic acid (1.0 mmol). Yield: 0.30 g (84%). Green solid. M.P.: 151°C.

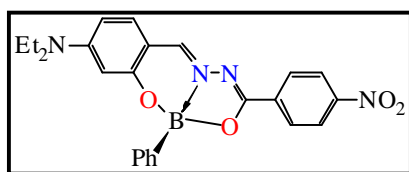
$\text{IR}_{\text{vmax}}$  (ATR): 3055, 3005, 2939, 2837, 1615, 1553, 1360, 1289, 1137, 1121, 915  $\text{cm}^{-1}$ .

UV/Vis (THF):  $\lambda_{\text{abs/max}}$ ,  $\epsilon_{\text{max}} * 10^4$ : 363 nm, 9.90  $\text{M}^{-1}\text{cm}^{-1}$ . Fluorescence (THF):  $\lambda_{\text{fluor/max}}$ :

439 nm.  $^1\text{H}$  NMR (400 MHz,  $\text{CDCl}_3$ )  $\delta$ : 3.88 (3H, s, H-15), 6.55 (1H, dd,  $J = 2.4, 8$  Hz, H-5), 6.73 (1H, d,  $J = 2$  Hz, H-3), 7.19 (1H, d,  $J = 2$  Hz, H-12), 8.17 (2H, m, H-10,14), 7.29 (1H, d,  $J = 8.8$  Hz, H-6), 7.21 (2H, m, H-11,13), 7.49 (2H, m, H-m), 7.56 (1H, m, H-p), 7.39 (2H, d,  $J = 8.4$  Hz, H-o), 8.23 (1H, s, H-7) ppm.  $^{13}\text{C}\{^1\text{H}\}$  NMR (100 MHz,

CDCl<sub>3</sub>)  $\delta$ : 55.7 (C-15), 102.9 (C-15), 109.5 (C-5), 112.0 (C-1), 158.6 (C-9), 128.5 (C-10,14), 127.5 (C-11,13), 128.5 (C-m), 132.7 (C-p) 131.1 (C-o), 128.0 (C-12), 133.5 (C-i), 132.1 (C-6), 145.2 (C-7), 158.9 (C-4), 166.9 (C-2), 171.7 (C-8) ppm. HETCOR correlation [ $\delta_{\text{H}}/\delta_{\text{C}}$ ]: 3.88/55.7 (H-15/C-15), 6.55/109.5 (H-5/C-5), 6.73/102.9 (H-3/C-3), 7.19/128.0 (H-12/C-12), 8.17/128.5 (H-10,14/C-10,14), 7.29/132.1 (H-6/C-6), 7.21/127.5 (H-11,13/C-11,13), 7.49/128.5 (H-m/C-m), 7.56/132.7 (H-p/C-p), 7.39/131.1 (H-o/C-o), 8.23/145.2 (H-7/C-7). COSY correlation [ $\delta_{\text{H}}/\delta_{\text{H}}$ ]: 6.73/6.55 (H-3/H-5), 7.49/7.56 (H-3/H-5), 7.48/7.57 (H-m/H-p), 7.21/8.17 (H-11,13/H-10,14), 7.49/7.39 (H-m/H-o). <sup>11</sup>B NMR (128 MHz, CDCl<sub>3</sub>)  $\delta$  7.7 ppm. APCI-MS: *m/z* (%): 357.20 (100) [M<sup>+</sup>1], 279.20 (60) [M<sup>+</sup>1-C<sub>6</sub>H<sub>5</sub>], 254.20 (12), 239.10 (12), 210.00 (6), 180.30 (16), 150.50 (11), 117.20 (18), 105.30 (24), 77.20 (44). Anal. Calc. for C<sub>21</sub>H<sub>17</sub>BN<sub>2</sub>O<sub>3</sub>: C; 70.81. H; 4.81. N; 7.86, Found: C; 70.05. H; 5.10. N; 8.05.

#### 4.7.9 (*E*)-N'-4-(diethylamino)-2-hydroxysalicylidine)-4-nitrobenzohydrazidato-phenyl boron (**9a**)

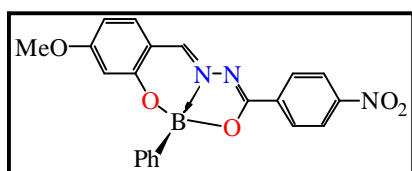


Preparation of **9a** was accomplished like that of **7a** from compound **3a** (1.0 mmol) and phenylboronic acid (1.0 mmol). Yield: 0.38 g (87%). Orange solid.

M.P.: 278 °C. IR<sub>vmax</sub> (ATR): 3028, 2972, 1610, 1593, 1342, 1245, 1185, 1144, 821, 670 cm<sup>-1</sup>. UV/Vis (THF):  $\lambda_{\text{abs/max}}$ ,  $\epsilon_{\text{max}} \cdot 10^4$ : 458 nm, 2.60 M<sup>-1</sup>cm<sup>-1</sup>. Fluorescence (THF):  $\lambda_{\text{fluor/max}}$ : 598 nm. <sup>1</sup>H NMR (400 MHz, CDCl<sub>3</sub>)  $\delta$ : 1.24 (6H, t, *J* = 7.2 Hz, H-16), 3.46 (4H, m, H-15), 6.32 (1H, dd, *J* = 2.4, 8.8 Hz, H-5), 6.39 (1H, d, *J* = 2.4 Hz, H-3), 7.17

(1H, d,  $J = 8.8$  Hz, H-6), 7.21 (1H, m, H-p), 7.22 (2H, m, H-m), 7.41 (2H, m, H-o), 7.54 (1H, d,  $J = 5.6$  Hz, H-10,14), 7.71 (2H, d,  $J = 5.6$  Hz, H-11,13), 8.15 (1H, s, H-7) ppm.  $^{13}\text{C}\{^1\text{H}\}$  NMR (100 MHz,  $\text{CDCl}_3$ )  $\delta$ : 12.6 (C-16), 44.9 (C-15), 99.1 (C-3), 106.3 (C-5), 107.8 (C-1), 149.7 (C-9), 131.0 (C-10,14), 128.9 (C-11,13), 127.5 (C-m), 127.9 (C-p), 130.8 (C-o), 134.0 (C-12), 131.3 (C-i), 132.9 (C-6), 146.1 (C-7), 155.2 (C-4), 158.9 (C-2), 167.5 (C-8) ppm.  $^1\text{H}/^{13}\text{C}$  HETCOR correlation [ $\delta_{\text{H}}/\delta_{\text{C}}$ ]: 1.24/12.6 (H-16/C-16), 3.46/44.9 (H-15/C-15), 6.39/99.1 (H-3/C-3), 6.32/106.3 (H-5/C-5), 7.22/127.5 (H-m/C-m), 7.21/127.9 (H-p/C-p), 7.41/130.8 (H-o/C-o), 7.54/131.0 (H-10,14/C-10,14), 7.71/128.9 (H-11,13/C-11,13), 7.17/132.9 (H-6/C-6), 8.15/146.1 (H-7/C-7). COSY correlation [ $\delta_{\text{H}}/\delta_{\text{H}}$ ]: 1.24/3.46 (H-16/H-15), 6.32/7.17 (H-5/H-6), 6.39/6.32 (H-3/H-5), 7.22/7.41 (H-m/H-o), 7.54/7.71 (H-10,14/H-11,13).  $^{11}\text{B}$  NMR (128 MHz,  $\text{CDCl}_3$ )  $\delta$ : 7.6 ppm. APCI-MS  $m/z$  (%): 443.00 (100) [ $\text{M}^+1$ ], 365.00 (8) [ $\text{M}^+1-\text{C}_6\text{H}_5$ ], 337.50 (78) [ $\text{M}^+1-\text{C}_6\text{H}_5\text{N}_2$ ], 319.20 (7), 291.00 (41) [ $\text{M}^+1-\text{C}_6\text{H}_5\text{N}_2\text{NO}_2$ ], 173.30 (12), 91.30 (6). Anal. Calc. for  $\text{C}_{24}\text{H}_{23}\text{BN}_4\text{O}_4$ : C; 65.18. H; 5.24. N; 12.67, Found: C; 67.22. H; 5.70. N; 11.62.

#### 4.7.10. (*E*)-*N'*-(4-(methoxy)-2-hydroxysalicylidine)-4-nitrobenzohydrazidato-phenyl boron (**10a**)

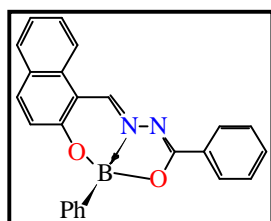


Preparation of **10a** was accomplished like that of **7a** from compound **4a** and phenylboronic acid. Yield: 0.38 g (94%). Yellow solid. M.P.: 242°C.  $\text{IR}_{\text{vmax}}$

(ATR): 3019, 3056, 1612, 1536, 1342, 1228, 1176, 1025, 701  $\text{cm}^{-1}$ . UV/Vis (THF):  $\lambda_{\text{abs/max}}$ ,  $\epsilon_{\text{max}} \cdot 10^4$ : 412 nm, 2.90  $\text{M}^{-1}\text{cm}^{-1}$ . Fluorescence (THF):  $\lambda_{\text{fluor/max}}$ : 502 nm.  $^1\text{H}$

NMR (400 MHz, DMSO- $d_6$ )  $\delta$  3.88 (3H, s, H-15), 6.70 (1H, sa, H-3), 6.79 (1H, dd,  $J = 2.4, 8.0$  Hz, H-5), 7.24 (2H, st,  $J = 8.0$  Hz, H-p), 7.18 (1H, m, H-m), 7.60 (1H, d,  $J = 8.0$  Hz, H-6), 8.32 (2H, d,  $J = 8.0$  Hz, H-10,14), 7.78 (2H, d,  $J = 8.0$  Hz, H-o), 8.38 (2H, d,  $J = 8.0$  Hz, H-11,13), 9.01 (1H, s, H-7) ppm.  $^{13}\text{C}\{^1\text{H}\}$  NMR (100 MHz, DMSO- $d_6$ )  $\delta$  56.0 (C-15), 102.8 (C-3), 109.4 (C-5), 111.1 (C-1), 149.9 (C-9), 124.2 (C-10,14), 129.3 (C-11,13), 127.6 (C-m), 130.6 (C-p), 134.0 (C-o), 138.6 (C-12), 132.5 (C-i), 133.7 (C-6), 149.4 (C-7), 158.0 (C-4), 162.3 (C-2), 168.5 (C-8) ppm. HETCOR correlation [ $\delta_{\text{H}}/\delta_{\text{C}}$ ]: 3.88/56.0 (H-15/C-15), 6.70/102.8 (H-3/C-3), 6.79/109.4 (C-5), 7.18/127.6 (H-m/C-m), 7.24/130.6 (H-p/C-p), 7.60/133.7 (H-6/C-6), 8.32/124.2 (H-10,14/C-10,14), 7.78/134.0 (C-o), 8.38/129.3 (H-11,13/C-11,13), 9.01/149.4 (H-7/C-7).  $^1\text{H}/^1\text{H}$  COSY correlation [ $\delta_{\text{H}}/\delta_{\text{H}}$ ]: 6.70/6.79 (H-3/H-5), 6.79/7.60 (H-5/H-6), 7.18/7.24 (H-m/H-p).  $^{11}\text{B}$  NMR (128 MHz,  $\text{CDCl}_3$ )  $\delta$  7.9 ppm. APCI-MS  $m/z$  (%): 402.50 (100) [ $\text{M}^+1$ ], 324.10 (53) [ $\text{M}^+1-\text{C}_6\text{H}_5$ ], 283.40 (33) [ $\text{M}^+1-\text{C}_6\text{H}_5\text{CHN}_2$ ], 277.80 (47) [ $\text{M}^+1-\text{C}_6\text{H}_5\text{CHN}_2\text{NO}_2$ ], 238.60 (13), 235.00 (13), 160.20 (20), 117.30 (16), 95.20 (16), 77.20 (22). Anal. Calc. for  $\text{C}_{21}\text{H}_{16}\text{BN}_3\text{O}_5$ : C; 62.87. H; 4.02. N; 10.47, Found: C; 62.60. H; 4.14. N; 10.02.

#### 4.7.11. (E)-(2-hydroxy-1-naphthalidene)benzohydrazidato-phenyl-boron (11a)



Preparation of **11a** was accomplished like that of **7a** from compound **5a** and phenylboronic acid. Yield: 0.33 g (89%).

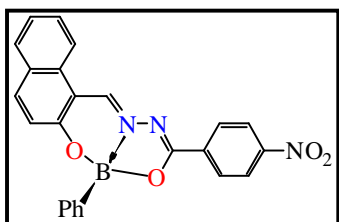
Yellow solid. M.P.: 302 °C. UV/Vis ( $\text{CHCl}_3$ ):  $\lambda_{\text{abs/max}}$ ,  $\epsilon_{\text{max}} \cdot 10^4$ : 426 [345] nm, 3.47 [3.11]  $\text{M}^{-1}\text{cm}^{-1}$ .  $^1\text{H}$  NMR (400

MHz, DMSO- $d_6$ )  $\delta$  7.20 (1H, sa, H-3), 7.21 (2H, sa, H-15,17), 7.41 (1H, st,  $J=8$  Hz, H-

7), 7.43 (1H, sa, H-m), 7.45 (1H, d,  $J = 1.6$  Hz, H-p), 7.52 (2H, t,  $J = 7.6$  Hz, H-14, 18), 7.57 (1H, st,  $J = 7.5$  Hz, H-8), 7.59 (1H, m, H-16), 7.80 (1H, d,  $J = 8.4$  Hz, H-6), 7.84 (1H, d,  $J = 8.4$  Hz, H-4), 8.03 (1H, d,  $J = 8.8$  Hz, H-9), 8.25 (2H, d,  $J = 7.2$  Hz, H-o), 8.85 (1H, s, H-11) ppm.  $^{13}\text{C}\{^1\text{H}\}$  NMR (100 MHz, DMSO- $d_6$ )  $\delta$ : 112.04 (C-1), 120.62 (C-p), 121.03 (C-4), 124.91 (C-7), 127.40 (C-5), 127.68 (C-15,17), 128.32 (C-3), 128.42 (C-10), 128.76 (C-o,14,18), 128.84 (C-i), 128.97 (C-8), 129.27 (C-6), 131.45 (C-m), 131.53 (C-13), 132.98 (C-16), 138.33 (C-9), 142.71 (C-11), 156.79 (C-2), 171.85 (C-12) ppm. HETCOR correlation [ $\delta_{\text{H}}/\delta_{\text{C}}$ ]: 7.20/128.32 (H-3/C-3), 7.21/127.68 (H-15,17/C-15,17), 7.41/124.91 (H-7/C-7), 7.43/131.45 (H-m/C-m), 7.45/120.64 (H-p/C-p), 7.52/128.76 (H-14,18/C-14,18), 7.57/128.97 (H-8/C-8), 7.59/132.98 (H-16/C-16), 7.80/129.27 (H-6/C-6), 7.84/121.03 (H-4/C-4), 8.03/138.33 (H-9/C-9), 8.25/128.76 (H-o/C-o), 8.85/142.11 (H-11/C-11), ppm. COSY correlation [ $\delta_{\text{H}}/\delta_{\text{H}}$ ]: 7.20/7.84 (H-3/H-4), 7.80/7.41 (H-6/H-7), 7.57/8.03 (H-8/H-9), 7.52/7.21 (H-14,18/H-15,17), 7.21/7.59 (H-15,17/H-16) ppm.  $^{11}\text{B}$  NMR (128 MHz,  $\text{CDCl}_3$ )  $\delta$ : 7.6 ppm. . Anal. Calc. for  $\text{C}_{24}\text{H}_{17}\text{BN}_2\text{O}_2$ : C; 76.62. H; 4.55. N; 7.45, Found: C; 76.66. H; 4.83. N; 7.61; TOF-MS calc. for  $[(\text{C}_{24}\text{H}_{17}\text{N}_2\text{O}_2\text{B}+\text{H})^+]$ : 376.1400 u.m.a; Exp.: 377.1467 u.m.a (Error = 1.25 ppm).

#### 4.7.12. (*E*)-(2-hydroxy-1-naphthalidene)4-nitro-benzohydrazidato-phenyl-boron

(12a)



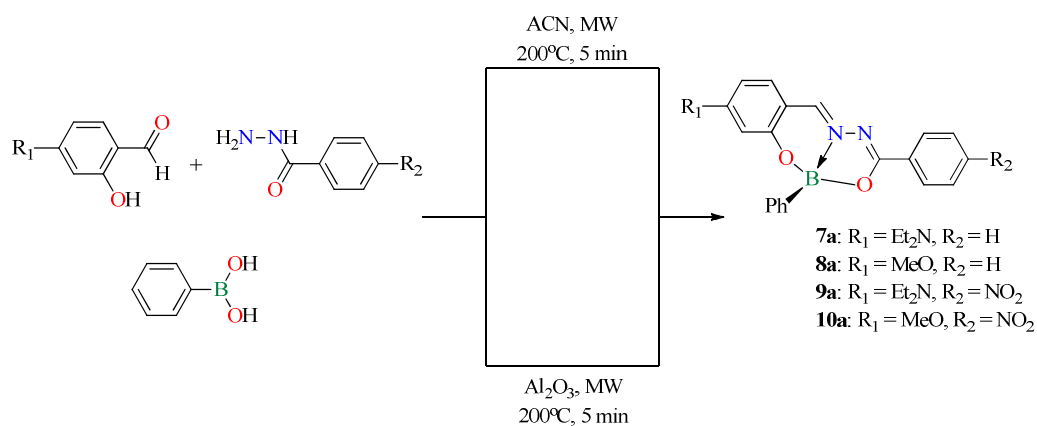
Preparation of **12a** was accomplished like that of **7a** from compound **6a** and phenylboronic acid. Yield: 0.38 g (90 %).

Orange solid. M.P.: 326 °C. UV/Vis (CHCl<sub>3</sub>):  $\lambda_{\text{abs/max}}$ ,  $\epsilon_{\text{max}} * 10^4$ : 441 [350] nm, 1.89 [1.51] M<sup>-1</sup>cm<sup>-1</sup>. Fluorescence

(THF):  $\lambda_{\text{fluor/max}}$ : 407 nm. <sup>1</sup>H NMR (400 MHz, DMSO-*d*<sub>6</sub>)  $\delta$ : 7.20 (2H, m, H-m), 7.22 (1H, m, H-p), 7.39 (1H, m, H-o), 7.43 (1H, d, *J* = 9.2 Hz, H-3), 7.47 (1H, st, *J* = 7.6 Hz, H-7), 7.62 (1H, t, *J* = 7.6 Hz, H-8), 7.83 (1H, d, *J* = 8.0 Hz, H-6), 7.89 (1H, d, *J* = 8.4 Hz, H-4), 8.08 (1H, d, *J* = 9.2 Hz, H-9), 8.34 (2H, d, *J* = 8.8 Hz, H-15,17), 8.38 (2H, d, *J* = 8.4 Hz, H-14,18), 8.92 (1H, s, H-11) ppm. <sup>13</sup>C{<sup>1</sup>H} NMR (100 MHz, DMSO-*d*<sub>6</sub>)  $\delta$ : 112.12 (C-1), 120.61 (C-3), 121.13 (C-4), 123.94 (C-15,17), 125.29 (C-7), 127.81 (C-m), 128.55 (C-5), 128.60 (C-p), 129.37 (C-8), 129.49 (C-6), 129.67 (C-14,18), 131.34 (C-o), 131.40 (C-i), 131.59 (C-10), 133.34 (C-13), 139.37 (C-9), 144.27 (C-11), 150.41 (C-16), 157.20 (C-2), 169.55 (C-12) ppm. HETCOR correlation [ $\delta_{\text{H}}/\delta_{\text{C}}$ ]: 7.20/127.81 (H-m/C-m), 7.22/128.60 (H-p/C-p), 7.39/131.34 (H-o/C-o), 7.43/120.61 (H-3/C-3), 7.47/125.29 (H-7/C-7), 7.62/129.37 (H-8/C-8), 7.83/129.49 (H-6/C-6), 7.89/121.13 (H-4/C-4), 8.08/139.37 (H-9/C-9), 8.34/123.94 (H-15,17/C-15,17), 8.38/129.67 (H-14,18/C-14,18), 8.92/144.27 (H-11/C-11) ppm. COSY correlation [ $\delta_{\text{H}}/\delta_{\text{H}}$ ]: 7.43/7.89 (H-3/H-4), 7.83/7.47 (H-6/H-7), 7.62/8.08 (H-8/H-9), 8.38/8.34 (H-14,18/H-15,17) ppm.

## 4.8 Synthesis under microwave irradiation

The organoboron compounds **7-10** were synthesized under microwave irradiation for two different methods for comparison purposes as is indicated in the **Scheme 15** shown below.



**Scheme 15.** Synthesis under microwave irradiation of compounds **7-10**.

### 4.8.1. Method A. Synthesis under microwave irradiation using an organic solvent, exemplified with **7a**.

A solution of 4-diethylaminosalicylaldehyde 0.050 g (0.260 mmol), benzoylhydrazide 0.035 (0.260 mmol) and phenylboronic acid 0.320 g (0.260 mmol) in acetonitrile was irradiated at 200 °C for 5 min. The progress of the reaction was monitored by thin layer chromatography. After cooling to room temperature, the excess solvent was removed and the solid precipitate was filtered and washed with hexane.

#### **4.8.2. Method B. Synthesis under microwave irradiation free-solvent using an inorganic solid support, exemplified with 7a.**

A homogeneous mixture of 4-diethylaminosalicylaldehyde 0.050 g (0.26 mmol), benzoylhydrazide 0.035 (0.26 mmol), phenylboronic acid 0.320 g (0.26 mmol), and 0.200 g (1.96 mmol) alumina free-solvent was irradiated at 200 °C for 5 min. The alumina was previously activated at 210°C for 3 min. After cooling, the solid support was eliminated, and the product was precipitated and washed with hexane.

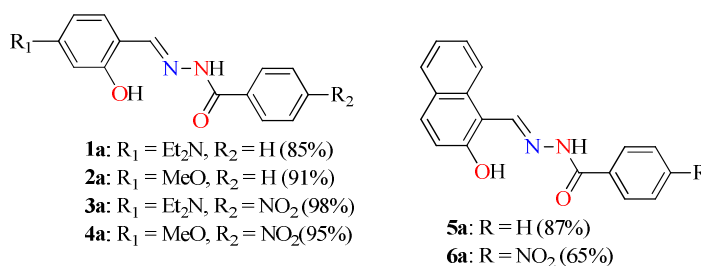
#### **4.8.3. Disposal of hazardous waste**

The organic waste generated in the condensation reactions: dimethylformamide, benzene, acetonitrile, as well as for the work up: hexane, acetone, ethyl acetate, were collected in the **container C**, which is assigned for halogen free-solvents. The alumina impregnated with organic material and solvent mixture containing waste of chloroform and dichloromethane were collected in the **containers B and D**, both assigned for solid inorganic waste and halogen containing solvents, respectively.

## RESULTS AND DISCUSSION

### 5.1. Synthesis.

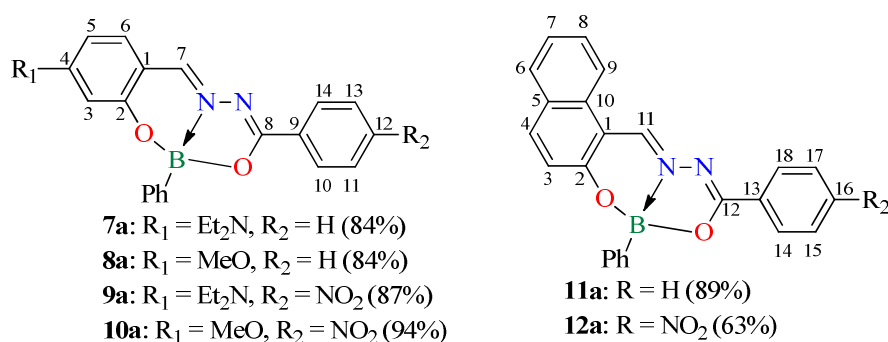
First of all, we carry out the synthesis of Schiff bases **1a-6a** (Scheme 16) by condensation reaction of the appropriate salicylaldehyde or naphthaldehyde with the corresponding benzohydrazides in benzene or dimethylformamide for 48 h and 10 min, respectively. The Schiff bases were isolated with good yields (85-98 %).



**Scheme 16.** Synthesis of Schiff bases **1a-6a**.

Consequently, their phenyl boron derivatives **7a-12a** (Scheme 17) were prepared by condensation of phenylboronic acid under reflux in benzene. The products were obtained as yellow, green, white and orange powders after filtration of the crude reaction and precipitation using hexane, where all compounds were soluble in common organic

solvents such as dichloromethane, chloroform, and acetone, while **6a** and **9a** were insoluble. Important to mention, all compounds were stable in solid-state however, compound **9a** in THF was unstable for one week resulting the free ligand (**3a**); which was evidenced by UV-vis.



**Scheme 17.** Synthesis of organic compounds derived from Schiff bases **7a-12a**.

In all the cases, the organoboron compounds were obtained in good yields after 48 h. Better yields and time reactions were determined for boron compounds **7a-10a** when the microwave irradiation are used. A comparison about both methods are summarized on **table 1**.

**Table 1.** Comparison of the time reaction and yields from different methods of compounds **7a-10a**.

Compound	Yield [%]			Reaction time [h]		
	Solution	Microwave		Solution	Microwave	
		Solvent	Free-solvent		Solvent	Free-solvent
<b>7a</b>	84	95	71	48	5	
<b>8a</b>	84	96	83			
<b>9a</b>	87	94	80			
<b>10a</b>	94	97	88			

The reactions *via* microwave irradiation proceeded very fast and cleanly, and reaction yields were increased around of 71 to 97 %. The most important change was given in reaction time, which decreased around of 570 times in comparison with the conventional synthesis.

## 5.2. Chemical structure elucidation.

<sup>1</sup>H-NMR spectra confirmed the formation of the Schiff bases **1a-6a** (See Appendix), with signals for H-7 and H-11 in the range 8.44 to 9.49 ppm, typical of an imine proton (**Table 2**), which are according to reported by Santillan *et al.* for salicylideneiminophenols.<sup>52</sup> The presence of two sharp singlets at high frequency in the range 12.02 to 12.83 ppm and 11.30 to 12.48 ppm were assigned to OH and NH protons, respectively. These signals are observed in the high  $\delta$  values due to they are attached to highly electronegative atoms oxygen and nitrogen. As example the figure **4** shows the <sup>1</sup>H NMR spectrum for the free-ligand **1a**.

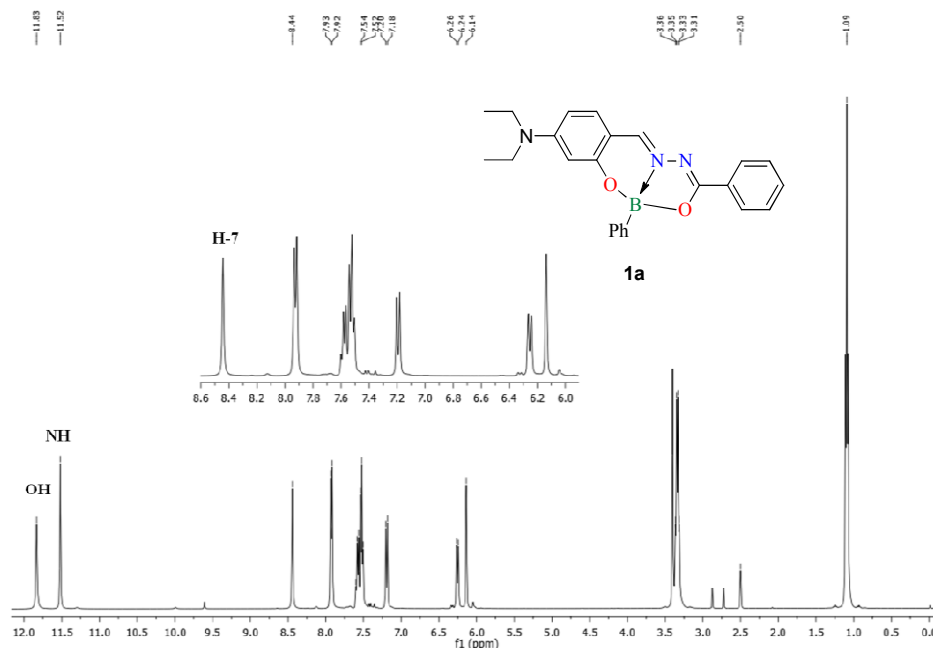


**Figure 4.**  $^1\text{H}$  NMR spectrum of free ligand **1a** in dimethyl sulfoxide- $d_6$ .

**Table 2.** Selected  $^1\text{H}$ ,  $^{11}\text{B}$ ,  $^{13}\text{C}$  NMR (ppm) and IR ( $\text{cm}^{-1}$ ) data for compounds **1a-6a** and **7a-12a**

Comp.	$^1\text{H}$ (H-7)	$^{13}\text{C}$				$^{11}\text{B}$	IR C=N
		C-2	C-4/C-9	C-7/C-11	C-8/C-12		
<b>1a</b>	8.44	159.8	150.1	150.0	162.2	-	1587
<b>2a</b>	8.55	162.1	159.4	148.8	162.6	-	1601
<b>3a</b>	8.45	159.8	150.4	150.7	160.5	-	1590
<b>4a</b>	8.58	160.9	159.4	149.3	162.3	-	1598
<b>5a</b>	9.49	157.9	120.6	146.8	162.5	-	1576
<b>6a</b>	9.48	158.1	120.9	147.9	160.9	-	1597
<b>7a</b>	8.11	167.7	158.4	144.9	169.9	7.5	1528
<b>8a</b>	8.23	166.9	158.9	145.2	171.7	7.7	1553
<b>9a</b>	8.15	158.9	155.2	146.1	167.5	7.6	1593
<b>10a</b>	9.01	162.3	158.0	149.4	168.5	7.9	1536
<b>11a</b>	8.85	156.8	138.3	142.7	171.9	7.6	*
<b>12a</b>	8.92	157.2	139.4	144.3	169.6	*	*

\* It was not possible to determine

The existence of the N $\rightarrow$ B coordination bond was evidenced by  $^{11}\text{B}$  NMR spectra for the compounds **7a-11a**. For example, one broad signal between 7.5 and 7.9

ppm indicative of tetracoordinated boron atoms (**Table 3**).<sup>53</sup> Also the  $^{11}\text{B}$  resonances of **7a-11a**, except **12a** due to it was not possible to determine, are shifted to lower frequencies with respect to phenylboronic acid ( $^{11}\text{B} = 9.3 \text{ ppm}$ )<sup>54</sup> by increasing the electron density on boron atoms, as a example the figure 5 shows the  $^{11}\text{B}$  spectrum for the boron compound **7a**.

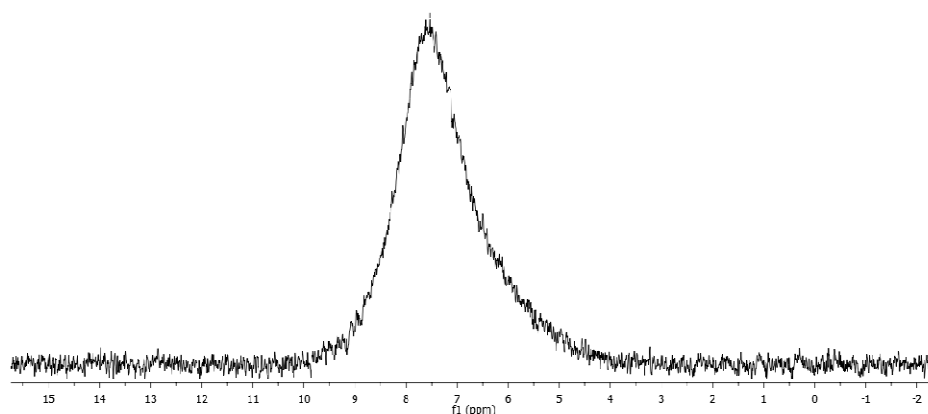
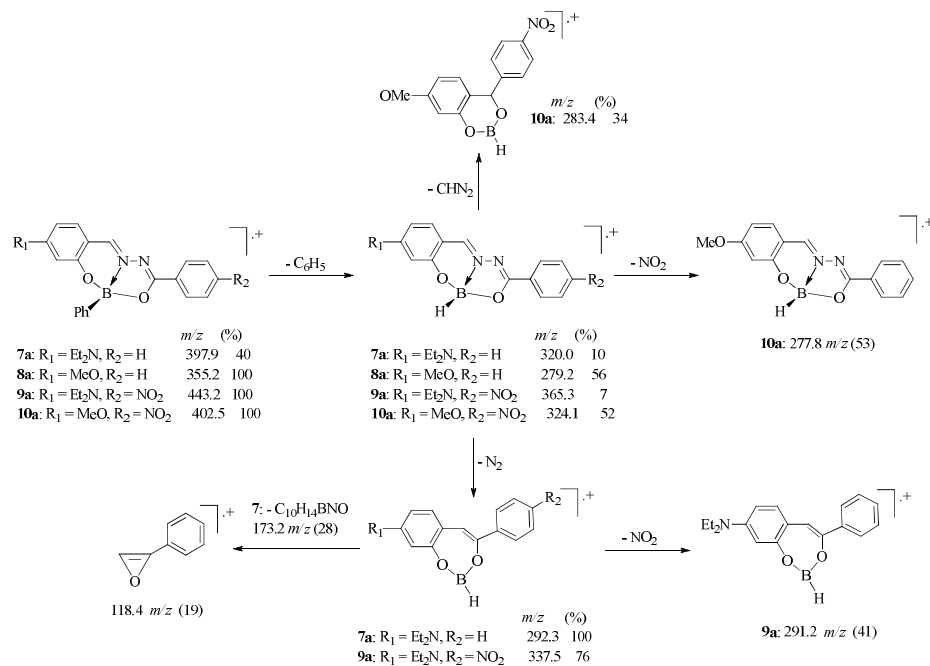


**Figure 5.**  $^{11}\text{B}$  NMR spectrum of boron compound **7a** in dimethyl sulfoxide- $d_6$ .

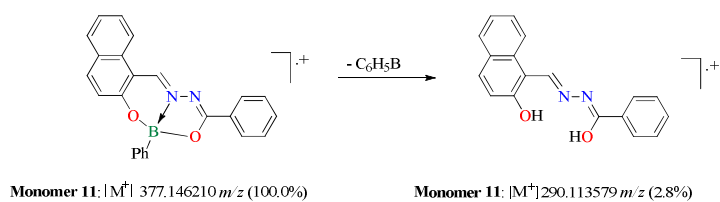
In the  $^{13}\text{C}$  NMR spectra of boron derivatives **7a-12a**, the signals for C-7 and C-11 (C=N) are shifted to low frequencies (144.9-149.4 ppm), with respect to the ligands (148.8-150.7 ppm) owing to the coordination to boron. In the solid state the IR spectral analysis showed that the C=N stretching vibration bands for compounds **7a-10a** were shifted to lower wavenumbers in comparison with the ligands, demonstrating a decrease in strength as the new dative bond is formed.<sup>55</sup> The mass spectra of boron derivatives showed first a mass loss corresponds to the phenyl group bonded to the boron atom (**Scheme 18**). Also, the base peak corresponding to the molecular ion peak for **8a-10a**, while **7a** showed a base peak after loss of the arylboron fragment and nitrogen.<sup>56</sup> The

presence of the base peak of the boron compounds are consistent with the theoretical molecular mass.



**Scheme 18.** Proposed fragmentation of boron compounds **7a-10a**.

In the case of boron compound **11a**, the high resolution mass spectrum confirm the expected molecular ion peak (377.146210 u.m.a), and as a characteristic of the molecular structure, the base peak corresponds to the loss of the phenyl group fragment bonded to the boron atom (**Scheme 19**).



**Scheme 19.** Proposed fragmentation of compound **11a**

The elemental analysis data of the Schiff bases and their boron compounds are given in the **table 3**. The results of elemental analysis for **C**, **H** and **N** obtained are in good agreement with those calculated for the suggested formula, indicating the purity of the Schiff bases **1a-2a**, and the boron compounds **7a**, **10a-12a**. In the case of the free ligand **6a**, the elemental analysis shows a great deviation in comparison with those calculated due to the presence of the hydrazine used as precursor in the condensation reaction, which was corroborated by NMR spectroscopy. For the boron compound **8a** is observed a slight deviation of 0.8 % in the percentage of carbon found in comparison with the calculated value, this behavior is attributed to the presence of a molecule of water in the molecular structure. Unfortunately, it was not possible to obtain the crystal structure due to the low stability in solution for this molecule but the thermal analysis confirms the presence of an endothermic peak attributed to dehydration process. In the case of boron compounds **9a** is observed a deviation of 2% in the percentage of experimental carbon in comparison with found value due to the presence in small amount of free ligand **4a**, which is confirmed by the NMR spectroscopy.

**Table 3.**  
Elemental analysis of compounds of free ligands **1a, 2a, 6a** and boron compounds **7a-12a**

Comp.	Formula	Calc. (%)			Found (%)		
		C	H	N	C	H	N
<b>1<sup>a</sup></b>	C <sub>18</sub> H <sub>21</sub> N <sub>3</sub> O <sub>2</sub>	69.43	6.80	13.49	69.44	7.06	13.57
<b>2<sup>a</sup></b>	C <sub>15</sub> H <sub>14</sub> N <sub>2</sub> O <sub>3</sub> · H <sub>2</sub> O	62.49	5.59	9.72	62.69	5.82	9.51
<b>6<sup>a</sup></b>	C <sub>18</sub> H <sub>13</sub> N <sub>3</sub> O <sub>4</sub>	64.50	3.90	12.50	55.34	4.04	17.47
<b>7<sup>a</sup></b>	C <sub>24</sub> H <sub>24</sub> BN <sub>3</sub> O <sub>2</sub>	72.56	6.09	10.58	72.57	6.34	10.53
<b>8<sup>a</sup></b>	C <sub>21</sub> H <sub>17</sub> BN <sub>2</sub> O <sub>3</sub>	70.81	4.81	7.86	70.05	5.10	8.05
<b>9<sup>a</sup></b>	C <sub>24</sub> H <sub>23</sub> BN <sub>4</sub> O <sub>4</sub>	65.18	5.24	12.67	67.22	5.70	11.62
<b>10<sup>a</sup></b>	C <sub>21</sub> H <sub>16</sub> BN <sub>3</sub> O <sub>5</sub>	62.87	4.02	10.47	62.60	4.14	10.02
<b>11<sup>a</sup></b>	C <sub>24</sub> H <sub>17</sub> BN <sub>2</sub> O <sub>2</sub>	76.62	4.55	7.45	76.66	4.83	7.61
<b>12<sup>a</sup></b>	C <sub>24</sub> H <sub>16</sub> BN <sub>3</sub> O <sub>4</sub>	68.39	3.80	9.97	68.70	3.94	9.73

\* The measurements were carried out by duplicated.

### 5.3. X-ray analysis

The structures of compounds **1a**, **2a**, **7a**, **8a** and **12a** are represented by the thermal ellipsoid plots in **figures 6, 7 and 8**. Selected bond distances and angles are listed in **table 6 and 7**. Compounds **1a**, **2a**, and **8a** belong to the monoclinic space group *P2<sub>1</sub>/c*, **7a** to the orthorhombic space group *Pna2<sub>1</sub>* and **12a** to the triclinic space group *P-1* (**table 4 and 5**). Boron compounds **7a**, **8a** and **12a** are chemically similar but crystallographically different molecules in the asymmetric unit. In the case of compound **2a**, a molecule of water is present in the asymmetric unit cell (see **Appendix**).

The crystal structures of **7a**, **8a**, **12a** show the molecules contain a tetra-coordinated boron atom, and the formation of three-ring-fused skeletons with N→B

coordination bond with lengths of 1.561(19), 1.571(16) and 1.564(19) Å, respectively. Boron atoms adopt tetrahedral geometry. The tetrahedral character of both boron atoms are 82.1, 82.7 and 99.7 %, <sup>57</sup>, which does not allow the total planar array, therefore the delocalization of the  $\pi$ -system is not optimal. For compounds **7a** and **8a** the bond lengths of B–O are 1.512(2);1.468(2), and 1.504(2);1.457(2) Å, respectively, whereas bond lengths for compound **12a** are 1.503(2) Å and 1.467(2) Å, which are similar to those of the organoboron complex previously reported.<sup>58</sup> The C=O bond lengths for **1a** and **2a** are 1.236(1) and 1.241(2) Å, respectively, which suggest they are in the keto form while in **7a**, **8a** and **12a** are closer to single bonds [**7a**: 1.339(2), **8a**: 1.334(1) and **12a**: 1.332(2) Å] due to the formation of new B–O bond. The crystal structures of **1a** and **2a** are stabilized by OH...N intramolecular hydrogen bonds.

It is worth noting that compound **8a** has a more planar structure than **7a** and **12a**, this is deduced from the dihedral angles between the two aromatic rings present in the molecules, which is 16.9° for **7a**, 6.2° for **8a** and 7.2° for **12a**. Undeniably, the boron atoms in both derivatives have great deviations ( $\theta$ ) from the salicylidenimino or naphthalidenimino -plane, 0.488 Å for **7a**, 0.749 Å for **8a** and 0.333 Å for **12a** (Scheme 20). It is likely that these parameters might affect the luminescent response as well as has been reported for the nonlinear optical properties.<sup>68</sup>

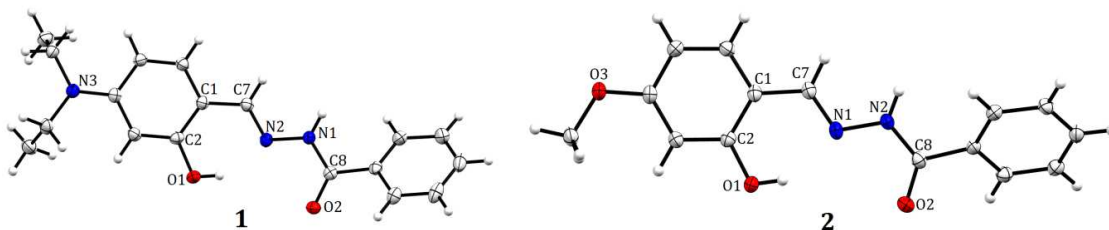


**Figure 6.** X-ray molecular structures of **1a** and **2a**. The anisotropic displacement parameters are depicted at the 50% probability level.

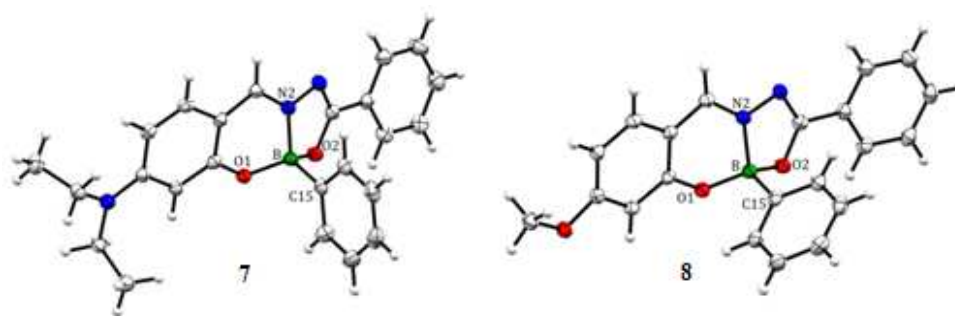


**Figure 7.** X-ray molecular structures of **7a** and **8a**. The anisotropic displacement parameters are depicted at the 50% probability level.

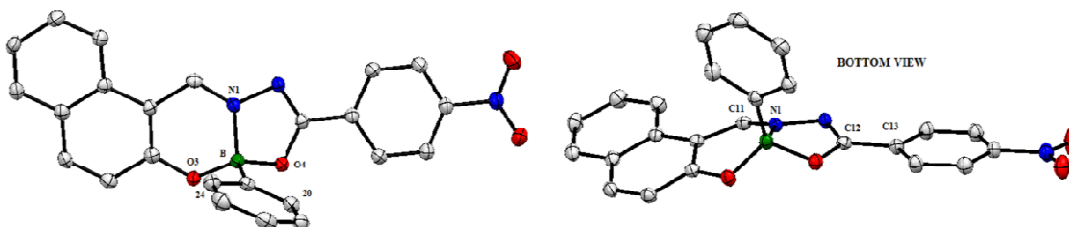
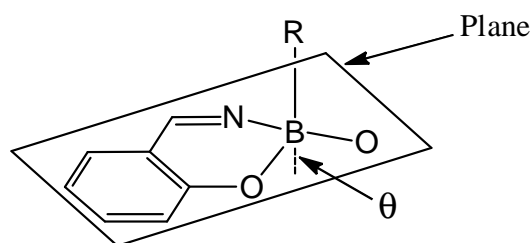


**Figure 8.** Molecular structure of **12a**. The anisotropic displacement parameters are depicted at the 30% probability level. Hydrogens were omitted by clarity.



**Scheme 20.** Deviation ( $\theta$ ) of the boron atom from the salicylideneimino/or naphthalidenimino-plane in compounds **7a**, **8a** and **12a**.

**Table 4.** Crystal data for compounds **1a**, **2a**, **7a**, and **8a**

	<b>1a</b>	<b>2a</b>	<b>7a</b>	<b>8a</b>
Empirical formula	C <sub>18</sub> H <sub>21</sub> N <sub>3</sub> O <sub>2</sub>	C <sub>15</sub> H <sub>14</sub> N <sub>2</sub> O <sub>3</sub> •H <sub>2</sub> O	C <sub>24</sub> H <sub>24</sub> BN <sub>3</sub> O <sub>2</sub>	C <sub>21</sub> H <sub>17</sub> BN <sub>2</sub> O <sub>3</sub>
Formula weight	311.16	288.10	397.20	356.13
Temperature, K	100(2)	100(2)	100(2)	100(2)
Wavelength	0.71073	0.71073	0.71073	0.71073
Crystal system	Monoclinic	Monoclinic	Orthorhombic	Monoclinic
Space group	<i>P</i> 2(1)/ <i>c</i>	<i>P</i> 2(1)/ <i>c</i>	<i>P</i> na2(1)	<i>P</i> 2(1)/ <i>c</i>
<b>Cell parameters</b>				
<i>a</i> , Å	10.6640(17)	15.245(6)	26.669(3)	9.0760(8)
<i>b</i> , Å	15.995(3)	7.292(3)	20.082(2)	7.8167(7)
<i>c</i> , Å	9.6691(15)	12.308(4)	7.8617(8)	24.901(2)
$\alpha$	90.00°	90.00°	90.00°	90.00
$\beta$	100.982(2)°	91.625(4)°	90.00°	98.717(1)
$\gamma$	90.00°	90.00°	90.00°	90.00
<i>V</i> , Å <sup>3</sup>	1619.1(4)	1367.5(8)	4210.4(8)	1746.2(3)
<i>Z</i>	4	4	8	4
$\rho_{\text{calc}}$ , mg.cm <sup>-3</sup>	1.277	1.400	1.253	1.355
$\mu$ , mm <sup>-1</sup>	0.085	0.103	0.080	0.091
<b>Data collection</b>				
2 $\theta$ range for data collection	1.95 – 28.34°	1.34 – 28.32°	1.27-28.32°	1.65-28.30°
Index ranges	-14 ≤ <i>h</i> ≤ 14,	-20 ≤ <i>h</i> ≤ 20	-35 ≤ <i>h</i> ≤ 35	-12 ≤ <i>h</i> ≤ 12
	-21 ≤ <i>k</i> ≤ 21,	-9 ≤ <i>k</i> ≤ 9	-26 ≤ <i>k</i> ≤ 26	-10 ≤ <i>k</i> ≤ 10
	-12 ≤ <i>l</i> ≤ 12	-16 ≤ <i>l</i> ≤ 16	-10 ≤ <i>l</i> ≤ 10	-33 ≤ <i>l</i> ≤ 32
No. of reflns collected	15745	13007	40824	16683
No. of indep reflns	4022	3410	10403	4337
<b>Refinement</b>				
[ <i>R</i> <sub>int</sub> ]	0.0278	0.0315	0.0336	0.0267
Goodness of fit	1.057	1.056	1.042	1.064
<i>R</i> 1, <i>wR</i> 2 ( <i>I</i> > 2 $\sigma$ ( <i>I</i> ))	0.0482/0.1318	0.0441/0.1207	0.0427/0.1011	0.0485/0.1219
<i>R</i> 1, <i>wR</i> 2 (all data)	0.0540/0.1387	0.0508/0.1283	0.0469/0.1045	0.0543/0.1295

**Table 5.** Crystal data for compound **12a**.

<b>12a</b>	
Empirical formula	C <sub>24</sub> H <sub>16</sub> N <sub>3</sub> O <sub>4</sub> B
Formula weight	421.21
Temperature, K	100(2)
Wavelength	0.71073
Crystal system	Triclinic
Space group	<i>P</i> -1
<b>Cell parameters</b>	
<i>a</i> , Å	9.0240(2)
<i>b</i> , Å	10.0680(2)
<i>c</i> , Å	11.3830(3)
$\alpha$	85.895(3) <sup>o</sup>
$\beta$	80.342(3) <sup>o</sup>
$\gamma$	76.498(3) <sup>o</sup>
<i>V</i> , Å <sup>3</sup>	990.80(4)
<i>Z</i>	2
$\rho_{\text{calc}}$ , mg.cm <sup>-3</sup>	1.412
$\mu$ , mm <sup>-1</sup>	0.097
<b>Data collection</b>	
2 $\theta$ range for data collection	2.35 – 28.19 <sup>o</sup>
Index ranges	-12 ≤ <i>h</i> ≤ 11 -21 ≤ <i>k</i> ≤ 21, -12 ≤ <i>l</i> ≤ 12
No. of reflns collected	4876
No. of indep reflns	3694
<b>Refinement</b>	
[ <i>R</i> <sub>int</sub> ]	0.0362
Goodness of fit	1.074
<i>R</i> 1, <i>wR</i> 2 ( <i>I</i> > 2 $\sigma$ ( <i>I</i> ))	0.0531/0.0699
<i>R</i> 1, <i>wR</i> 2 (all data)	0.1357/0.1480

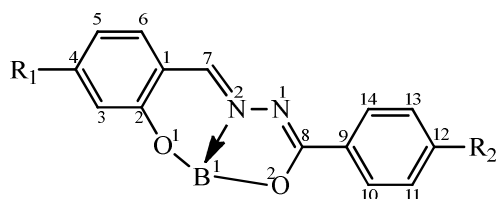


**Table 6.** Selected bond distances (°) and angles (deg) for **1a-2a** and **7a-8a**.

	<b>1a</b>	<b>2a</b>	<b>7a</b>	<b>8a</b>
B(1)- N(2)			1.561(2)	1.571(2)
B(1)-O(2)			1.512(2)	1.504(2)
B(1)-O(1)			1.468(2)	1.457(2)
B(1)-C(15)			1.603(2)	1.610(2)
C(1)-O(2)	1.364(1)	1.355(2)	1.355(2)	1.365(1)
N(2)-C(7)	1.297(1)	1.289(2)	1.294(2)	1.287(2)
N(2)-N(1)	1.388(1)	1.386(13)	1.402(2)	1.395(1)
N(1)-C(8)	1.236(1)	1.343(2)	1.305(2)	1.312(2)
C(10)-C(11)	1.393(2)	1.393(2)	1.389(2)	1.386(2)
C(11)-C(12)	1.390(2)	1.387(2)	1.390(2)	1.393(2)
C(12)-C(13)	1.388(2)	1.392(2)	1.390(2)	1.385(2)
C(13)-C(14)	1.387(2)	1.388(2)	1.388(2)	1.395(2)
O(2)-C(8)	1.236(1)	1.241(2)	1.339(2)	1.334(1)
O(2)-B(1)-N(2)			96.34(10)	96.34(9)
O(2)-B(1)-C(15)			109.86(11)	110.92(9)
O(1)-B(1)-N(2)			107.81(11)	107.19(9)
O(1)-B(1)-C(15)			114.85(12)	113.08(10)
C(8)-N(1)-N(2)	118.14(9)	119.62(10)	102.98(11)	103.05(9)
C(14)-C(13)-C(12)	120.02(13)	119.91(11)	120.00(15)	119.95(12)
N(1)-C(8)-O(2)	122.46(10)	124.03(11)	119.58(13)	119.46(11)
O(2)-C(8)-C(9)	121.84(10)	119.65(11)	118.55(12)	118.82(10)
N(1)-C(8)-C(9)	115.68(9)	116.32(10)	121.87(12)	121.62(11)
C(10)-C(11)-C(12)	119.78(12)	120.21(11)	120.28(14)	119.80(12)

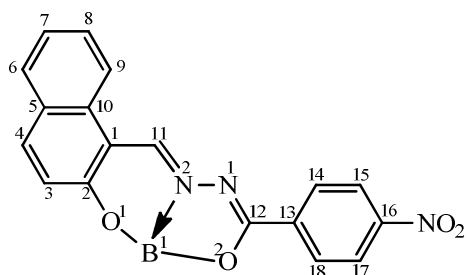


**Table 7.** Selected bond distances ( $^{\circ}$ ) and angles (deg) for **12a**.

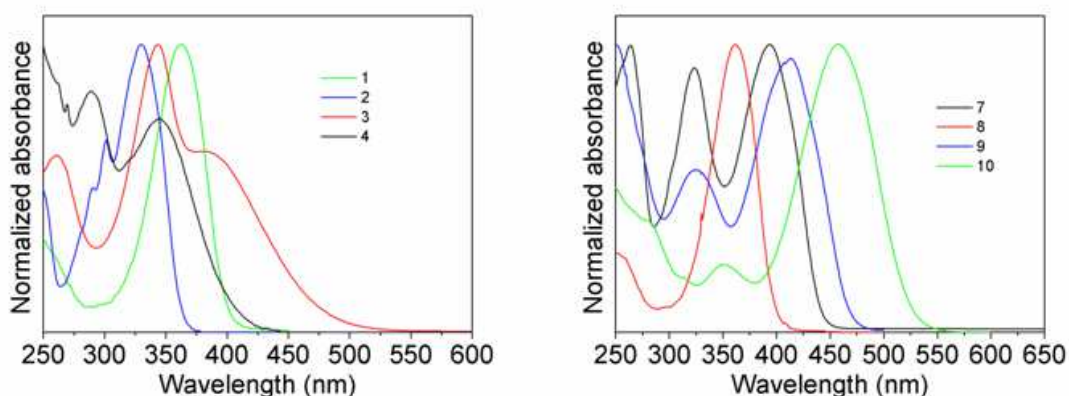
<b>12a</b>	
B(1)-N(2)	1.565(2)
B(1)-O(2)	1.467(2)
B(1)-O(1)	1.503(2)
B(1)-C(19)	1.605(2)
C(2)-O(1)	1.346(2)
N(2)-C(11)	1.287(2)
N(2)-N(1)	1.405(2)
N(1)-C(12)	1.305(2)
C(14)-C(15)	1.308(2)
C(15)-C(16)	1.384(2)
C(16)-C(17)	1.382(2)
C(17)-C(18)	1.386(2)
O(2)-C(12)	1.332(2)
O(2)-B(1)-N(2)	96.66(10)
O(2)-B(1)-C(19)	110.51(11)
O(1)-B(1)-N(2)	106.14(11)
O(1)-B(1)-C(19)	114.21(12)
C(12)-N(1)-N(2)	102.68(11)
C(18)-C(17)-C(16)	117.94.12(15)
N(1)-C(12)-O(2)	120.12(13)
O(2)-C(12)-C(13)	118.89(12)
N(1)-C(12)-C(13)	120.98(12)
C(14)-C(15)-C(16)	118.37(14)

#### 5.4. Optical properties

The optical properties of the free-ligands **1a-4a** and their boron compounds **7a-10a** were obtained in THF (**Table 8**). **Figure 9** shows the absorption spectra of these compounds. In general, the ligands present a main absorption peak in the UV region, due to the HOMO-LUMO electronic transition through the molecule. The shift from 330 to 362 nm into the series depends on the overall electronic contribution of the substituents in the *para* position of the two terminal phenyl rings. An additional band can also be observed in the short wavelength region, which can be related to electronic transitions from low lying occupied molecular orbitals to the LUMO as previously reported for similar molecules<sup>52</sup> being the maximum at 260 and 288 nm for **3a** and **4a**, while for **1a** and **2a** this band cannot be clearly visualized as it is likely blue shifted into the optical cut-off of the solvent. For molecule **3a** a shoulder at 385 nm is also evident and has been attributed to n-p\* transitions of the nitro substituents by Bessy and Prathapachandra for the same molecule in DMF.<sup>49</sup> Contrary to these authors findings<sup>59</sup>, we consider that the 345 nm band could not be assigned purely to the n-p\* transition of the nitro group in **4a**, but rather to its overlap with the broader HOMO-LUMO transition. When the boron complex is formed (**Figure 9**), the bands are red-shifted due to the larger electronic delocalization because of the formation of the diimine system, in agreement with the <sup>1</sup>H NMR results.

**Table 8.** Photophysical data of Schiff bases **1a-4a** and boron compounds **7a-10a**.

Comp.	$\lambda_{\text{abs}}$ [nm]	$\epsilon * 10^4$ [M <sup>-1</sup> cm <sup>-1</sup> ]	$E_g$ [eV]	$\lambda_{\text{em}}$ [nm]	$\Delta\nu$ [cm <sup>-1</sup> ]	$\Phi$ [%]	$\tau$ [ns]	$K_{\text{rad}} * 10^9$ [s <sup>-1</sup> ]	$K_{\text{nr}} * 10^9$ [s <sup>-1</sup> ]
<b>1a</b>	362	6.5	3.03	453	5549	0.32	0.01	0.32	99.7
<b>2a</b>	330	4.2	3.38	-	-	-	-	-	-
<b>3a</b>	343	5.7	2.49	411	4824	0.75	1.36	0.0055	0.73
<b>4a</b>	345	1.8	2.97	-	-	-	-	-	-
<b>5a</b>	364	1.3	3.08	406	3940	1.0	0.52	0.019	1.90
<b>7a</b>	394	3.8	2.71	452	3257	0.34	0.03	0.110	33.2
<b>8a</b>	363	9.9	3.02	439	4770	0.31	0.11	0.028	9.06
<b>9a</b>	458	2.6	2.34	598	5111	0.10	0.56	0.002	1.78
<b>10a</b>	412	2.9	2.58	502	4352	0.15	0.09	0.017	11.09
<b>11a</b>	345(426)	3.1(3.5)	2.59	-	-	-	-	-	-
<b>12a</b>	350(441)	1.5(1.89)	2.46	407	4001	1.3	0.22	0.059	4.49

**Figure 9.** UV-Vis spectra in THF of compounds **1a-4a** and **7a-10a**.

The optical band gap  $E_g$  between 2.34-3.38 eV, permits a general classification of the materials as semiconductors. Compounds **2a** and **4a** do not emit at all under our experimental conditions, but the fluorescence spectra of the ligands **1a**, **3a** and of the complexes **7a-10a** are presented in **Figure 10**. With respect to ligand **1a**, one broad band at 453 nm is observed. This is consistent with the emission spectrum reported by Tong *et al* in ethanol 10: water 90 (v/v) mixture.<sup>60</sup> In that solvent mixture, the authors found also a second band at *ca.* 530 nm that is assigned to aggregation-induced emission (AIE). In

our studies that were performed in pure THF, no aggregation was found in concentration dependent UV-Vis studies for **1a** or any other molecule. For this reason, AIE was not observed. The fluorescence spectrum of its complex **7a** is practically identical and the same occurs with their excitation spectra (**Figure 11**), contrary to what found for the UV-Vis spectra. This suggests that the boron complexation affects the geometry at the ground but not at the excited state. Interestingly, the behavior in the couple ligand/complex **3a/9a** is completely different. For the ligand **3a**, actually an excitonic emission spectrum with the main peak at 412 nm and a vibronic replica at 431 nm can be observed, while the complex **9a** presents a broad band centered at 598 nm, with a red shift of 186 nm with respect to **3a**. This implies that the complexation with boron strongly affects the geometry in the excited state of the salicylidene fluorophore when it is *para* nitro substituted. Complex **10a** shows a broad fluorescence band, similarly to **9a**, but blue shifted to 502 nm, in agreement with the blue shift observed in the corresponding absorption spectra. Unfortunately as its ligand **4a** does not emit, it is not possible to make a comparison to confirm the effect of the nitro substituents on the spectral changes in the fluorescence between ligand and complex. An interesting aspect is that the emission can be tuned from the blue (**8a**) to the green (**10a**) and red (**9a**) regions by changing the substituents in the *para* position on the phenyl rings. As a general remark, the fluorescence quantum yield is very low for all the molecules; below 1% with lifetime values in the  $10^{-10}$ - $10^{-11}$  s range and radiative constant very small that are in agreement with the poor values of quantum yields measured. The non-radiative constant is high, which suggests a large contribution of non-radiative processes in the fluorescence quenching. The Stokes's shift ( $\Delta\nu$ ) is also large, indicating that the

geometry of the molecules change dramatically after excitation and non-radiative losses are probably mainly due to internal conversion.<sup>61</sup> Due to the “push-pull” character of the molecules, charge transfer from the electron donating MeO or Et<sub>2</sub>N to the electron acceptor (NO<sub>2</sub>) groups, as previously reported by Farfán *et al.*<sup>52</sup> is also possible and could be also the responsible of the low quantum yield.

The absorption spectra of the boron compounds indeed became identical to those of their ligands after one day of storage in ambient conditions revealing de-complexation. For this reason, THF was freshly distilled and the solutions were studied just as prepared. However, and based on results reported by Tong *et al* for **1a**,<sup>60</sup> fluorescence intensity could be enhanced by inducing their aggregation emission in solvent and solvent free mixtures.

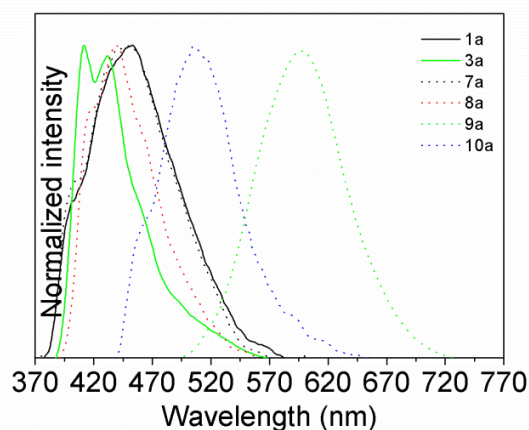


**Figure 10.** Emission spectra of compounds **1a**, **3a**, and **7-10a** in THF.

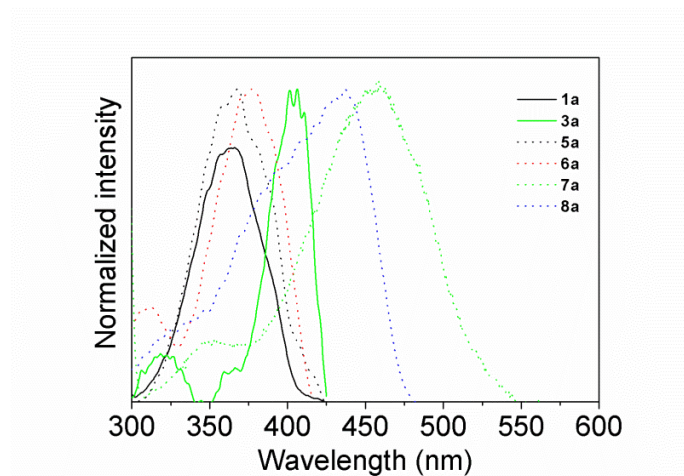
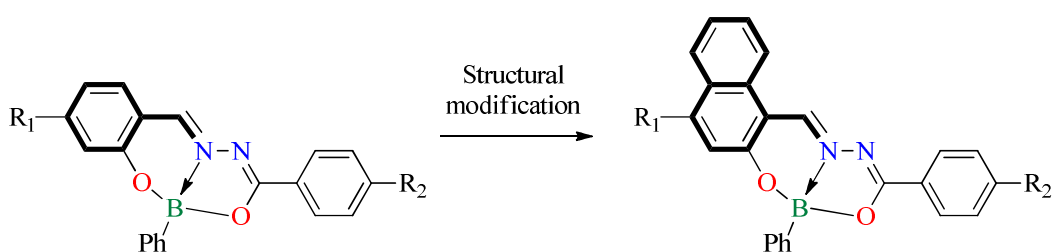


**Figure 11.** Excitation spectra of compounds **1a**, **3a**, **7a-10a** in THF.

In general, the boron compounds **7a-10a** showed interesting optical properties such as the ability of tuning of emission band from blue to red region but unfortunately, fluorescent quantum yields were very low for all the molecules (below 1%). It is known that fluorescent properties are mainly affected for the solvent nature, temperature, concentration, pH, dissolved oxygen, structural rigidity and fluorophore structure.<sup>61b</sup> In order to improve the fluorescent properties it has been reported that naphthyl derivatives improve this properties,<sup>63</sup> we decided to make a change on the structure of the Schiff base by changing the salicylaldehyde to naphthaldehyde as indicated in the **scheme 21**.



**Scheme 21.** Structural modification of boron compound.

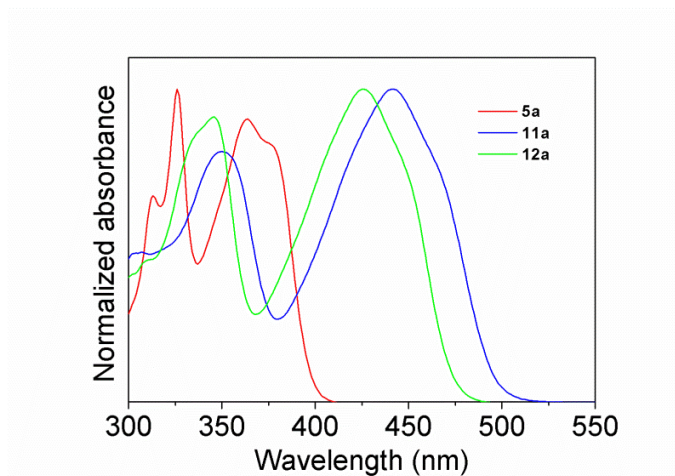


**Figure 12.** UV-Vis spectra in chloroform of compounds **1a**, **11a-12a**.

The electronic absorption spectra of the ligand **5a** and the boron compounds **11-12a** in chloroform are showed in **figure 12**. The ligand presents a main peak at 364 nm due to the HOMO-LUMO electronic transition through the molecule with band gap in the semiconducting range. The  $\pi-\pi^*$  intraligand electronic transition is observed for boron complex **11a** at lower wavelength relative to their corresponding ligand, likely because of distortion of the naphthol imine system after complexation torsion angle of (N2-C12-C13-C18) is  $7.2^\circ$  (12). The ligand **5a** and the boron complex **12a** have a weak fluorescence at around 410 nm whose excitation spectrum is practically identical, suggesting that the fluorescence comes from the naphthoyl fluorophore (**figure 13**). The fluorescent quantum yield measurement is in the range of 1.0-1.3 % with lifetimes in the order of  $10^{-10}$  s. Due to the large Stokes' shift the nonradiative losses can be easily associated with strong deviation of the geometry from the ground to the excited state, as we previously found for salicylidenbenzoylhydrazones. However, internal charge transfer to the nitro substituted benzene can also occur.

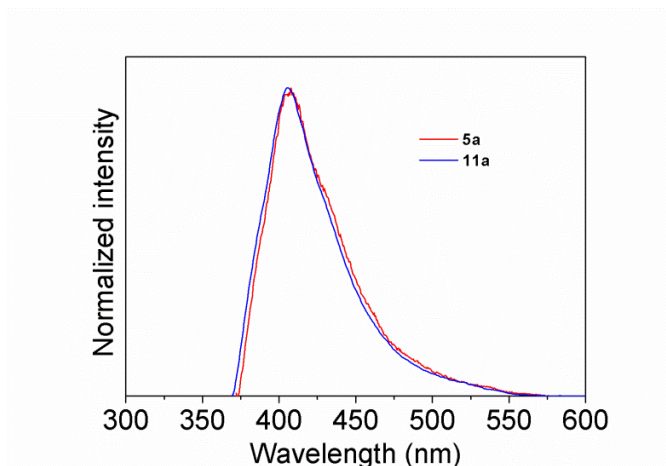


**Figure 13.** Fluorescence spectra of Schiff base **5a** and boro compound **12a**.

Interestingly, the quantum yields are a bit higher than the corresponding salicylidenebenzoylhydrazone. This could be related to the change in the fluorophore from benzene to the more fluorescent naphthalene.<sup>61a</sup> A moderate enhancement of the fluorescence quantum yield is observed for the boron complex **12a** (**Table 10**). A similar behavior was observed by other authors for different main group complexes and generally attributed to an increase of the molecular rigidity or co planarity upon complexation that reduces the number of nonradioactive pathways.<sup>62</sup>

### 5.5 Optical nonlinear properties.

The compounds **1a** and **2a** exhibit the electronic effect induced by a stronger donor substituent<sup>63</sup> on the salicylidenebenzohydrazide, which was observed for optical band gap determinate (**Table 9**). For the molecules **3a** and **4a**, it is interesting the fact that the “*push-pull*” character decreases the optical band gap ( $E_g$ ) values, when the electron donating substituent changes from MeO- to Et<sub>2</sub>N-. These results are consistent with

study reported by Santillan *et al* for salicylideniminophenols.<sup>52</sup> In this study the authors found that the “*push-pull*” character increase by using stronger donor-acceptor substituents and it is consistent with the well-known electronic effect induced on a stilbene backbone.<sup>64</sup> In the case of boron compounds **7a-10a** is observed a change of  $E_g$  values in passing of free ligands to the complexes, which is indicating that the N→B coordinate bond decreased the energy needed for the polarization of the conjugated  $\pi$  system. This is consistent with tetracoordinate organoboron compounds reported by Farfán and Ramos-Ortiz for multidentate ligands.<sup>52,56</sup>

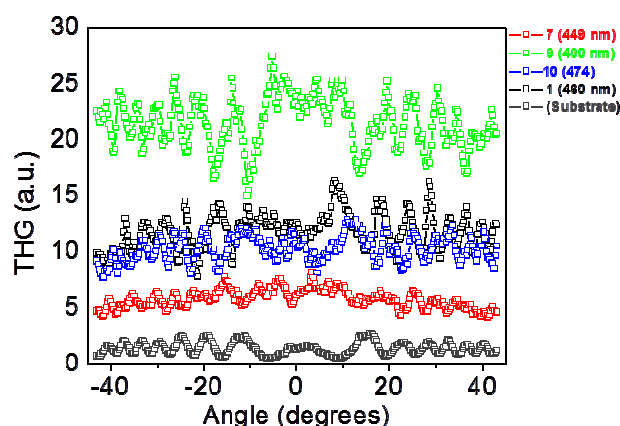


**Figure 14.** THG Maker-fringe patterns for thin solid films doped with 30 wt% of compounds **1a**, **7a**, **9-10a**.

**Figure 14** shows typical plots of the THG signal from solid PS films doped with compounds **1a**, **7a** and **9a-10a**, and from the substrate alone as a function of the incident angle for the excitation beam. The excitation wavelength in this case is 1300 nm with THG signal at 433 nm. The THG curves display an oscillatory behavior typical of Marker-Fringe pattern with average intensity values for the solid films between **4** to **15** times more intense than the substrate alone.

The third order nonlinear susceptibilities for the free ligands and their complexes are summarized in **table 9**. For ligands **2a-3a**, and the boron compound **8a**, the THG signal was very weak and below the range of sensitivity for our experimental setup, so the estimation of their  $\chi^3$  values was not possible. In the case of **4a** the poor of solubility does not permit the preparation of solid films for the analysis. The modest nonlinearities values were observed for the compounds **1a** and **7a** having the strong donor Et<sub>2</sub>N resulting to be  $3.53 \times 10^{-12}$  esu, and  $1.51 \times 10^{-12}$  esu, respectively.

**Table 9.** Optical nonlinear response and thermal properties of compounds **1a-12a**.

Compound	$\chi^3 * 10^{-12}$ [esu]	Td <sub>5</sub> [°C]	Tm [°C]
<b>1a</b>	3.53	286	224
<b>2a</b>	-	233	184
<b>3a</b>	-	261	224
<b>4a</b>	-	274	218
<b>5a</b>	-	269	217
<b>6a</b>	-	257	216
<b>7a</b>	1.51	278	151
<b>8a</b>	-	225	172
<b>9a</b>	3.39	230 243	316
<b>10a</b>	2.42	263	226
<b>11a</b>	-	299	140
<b>12a</b>	-	305	280

-It was not determined

It important to notice that the value of susceptibility for **1a** is larger than boron complexes due to the thickness of the film (460 nm) but the ability to generate the THG intensity shows that the best materials are the molecules with dipolar design type *push-pull*, actually, the best response corresponding to the molecule **9a** (**Figure 14**). However, the nonlinear susceptibility value determined for **1a** is larger than those reported for

other tridentate, and bidentate Schiff bases with similar thicknesses.<sup>56,63b</sup> In the cases of the boron compounds **7a**, **9a-10a**, the enhancement of the nonlinear properties it is observed from the ligand to their corresponding complexes, except **8a**, which does not have the ability for to generate the non linear response. A similar behavior was observed by other authors for different four-coordinate boronates.<sup>52,56,65</sup> Unfortunately, it was not possible obtaining the crystal structure for **9a-10a**, for to make a comparison and confirm the effect of the conformation on the nonlinear behavior between ligand-free and complexes but these materials are instable in solution.

However, the analysis of crystal structure for **7a-8a** suggested that tetrahedral character of boron atom in **7a** generated a high deformation of conjugated  $\pi$ -system compared with molecule **8a**, which could be explains the non linear optical response. This result is consistent with non linear properties in boron compounds derived from salicylideniminophenols.<sup>52</sup>

## 5.6 Thermal analysis

Simultaneous analysis of thermal stability of boron compounds **7a-12a** and the Schiff bases **1a-6a** were determined by differential thermal analysis (DTA) and thermogravimetric analysis (TGA) in the temperature range 25 to 600 °C under a nitrogen atmosphere. The melting transition ( $T_m$ ) and decomposition temperature ( $T_{d5}$ ) are summarized in **table 10**. The figure **15** show the decomposition temperature curves for the Schiff bases **1a-6a**, which exhibited thermal stability in the range of 233-286 °C.

In the case of free ligands **3a** and **4a**, the DTA curves (See appendix) show an endothermic peak at 112 °C and 100 °C with a loss of mass of 4.2 and 5.4 %, respectively, which is attributed to the dehydration process. Additionally, the free ligands showed a remarkable endothermic peak from 184 to 224 °C range due to the melting process, this thermal behavior has been reported for another Schiff bases.<sup>66-67</sup>

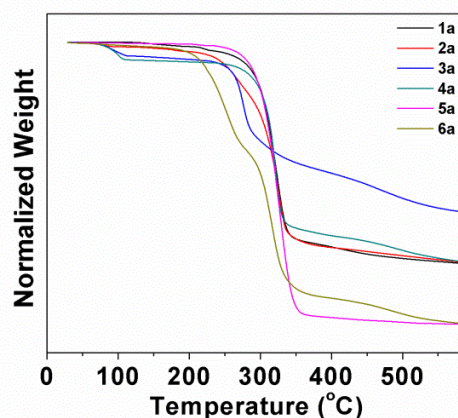


**Figure 15.** TGA thermogram of Schiff bases **1a-6a**.

For the boron compounds **7a-12a**, the introduction of boron atom in the conjugate  $\pi$  system resulted in the increment of  $T_{d5}$  in comparison with the corresponding free-ligand (**Figure 16**). The DTA curve for boron compound **9a** shows an endothermic peak at 107 °C with a loss of mass of 4.2% due to dehydration process (See appendix). The most interesting change of the thermal stability was observed in the complexes **11a** and **12a**, where the decomposition temperature was increased around of 80 °C in comparison with the complexes derived from salicylbenzohydrazide. The high decomposition temperature of these molecules may be related to the slight increment of the molecular weight. This results are in agreement with the report by Zhang *et al.* where

the author reported the improvement of the thermal properties due to significantly increment of molecular weights in a serie of boron complexes.<sup>32</sup> It is important to notice that the boron compounds show an important thermal stability in a temperature range (225-305°C), which is a requirement for those boron compounds that wants to be deposited by thermal evaporation.

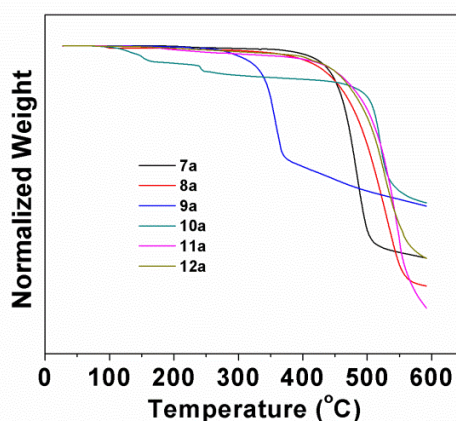


**Figure 16.** TGA thermograms of boron compounds **7a-12a**.

## 5.7 Computational study

In order to explain the experimental results from the photoluminescence a computational study was carried out for the boron complexes in gas phase and in different solvents (**Table 10**). We can observe from this table, that the calculated  $\lambda_{\max}$  suffers a bathochromic shift when including the effect of the dielectric constant through a solvent model.  $\lambda_{\max}$  of the unsubstituted compounds seems rather insensitive to the dielectric constant but  $-\text{NO}_2$  substitution seems to increase the sensitivity of  $\lambda_{\max}$  to the dielectric constant of the solvent, with higher values of the dielectric constant yielding a larger bathochromic shift. All the active transitions are of  $\pi-\pi^*$  nature, corresponding to

transitions between HOMO and LUMO. Taking the structures in the gas phase as examples, the figures **17-18** show that the presence of the nitro group localizes the LUMO on one side of the molecule, thus favoring push-pull character.

**Table 10.** Calculated values of maximum absorption wavelength using TDDFT at the level B3LYP/6-311++G\*\*//B3LYP/6-31G\* and PCM solvent model.

Compound	Solvent	$\lambda_{\max}$ [nm]	Transition	Compound	Solvent	$\lambda_{\max}$ [nm]	Transition
	None	408	$\pi$ - $\pi^*$		none	393	$\pi$ - $\pi^*$
<b>7a</b>	Toluene	421 (426)	$\pi$ - $\pi^*$	<b>8a</b>	toluene	399 (397)	$\pi$ - $\pi^*$
	CHCl <sub>3</sub>	422 (428)	$\pi$ - $\pi^*$		CHCl <sub>3</sub>	396 (395)	$\pi$ - $\pi^*$
	THF	422 (394)	$\pi$ - $\pi^*$		THF	395 (363)	$\pi$ - $\pi^*$
	Acetone	421(428)	$\pi$ - $\pi^*$		acetone	393 (391)	$\pi$ - $\pi^*$
	None	506	$\pi$ - $\pi^*$		<b>10a</b>	None	452
<b>9a</b>	Toluene	561 (457)	$\pi$ - $\pi^*$		toluene	477 (417)	$\pi$ - $\pi^*$
	CHCl <sub>3</sub>	586 (461)	$\pi$ - $\pi^*$		CHCl <sub>3</sub>	486 (416)	$\pi$ - $\pi^*$
	THF	595 (458)	$\pi$ - $\pi^*$		THF	489 (412)	$\pi$ - $\pi^*$
	Acetone	607 (456)	$\pi$ - $\pi^*$		acetone	493 (409)	$\pi$ - $\pi^*$

The analysis of the optimized structures in gas phase (**Figure 17** and **18**), revealed that the HOMOs of all compounds are mainly located on the salicylaldehyde, whereas the LUMOs are founded on the benzohydrazine. The HOMO-LUMO levels do not show a significant contribution from the boron center, thus suggesting that the HOMO and LUMO energies are dominated by the salicylidenebenzohydrazide ligand. A similar behavior has been reported by Ko *et al.* In this study the author found that the boron atom did not show an important contribution from the frontier orbital in the boron complexes derived from oxazolylphenolate ligand.<sup>35</sup>

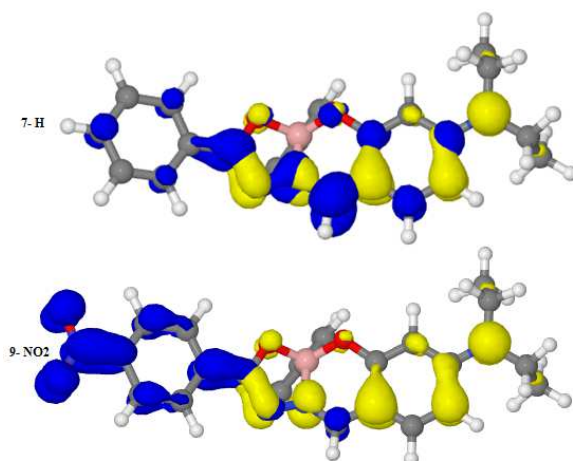


**Figure 17.** Occupied orbitals (HOMO, yellow) and virtual orbitals (LUMO, blue) for the  $\pi$ - $\pi^*$  transition in compound **7a** (top) and **9a-NO<sub>2</sub>** (bottom).

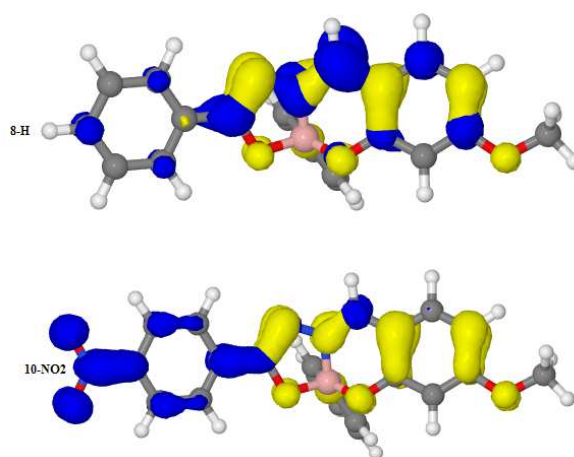


**Figure 18.** Occupied orbitals (HOMO, yellow) and virtual orbitals (LUMO, blue) for the  $\pi$ - $\pi^*$  transition in compound **8a** (top) and **10a-NO<sub>2</sub>** (bottom).

### 5.8 Fabrication of electroluminescent device type OLED derived from **9a** and **10a**

An atypical double-layered device was therefore fabricated with a structure ITO/PEDOT:PSS/**9a-10a**/Al, where the boron complex **9a** and **10a** were used as an emitting and electron transport due to its interesting optical and thermal characteristics as well as the good solubility. The figure **19** shows the current density (J)-bias (V) for **9a**

and **10a** , respectively. The curves for **9a-10a** display an insignificant current density, and due to its low fluorescent quantum yield in solution (0.15%), these materials show a poor electroluminescence performance in comparison with other electroluminescent materials such as Alq<sub>3</sub> (~15%).<sup>5c</sup>

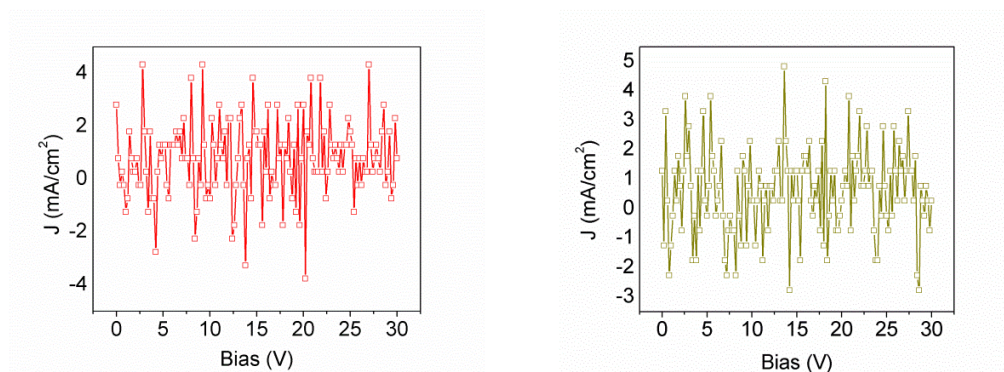


**Figure 19.** Current density-Voltage **9a** (left) and **10a** (right) using a configuration ITO/PEDOT:PSS/**9a-10a**/Al OLED.

## CONCLUSION

In summary, we have synthesized six new boron compounds with three-ring-fused skeletons derived from Schiff bases, and three new free ligands type Schiff base in good yields. The synthesis under microwave method for the boron compound **7a-10a** proceeded very fast and cleanly. The reaction times decreased around of 570 times in comparison with the conventional synthesis.

The crystal structures for the ligands **1-2a** show that these molecules have a near planar array, whereas that the boron compounds **7a**, **8a** and **12a**, due to the tetrahedral characters of the boron atom, these molecules have a great distortion, when the coordinate bond  $N \rightarrow B$  is formed.

The absorption, fluorescence emission, and fluorescence lifetimes for all compounds, except **2a**, **4a** and **6a**, were studied in solution. The absorption spectra of the free ligands **1-6a** revealed that these molecules have maximum absorption peaks

mainly in the ultraviolet region, and the bands show a displacement towards to the red region, after that the coordinate bond is formed N→B.

The emission spectra of free-ligands **1a-4a** and their boron compounds **7a-10a** showed that the emission peaks can be tuned from region of blue, green to red regions by changing the substituents on the *ortho* positions of the external aromatic rings.

For the salicylidenebenzohydrazine and their boron complexes were found that all compounds studied exhibit low fluorescence emission ( $\phi < 1\%$ ), mainly because of strong internal conversion as indicated by the large Stokes' shift values. The boron atom deviation from salicylidenimino-plane might affect the luminescence response.

In the case of boron compound derived from naphthalidenbenzohydrazide, the change in the fluorophore from benzene to naphthyl showed a moderate enhancement of the fluorescent quantum yield ( $\phi > 1\%$ ), in the comparison with the salicylidenbenzoylhydrazone.

The computational study for the boron compounds **7a-10a** showed that the boron center has not a significant contribution in the HOMO-LUMO levels and suggested that these frontier orbitals are dominated by the salicylidenebenzohydrazide.

The simultaneous thermal analysis under nitrogen of molecules **1a-12a** showed that the complexes have high decomposition temperatures in comparison with the corresponding free-ligands (233-286 °C). The introduction of the boron atom in the  $\pi$ -conjugated system increment the decomposition temperature.

The third-order susceptibility values measured for the salicylidenbenzohydrazides and their organoboron compounds showed that it increases when the coordination bond  $N \rightarrow B$  is formed. This behavior is more evident for the organoboron compounds **7a**, **9a** and **10a**, where the optical energy gap is smaller than the ligand.

The electroluminescent device type OLED fabricated using **9a-10a** as an emitter and electron transport, displayed an insignificant current density in a range from 0 to 20 V. In addition, due to its low fluorescent quantum yield in solution, **9a-10a** have a poor electroluminescence performance.

The results obtained in this thesis contribute to knowledge of boron chemistry, providing the determination of optical linear and non linear properties and evaluation of the electroluminescent behaviour of these materials, being an interesting area for their potential study.

## **PERSPECTIVES**

As a part of the knowledge generated in this research work was demonstrated that boron compounds derived from Schiff bases are candidates for their use as emitter materials with application in electroluminescent devices type OLED.

To continue with this work, we are going to carry out the synthesis of new bidentate ligands and their boron compounds, which allows boron atom is into the planar array of the ligand. Probably, this new structure improves the electronic delocalization through of conjugated  $\pi$ -system. As a result of the structural change, the new boron compounds are going to show improvement optoelectronic properties that allows a good performance of the electroluminescent devices are going to fabricate using these materials as an emitter and electron transport layers.

## REFERENCES

1. Valeur B., Berberan-Santos M. N. A brief history of fluorescence and phosphorescence before the emergency of quantum theory. *J. Chem. Educ.* 88: 731-738. (2011).
2. Rao Y. L., Wang S. Four-coordinate organoboron compounds with a  $\pi$ -conjugated chelate ligand for optoelectronic applications. *Inorg. Chem.* 50: 12263-12274. (2011).
3. a) Tang C. W., VanSlyke S. A. Organic electroluminescent diodes. *Appl. Phys. Lett.* 51: 913-915. (1987); b) Tang C. W., VanSlyke, S. A., Chen, C. H. Electroluminescent of doped organic thin films. *J. Appl. Phys.* 65: 3610-3616. (1989).
4. (a) Aziz H., Popovic Z. D., Hu N. X., Hor A., Xu G. Degradation mechanism of small molecule-based organic light emitting devices. *Science* 283: 1900-1902. (1999); (b) Papadimitrakopolus, F., Zhang X. M., Thomsen, D. L., Higginson, K. A. A chemical failure mechanism for aluminum(III) 8-hydroxyquinoline light-emitting device. *Chem. Mater.* 8: 1363-1365. (1996); (c) Higginson K. A., Zhang X. M., Papadimitrakopolus, F. Thermal and Morphological effects on the hydrolytic stability of aluminum tris(8-hydroxyquinoline) ( $\text{Alq}_3$ ). *Chem. Mater.* 10: 1017-1020 . (1998); (d) Knox J.E., Halls M.D., Hrachian H.P. and Schlegel H.B. Chemical failure modes of  $\text{AlQ}_3$ -based OLEDs:  $\text{Alq}_3$  hydrolysis. *Phys. Chem. Chem. Phys.* 8:1371-1377. (2006).
5. (a) Chen H., Chi Y., Liu C.S., Yu J.K., Cheng Y.M., Chen K.S., et al. Rational color tuning and luminescent properties of functionalized boron containing 2-pyridyl pyrrolide complexes. *Adv. Funct. Mater.* 15:567-574. (2005); (b) Cui Y., Liu Q., Bai D.R., Wen-Li J., Tao Y., Wang S., et al. Organoboron compounds with an 8-

- hydroxyquinolato chelate and its derivatives: substituent effects on structures and luminescence. *Inorg. Chem.* 44:601-609. (2005). (c) Zhang H., Cheng H., Kaigi Y., Peng Z., Wenjing T., Wang Y. Synthesis, structures, and luminescent properties of phenol-pyridyl boron complexes. *Inorg. Chem.* 45:2788-2794. (2006).
6. Costa R. D., Orti E., Bolink H.J. Luminescent ionic transition-metal complexes for light-emitting electrochemical cells. *Angew. Chem. Int. Ed.* 51:8178-8211. (2012).
  7. You Y.G., Nam W.W. Photofunctional triplet excited states of cyclometalated Ir(III) complexes: beyond electroluminescence. *Chem. Soc. Rev.* 41: 7061-7084. (2012).
  8. Vezzu D.A.K., Deaton J.C., Jones J.S., Bartolotti L., Harris C.F., Marchetti A.P., Kondakova M., Pike R.D., Huo S. Highly luminescent tetradentate bis-cyclometalated platinum complexes: Design, synthesis, structure, photophysics, and electroluminescence Application. *Inorg. Chem.* 49: 5107-5119. (2010).
  9. Lotitoz K.J., Peters J.C. Efficient luminescence from easily prepared three-coordinate copper(I) arylamidophosphines. *Chem. Commun.* 46:3690-3692. (2010).
  10. a) Desiraju G. R. Supramolecular synthons in crystal engineering-A new organic synthesis. *Angew. Chem. Int. Ed.* 34: 2311-2327. (1995); b) Davis C. J., Lewis, P. T., Billodeux D. R., Fronczek F. R., Escobedo J. O., Strongin R. M. Solid-State Supramolecular structures of resorcinol-arylboronic acid compound. *Org. Lett.* 3: 2443-2445. (2001).
  11. Killoran, J., Allen L., Gallagher J. F., Gallagher W.M., O' Shea, D.F. Synthesis of BF<sub>2</sub> chelates of tetraaryllazadipyrromethenes and evidence for their photodynamic therapeutic behaviour. *Chem. Commun.* 17: 1862-1863. (2002).
  12. Kollmannsberger M., Rurack K., Resch-Genge U., Daub J. Ultrafast charge transfer in amino substituted boron dipyrromethene dyes and its inhibition by cation complexation: a new design concept for highly sensitive fluorescent probes. *J. Phys. Chem. A.* 50: 10211-10220. (1998).

13. Zeng L., Miller E.W., Pralle A., Isacoff E., Chang C.J. A selective turn-on fluorescent sensor for imaging copper in living cells. *J. Am. Chem. Soc.* 128: 10-11. (2006).
14. Boyer J.H., Haag A.M. Sathyamoorthi G., Soong M.L., Thangaraj K., Pavlopoulos T.G. Pyrromethene-BF<sub>2</sub> complexes as laser dyes: 2. *Heteroat. Chem.* 4: 39-49. (1993).
15. Kubo Y., Yamamoto M., Ikeda M., Shinkai S., Yamaguchi S., Tamao, K., A colorimetric and ratiometric fluorescent chemosensor with three emission changes: fluoride ion sensing by a triarylborane-porphyrin conjugate. *Angew. Chem. Int. Ed.* 42: 2036-2040. (2003).
16. Wang S. Luminescence and electroluminescence of Al (III), B (III), Be (II) and Zn (II) complexes with nitrogen donors. *Coord. Chem. Rev.* 215: 79-98. (2001); b) Huang L.S., Chen C.H. Recent progress of molecular organic electroluminescent materials and devices. *Mater. Sci. Eng. R.* 39: 143-222. (2002).
17. Sun Y., Rohde D., Liu Y., Wan L., Wang Y., Wu W., Di C., Yu G., Zhu D. A novel air-stable n-type organic semiconductor; 4-4'-bis [(6,6'-diphenyl)-2,2-difluoro-1,3,2-dioxaborine] and its application in organic ambipolar field effect transistors. *J. Mater. Chem.* 16: 4499-4503. (2006).
18. a) Rao Y.L., Amarne H., Chen L.C., Mosey N., Wang S. Photo- and thermal-induced multistructural transformation of 2-phenylazolyl chelate boron compounds. *J. Am. Chem. Soc.* 135: 3407-3410. (2013); b) Hudson Z. M., Ko S. B., Yamaguchi S., Wang S. Modulating the photoisomerization of N,C-chelate organoboranes with triplet acceptors. *Org. Lett.* 14: 5610-5613. (2012); c) Rao Y., Amarne H., Wang S. Photochromic four-coordinate N, C-chelate boron compounds. *Coord. Chem. Rev.* 256: 759-770. (2012).
19. Branger C., Lequan R.M., Large M., Kajzar F. Polyurethanes containing boron chromophores as sidechains for nonlinear optics. *Chem. Phys. Lett.* 272: 265-270. (1997).
20. Tushar B. B., Cheerfulman S. M., Willem W., Monique B. Self-assembly of diorganotin(IV) 2-[(E)-1-(2-oxyaryl)alkylidene]amino}acetates: An investigation of

structures by X-ray diffraction, solution and solid-state tin NMR, and electrospray ionization MS. *J. Organomet. Chem.* 690:3080-3094. (2005).

21. Nath M., Pramendra K. S. Chemistry and applications of organotin (IV) complexes of Schiff bases. *Dalton. Trans.* 40:7077-7121. (2011).
22. Petasis N.A. Expanding roles for organoboron compounds-versatile and valuable molecules for synthetic, biological, and medicinal chemistry. *Aust. J. Chem.* 60: 795-798. (2007).
23. Hassan, A., Wang S. First blue luminescent diborate compound:  $B_2(\mu-O)Et_2(7\text{-azain})_2$  (7-azain = 7-azaindole anion). *Chem. Commun.* 2: 211-212. (1998).
24. Wu, Q. G., Wu G., Brancalon L., Suning W.  $B_3O_3Ph_3(7\text{-azaindole})$ : Structure, luminescence, and fluxionality. *Organometallics.* 18: 2553-2556. (1999).
25. Anderson S., Weaver M. S., Hudson A. J. Materials for organic electroluminescence: aluminium vs. boron. *Synthetic. Met.* 111-112: 459-463. (2000).
26. Lim H.J., Kim S.M., Lee S.J, Jung S., Kwan K. Y., Ha Y. Synthesis of new boron complexes containing aromatic moieties and their application to organic electroluminescent devices. *Opt. Mat.* 21: 211-215. (2002).
27. Cheng C.C., Yu W.S., Chou P.T., Peng S.M., Lee G.H., Wu P.C., Song Y.H., Chi Y. Syntheses and remarkable photophysical properties of 5-(2-pyridyl)pyrazolate boron complexes; photoinduced electron transfer. *Chem. Commun.* 20: 2628-2629. (2003).
28. Chen H.Y., Chi Y., Liu C.S., Yu J.K., Cheng Y.M., Chen K.S., Chou P.T., Peng S.M., Lee G.H., Carty A.J., Yeh S.J., Chen C.T. Rational color tuning and luminescent properties of functionalized boron-containing 2-pyridyl pyrrolide complexes. *Adv. Funct. Mater.* 15: 567-574. (2005).
29. Cui Y., Lui Q.D., Bai D.R., Jia W.L., Tao Y., Wang S. Organoboron compounds with an 8-hydroxyquinolato chelate and Its derivatives: substituent effects on structures and luminescence. *Inorg. Chem.* 44: 601-609. (2005).

30. Liu Q.D., Mudadu M. S., Thummel R., Tao Y., Wang S. From blue to red: Syntheses, structures, electronic, and electroluminescent properties of tunable luminescent N,N chelate boron complexes. *Adv. Funct. Mater.* 15: 143-154. (2005).
31. Zhang H., Huo C., Ye K., Zhang P., Tian W., Wang Y. Synthesis, structures, and luminescent properties of phenol-pyridyl boron complexes. *Inorg. Chem.* 45: 2788-2794. (2006).
32. Qin Y., Kiburu I., Shah S., Jäkle F. Luminescence tuning of organoboron quinolates through substituent variation at the 5-position of the quinolato moiety. *Org. Lett.* 8: 5227-5230. (2006).
33. Zhang H., Huo C., Zhang J., Zhang P., Tian W., Wang Y. Efficient single-layer electroluminescent device based on a bipolar emitting boron-containing material. *Chem. Commun.* 3: 281-283. (2006).
34. Zhang Z., Bi H., Zhang Y., Yao D., Gao H., Fan Y., Zhang H., Wang Y., Wang Y., Chen Z., Ma D. Luminescent boron-contained ladder-type  $\pi$ -conjugated compounds. *Inorg. Chem.* 48: 7230-7236. (2009).
35. Son H. J., Han W. S., Wee K. R., Chun J. Y., Choi K. B., Han S. J., Kwon S. N., Ko J., Lee C., Kang S. O. Systematic electronic control in ambipolar compounds optimizes their photoluminescence properties: synthesis, characterization, and device fabrication of four-coordinate boron compounds containing an N,O-chelating oxazolyphenolate ligand. *Eur. J. Inorg. Chem.* 11:1503-1513. (2009).
36. Zhang Z., Yao D., Zhao S., Gao H., Fan Y., Su Z., Zhang H., Wang Y. Carbazolyl-contained phenol-pyridyl boron complexes: syntheses, structures, photoluminescent and electroluminescent properties. *Dalton. Trans.* 39: 5123-5129. (2010).
37. Suresh D., Gomes C. S., Gomes P. T., Di Paolo R. E., Maçanita A. L., Calhorda M. J., Charas A., Morgado J., Duarte M. T. Syntheses and photophysical properties of new iminopyrrolyl boron complexes and their application in efficient single-layer non-doped OLEDs prepared by spin coating. *Dalton. Trans.* 41: 8502-8505. (2012).

38. Suresh D., Lopes P. S., Ferreira B., Figueira C., Gomes C., Gomes P. T., Di Paolo R. E., Macanita A. L., Duarte M. T., Charas A., Morgado J., Calhorda M. J. Tunable fluorophores based on 2-(N-Arylimino)pyrrolyl chelates of diphenylboron: synthesis, structure, photophysical characterization, and application in OLEDs. *Chem. Eur. J.* 20: 1-16. (2014).
39. Li H.J., Fu W.F., Li L., Gan X., Mu W. H., Chen W. Q. Duan X. M., Song H. B. Intense one- and two-photon excited fluorescent bis (BF<sub>2</sub>) core complex containing a 1,8-naphthyridine. *Org. Lett.* 12: 2924-2927. (2010).
40. Felouat A., D'Aléo A., Fages F. Synthesis and photophysical properties of difluoroboron complexes of curcuminoid derivatives bearing different terminal aromatic units and meso-aryl ring. *J. Org. Chem.* 78: 4446-4455. (2013).
41. Sheldrick G.M. Phase annealing in SHELX-90: direct methods for larger structures. *Acta. Crystallogr. Sec. A.* 46: 467-473. (1990).
42. Sheldrick GM. SHELX-97: Program for the Solution and Refinement of Crystal Structures; Universität Göttingen: Göttingen, Germany. (1997).
43. Williams A.T.R., Winfield S.A., Miller J.N. Relative fluorescence quantum yields using a computer-controlled luminescence spectrometer. *Analyst.* 108: 1067-1107. (1983).
44. Ramos-Ortiz, G.; Maldonado, J.L.; Meneses-Nava, M.A.; Barbosa-García, O.; Olmos, M., Cha, M. Third harmonic generation performance of organic polymers films doped with triphenyl methane derivative dyes. *Opt. Mater.* 29: 636-641. (2007).
45. Schmidt M. W., Kim K. Baldrige K.K., Boatz J.A., Elbert S.T., Gordon M.S., Jensen J.H., Koseki S., Matsunaga N., Nguyen K.A., Nguyen K.A., Su S., Windus T.L., Dupuis M., Montgomery Jr J.A. General atomic and molecular electronic structure system. *J. Comp. Chem.* 14: 1347-1363. (1993).
46. a) Becke A. Density-functional thermochemistry.III. The role of exact exchange. *J. Chem. Phys.* 98: 5648-5652. (1993); b) Lee C., Yang W., Parr R. Development of the Colle-Salvetti correlation-energy formula into a functional of the electron density. *Phys. Rev. B.* 37: 785-789. (1988); c) Vosko S.H. , Wilk L., Nusair M., Accurate

- Spin-Dependent Electron Liquid Correlation Energies for Local Spin Density Calculations: A Critical Analysis. *Can. J. Phys.* 58: 1200-1211. (1980); d) Stephens P., Devlin F., Chabalowski C., Frisch M. *J. Phys. Chem.* 98: 11623-11627. (1994).
47. Cossi, M., Rega N., Scalmani G., Barone V. Energies, structures, and electronic properties of molecules in solution with the C-PCM solvation model. *J. Comp. Chem.* 24: 669-681. (2003).
48. Allouche A.R. Gabedit-A Graphical user interface for computational chemistry softwares. *J. Comp. Chem.* 32:174-182. (2011).
49. Bessy R.B.N., Prathapachandra K.M.R., Suresh E. Synthesis, spectral characterization and crystal structure of N-2-hydroxy-4-metoxybenzaldehyde-N-4-nitrobenzoylhydrazone and its square planar Cu(II) complex, *Spectroch Acta Part A.* 71:1253-1260. (2008).
50. Cariati F, Caruso U, Centore R, Marcolli W, De Maria A, Panunzi B, Roviello A and Tuzi A. Synthesis, structure, and second-order nonlinear optical properties of copper(II) and palladium(II) acentric complexes with N-Salicylidene-N-aryloylhydrazine tridentate ligands. *Inorg. Chem.* 41:6597-6603. (2002).
51. Ioannou P.C., Konstantianos D.G. Fluorometric determination of Magnesium in serum with 2-hydroxy-1-naphthaldehyde salicyloylhydrazone. *Clin. Chem.* 35: 1492-1496. (1989).
52. Muñoz B.M., Santillan R., Rodríguez M., Méndez J.M., Romero M., Farfán N., Lacroix P.G., Nakatani K., Ramos-Ortíz G., Maldonado J.L. et al. Synthesis, crystal structure and non-linear optical properties of boronates derivatives of salicylideniminophenols. *J. Organomet. Chem.* 693:1321-1334. (2008).
53. Barba V., Vazquez J., López F., Santillan R., Farfán N. Mono- and diboronates derived from tridentate ONO ligands and arylboronic acids. *J. Organomet. Chem.* 690:2351-2357. (2005).
54. Beachell H.C., Beistel D.W. Nuclear magnetic resonance spectra of phenylboronic acids. *Inorg. Chem.* 3:1028-1032. (1964).

55. Barba V., Cuahutle D., Santillan R., Farfán, N. Stereoselective addition of acetone to C=N bond of [4.3.0] boron heterobicycles. *Can. J. Chem.* 79:1229-1237. (2001).
56. Rodríguez M., Ramos-Ortíz G., Alcalá-Salas M.L., Maldonado K.A., López Y., Domínguez .O. One-pot synthesis and characterization of novel boronates for the growth of single crystals with nonlinear optical properties. *Dyes and Pigm.* 87:76-83. (2010).
57. Höpfl H. The tetrahedral character of the boron atom newly defined a useful tool to evaluate the N→B bond. *J. Organomet. Chem.* 581:129-149. (1999).
58. a) Li D., Zhang H., Wang C., Huang S., Guo J., Wang Y. Construction of full-color-tunable and strongly emissive materials by functionalizing a boron-chelate four-ring-fused  $\pi$ -conjugated core. *J. Mater. Chem.* 22:4319-4348. (2012); b) Li D., Zhang Z., Zhao S., Wang Y., Zhang H. Diboron-containing fluorophores with extended ladder-type  $\pi$ -conjugated skeletons. *Dalton. Trans.* 40:1279-1285. (2011); c) Li D., Yuan Y., Bi H., Yao D.D., Zhao X.J., Tian W.J. Boron-Bridged  $\pi$ -Conjugated Ladders as Efficient Electron-Transporting Emitters. *Inorg. Chem.* 50: 4825-4831. (2011); d) Li D., Wang K., Huang S., Qu S.N., Liu X.Y., Zhu Q.X. Brightly fluorescent red organic solids bearing boron-bridged  $\pi$ -conjugated skeletons. *J. Mater. Chem.* 21: 15298-15304. (2011).
59. Bessy R.B.N., Prathapachandra K.M.R. Synthesis, spectroscopic characterization and crystal structure of mixed ligand Ni(II) complex of N-4-diethylaminosalicylidine-N'-4-nitrobenzoyl hydrazone and 4-picoline, *Struct Chem* 17: 201-208. (2006).
60. Li N., Tang W., Xiang Y., Tong A., Jin P., Ju Y. Fluorescent salicylaldehyde hydrazone as selective chemosensor for Zn<sup>+2</sup> in aqueous ethanol : a radiometric approach. *Luminescence.* 25: 445-451. (2010).
61. a) Berlman I.B., *Handbook of Fluorescence Spectra of Aromatic Molecules*, second ed., Academic Press, London, New York: 1971; b) Lakowicz J.R., *Principles of Fluorescence Spectroscopy*, second ed., Kluwer Academic/Plenum Publishers, New York: 1999.
62. a) Crawford S.M., Ali A.A., Cameron S.T., Thompson A. Synthesis and characterization of fluorescent pyrrolyldipyrinato Sn (IV) complexes. *Inorg. Chem.*

- 50, 8207-8213. (2011); b) López-Torres E., Medina-Castillo A.L., Fernández-Sánchez J.F., Mendiola M.A. Luminescent organotin complexes with the ligand benzil bis(benzoylhydrazone). *J. Organomet. Chem.* 695: 2305-2310. (2010); c) Li S.H., Chen F.R., Zhou Y.F., Wang J.N., Zhang H., Xu J.G. Enhanced fluorescence sensing of hydroxylated organotins by a boronic acid-linked Schiff base. *Chem. Commun.* 28:4179-4181. (2009).
63. Maity D., Govindaraju D. Naphthaldehyde-urea/thiourea conjugates as turn on fluorescent probes  $Al^{3+}$  based on restricted C=N isomerization. *Eur. J. Inorg. Chem.* 36: 5479-5485. (2011).
64. a) Rivera, J.M., Méndez, E., Colorado-Peralta, R., Rincón, S., Farfán, N., Santillan, R. Synthesis, characterization and X-ray studies of new six-seven membered rings[4.5.0] heterobicyclic system of monomeric boronates. *Inorg. Chim. Acta.* 390: 26-32. (2012); b) Rodríguez, M., Maldonado, J.L., Ramos-Ortíz, G., Domínguez, O., Ochoa, Ma. E., Santillán, R., Farfán, N., Meneses-Nava, M.A., Barbosa-García, O. Synthesis, X-ray diffraction analysis, and chemical-optical characterizations of boron complexes from bidentate ligands. *Polyhedron.* 3: 194-200. (2012).
65. Cheng, L.T., Tam, W., Marder, S.R., Stiegman, A.E., Rikken, G., Spangler, C.W. Experimental investigations of organic molecular nonlinear optical polarizabilities. I. Methods and results on benzene and stilbene derivatives. *J. Phys. Chem.* 95, 10631-10643. (1991).
66. Reyes H.; García C.; Farfán N.; Santillan R.; Lacroix P.G., Lepetit, C., Nakatani, K. Synthesis, crystal structures, and quadratic nonlinear optical properties in four "push-pull" diorganotin derivatives. *J. Organomet. Chem.* 689:2303-2310. (2004).
67. Mohamed, G.G.; Omar, M.M.; Ibrahim. A.A. Biological activity studies on metal complexes of novel tridentate Schiff bases ligand, spectroscopic and thermal characterization. *Eur. J. Med. Chem.* 44: 4801-4812. (2009).
68. Ceyhan, G., Köse M., Tümer, M., Demirtaş I., Yağlıoğlu A.S., McKee, V. Structural characterization of some Schiff bases compounds: investigation of their electrochemical, photoluminescence, thermal and anticancer activity properties. *J. Lumin.* 143, 623-634. (2013).

# APPENDIX

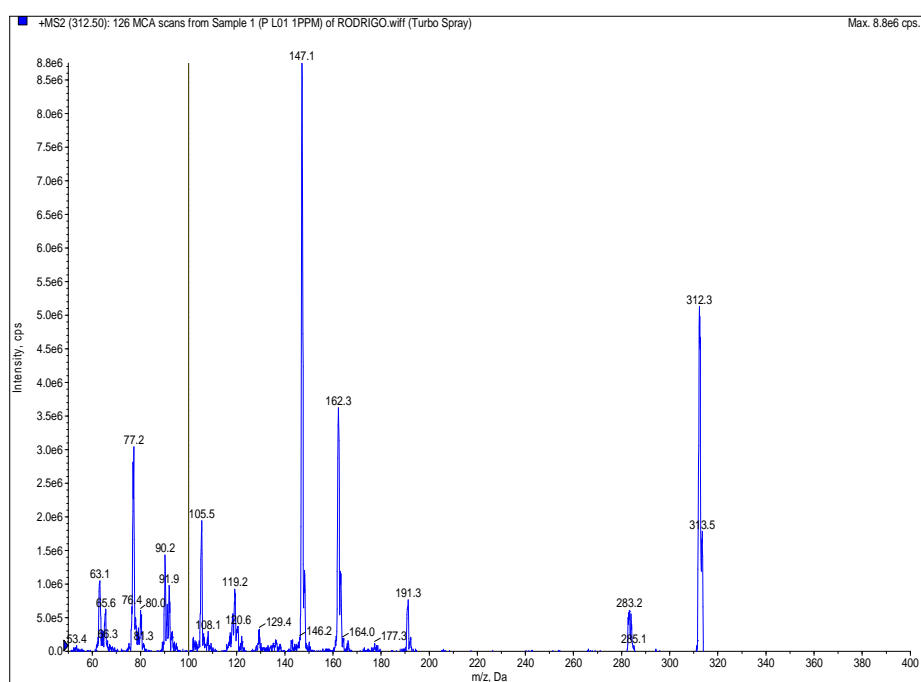


**Figure S1.** Mass spectrum of compound **1a**.

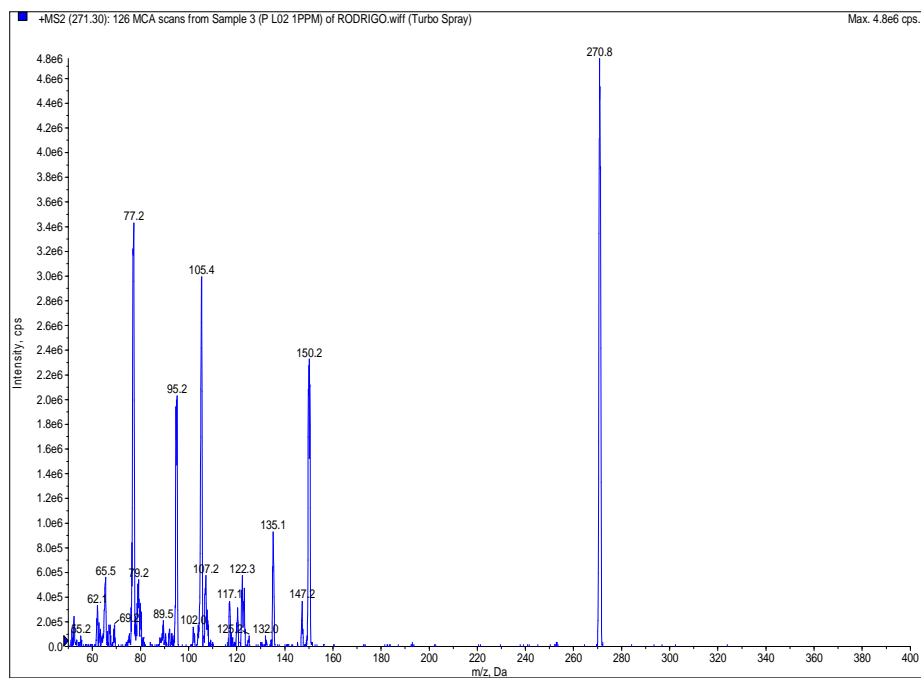


**Figure S2.** Mass spectrum of compound **2a**.

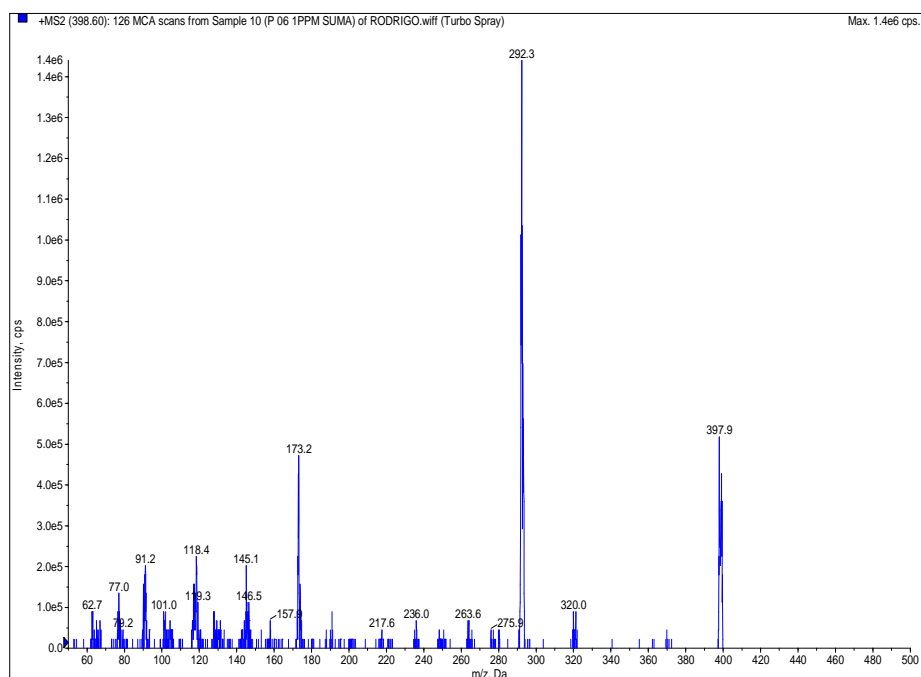


**Figure S3.** Mass spectrum of compound **7a**.

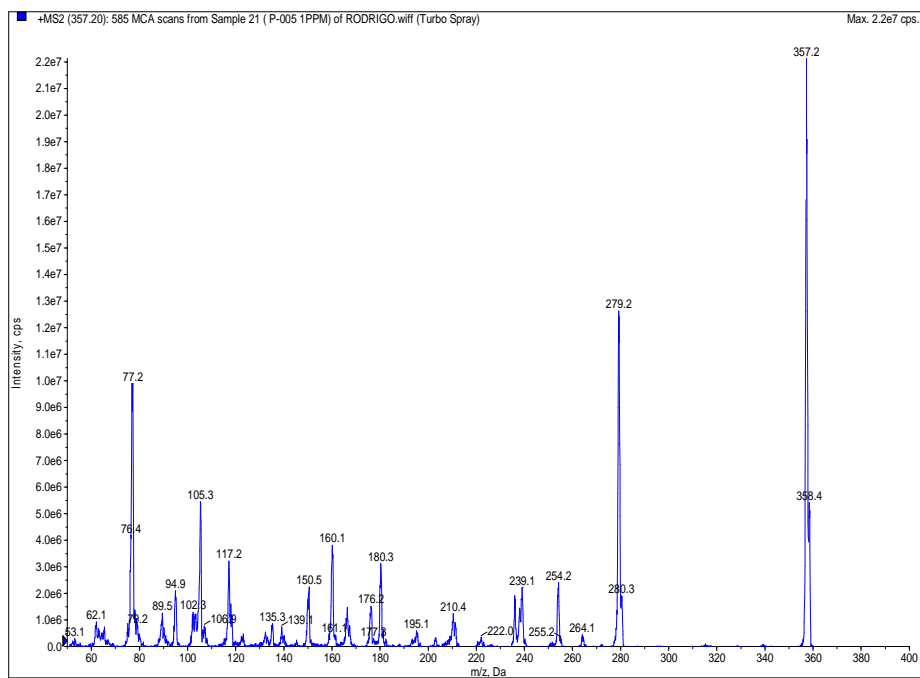


**Figure S4.** Mass spectrum of compound **8a**.

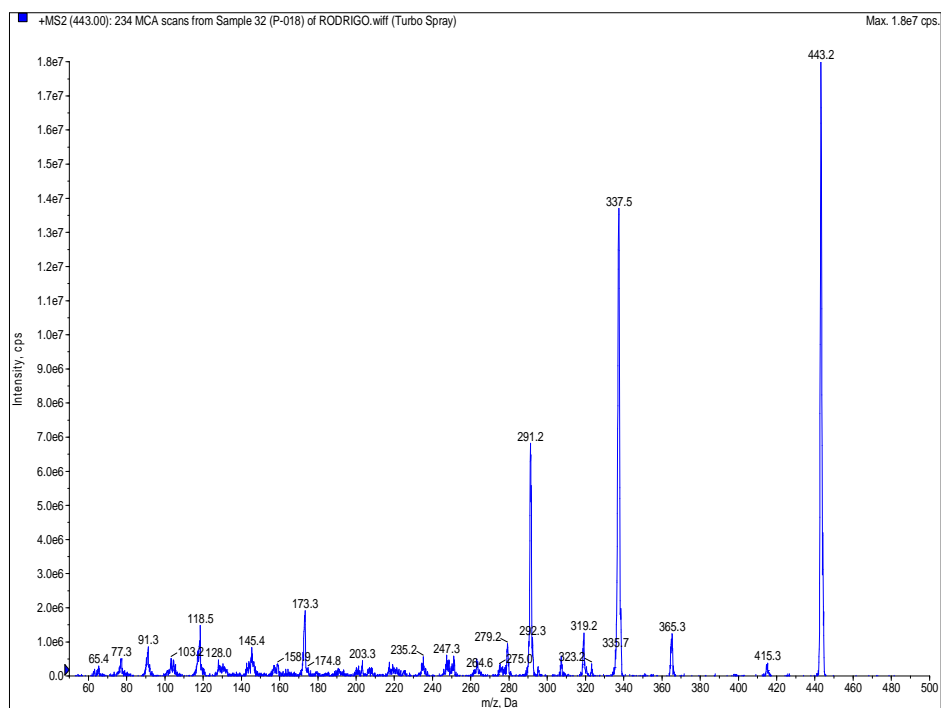


**Figure S5.** Mass spectrum of compound **9a**.

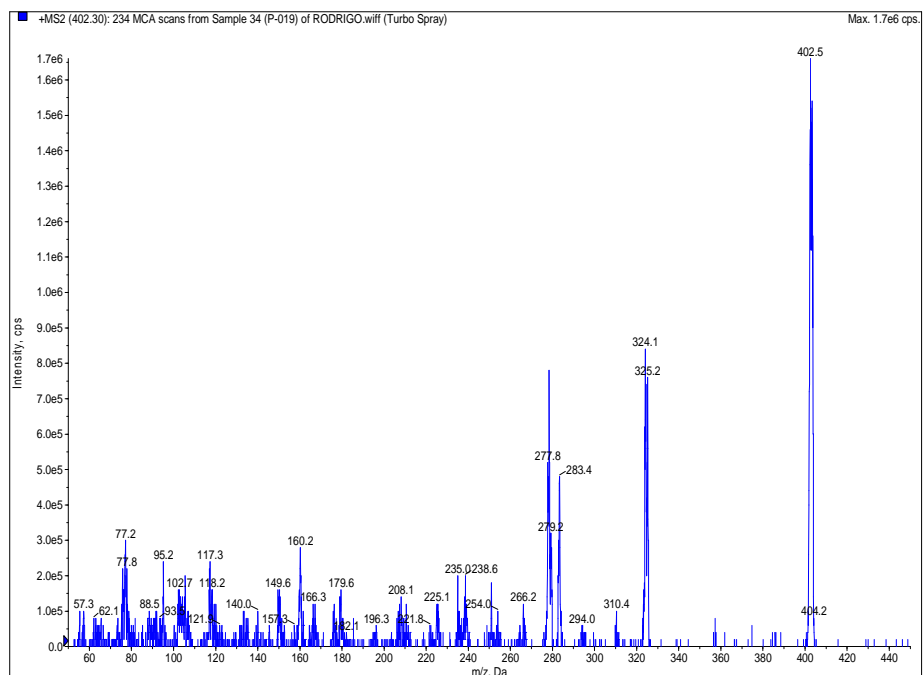


**Figure S6.** Mass spectrum of compound **10a**.

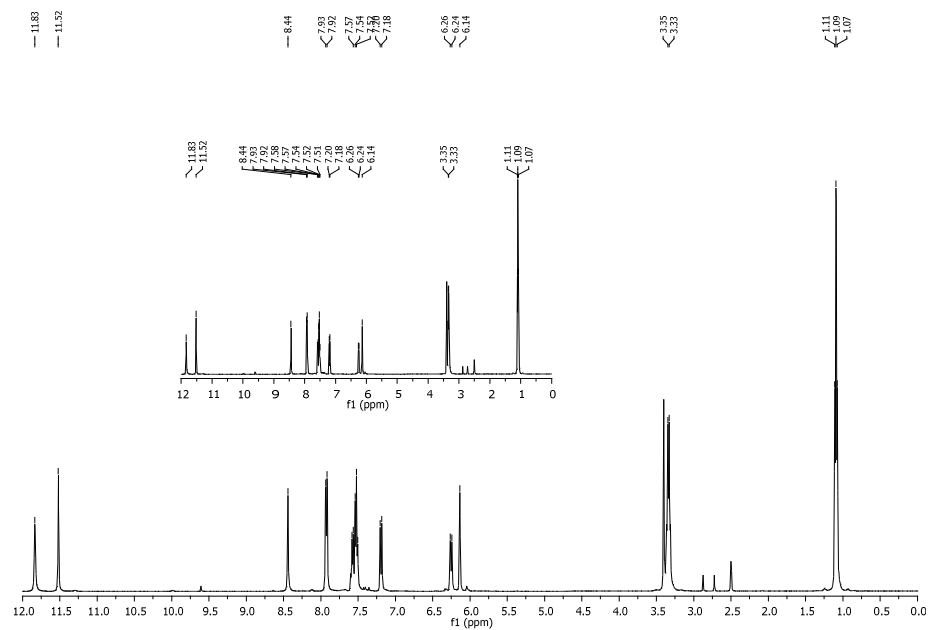


**Figure S7.** Mass spectrum of compound **1a**.

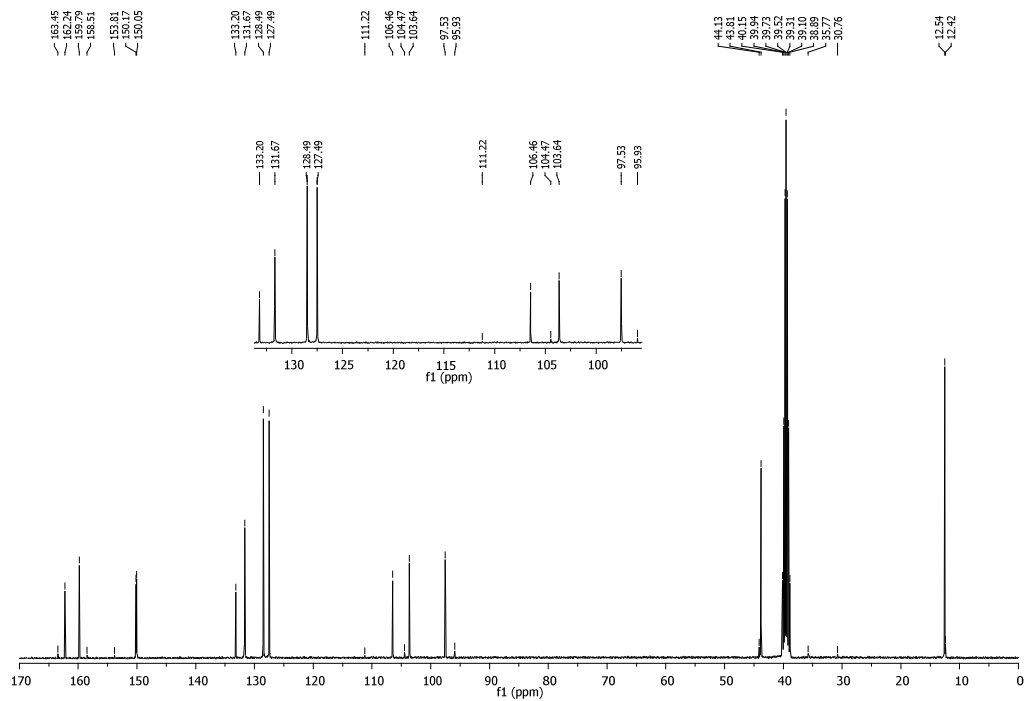


Figure S8.  $^{13}\text{C-NMR}$  spectrum of compound 1a.

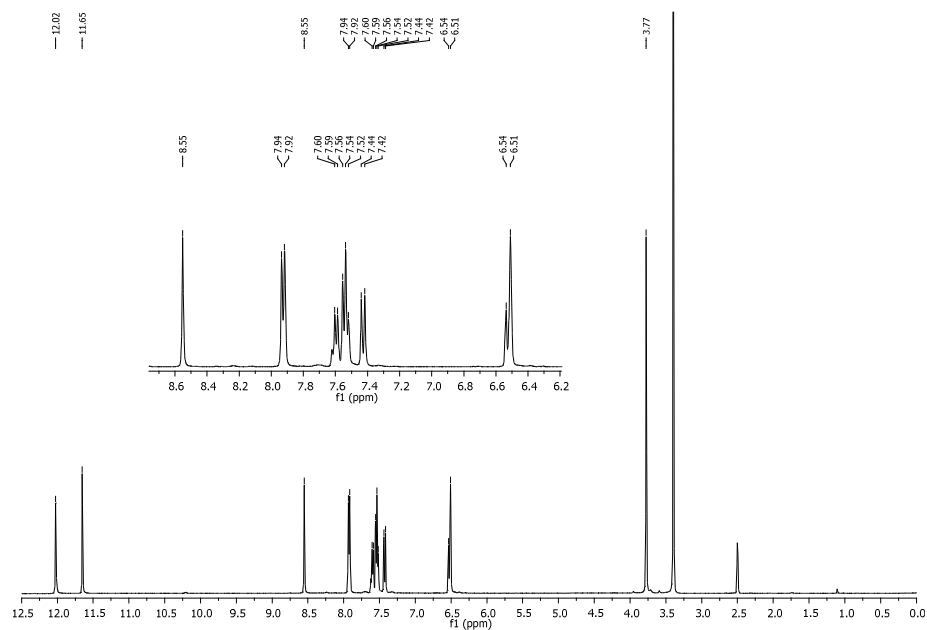


Figure S9.  $^1\text{H-NMR}$  spectrum of compound 2a.

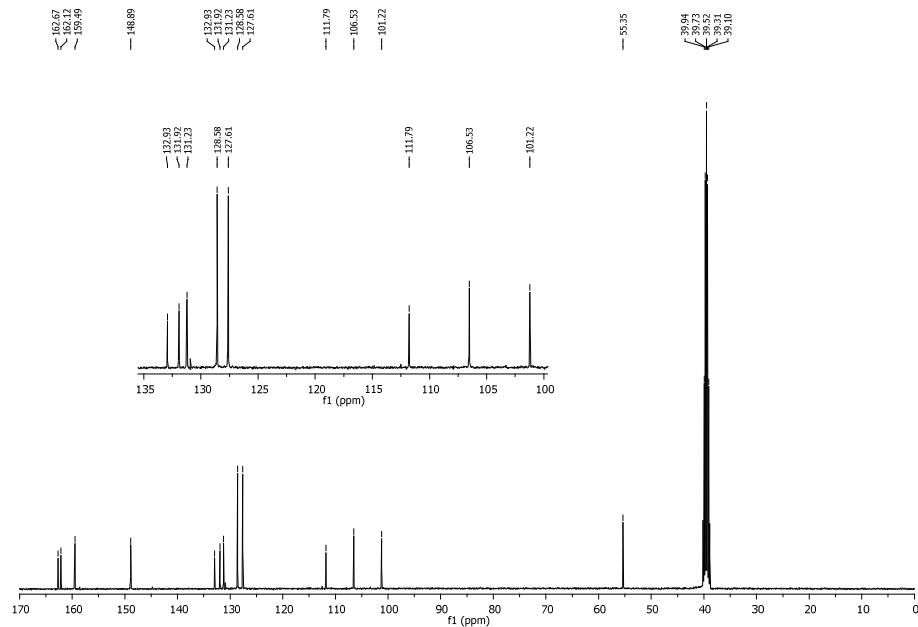


Figure S10.  $^{13}\text{C}$ -NMR spectrum of compound **2a**.

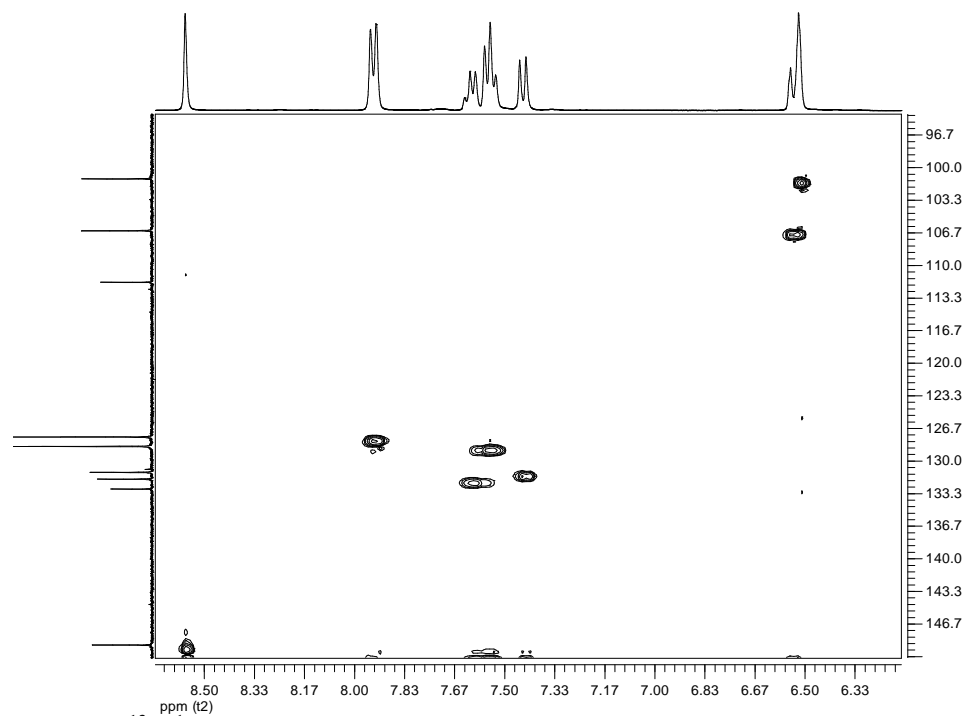


Figure S11.  $^{13}\text{C}$ - $^1\text{H}$  HETCOR spectrum corresponding aromatic region of compound **2a**.



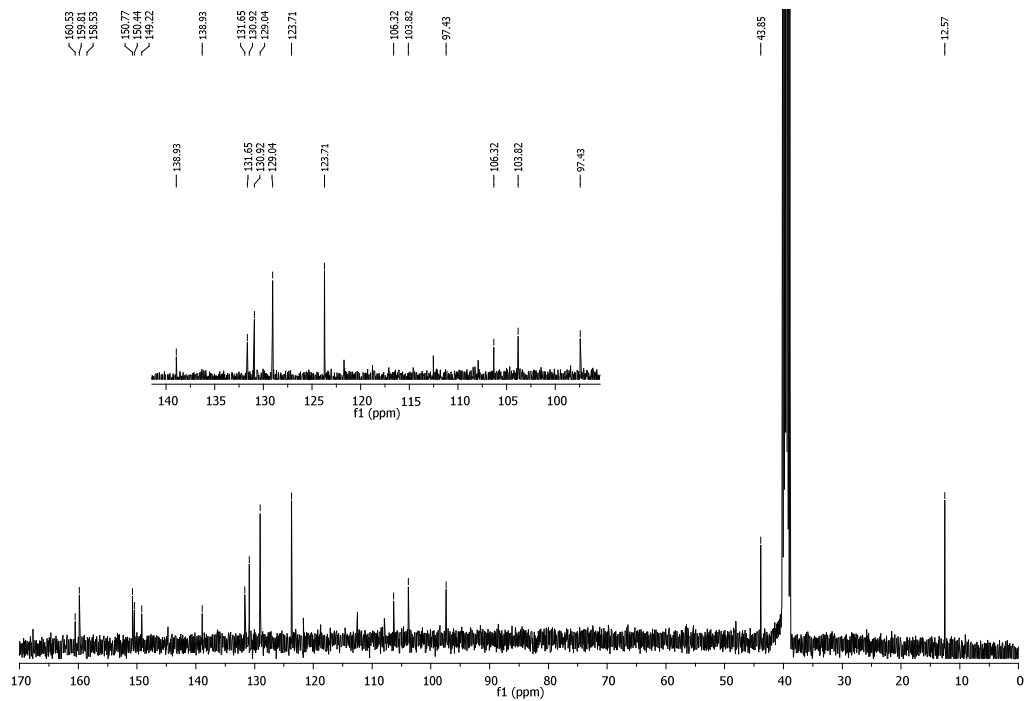


Figure S14.  $^{13}\text{C}$ -NMR spectrum of compound 3a.

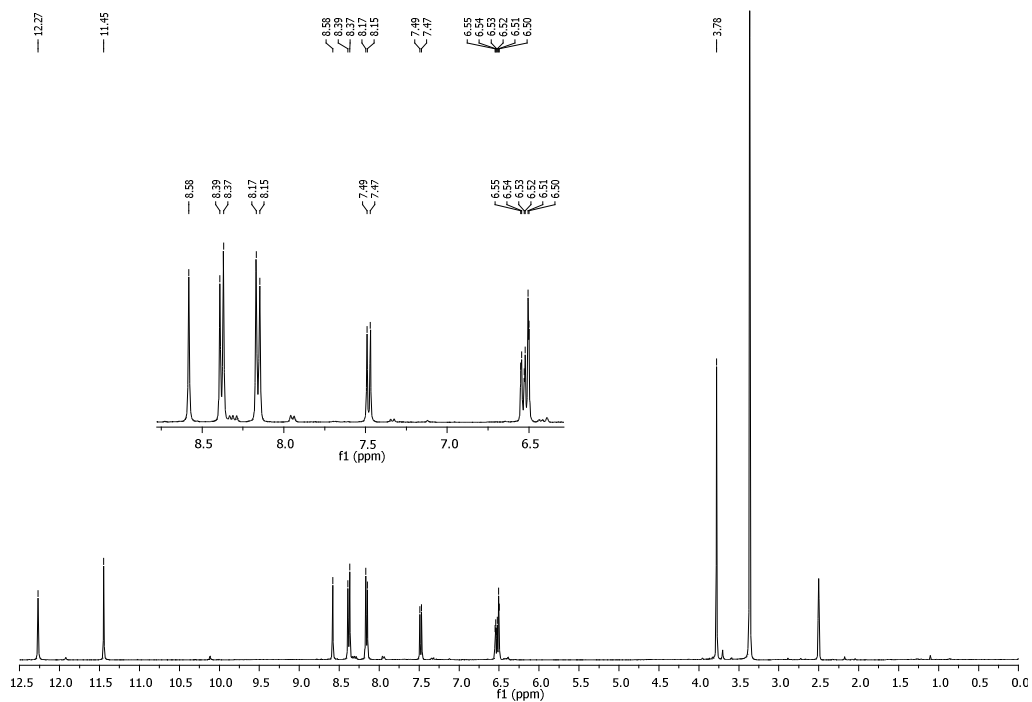


Figure S15.  $^1\text{H}$ -NMR spectrum of compound 4a.

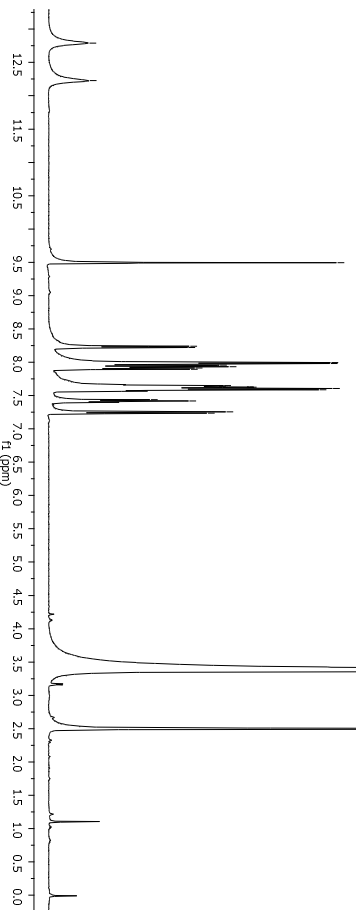
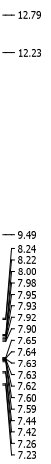


Figure S16. <sup>1</sup>H-NMR spectrum of compound 5a.

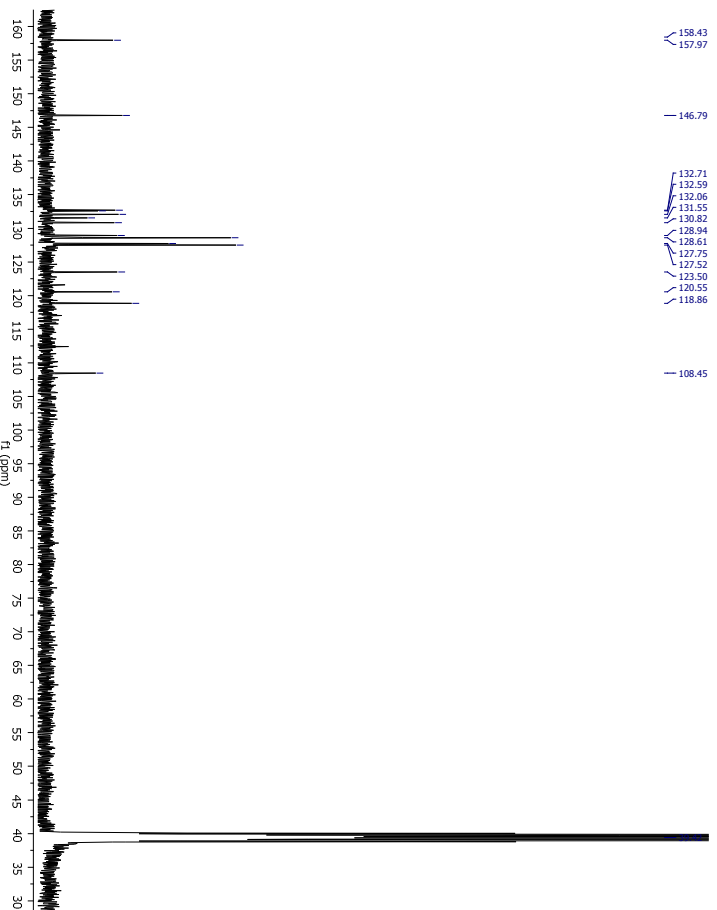
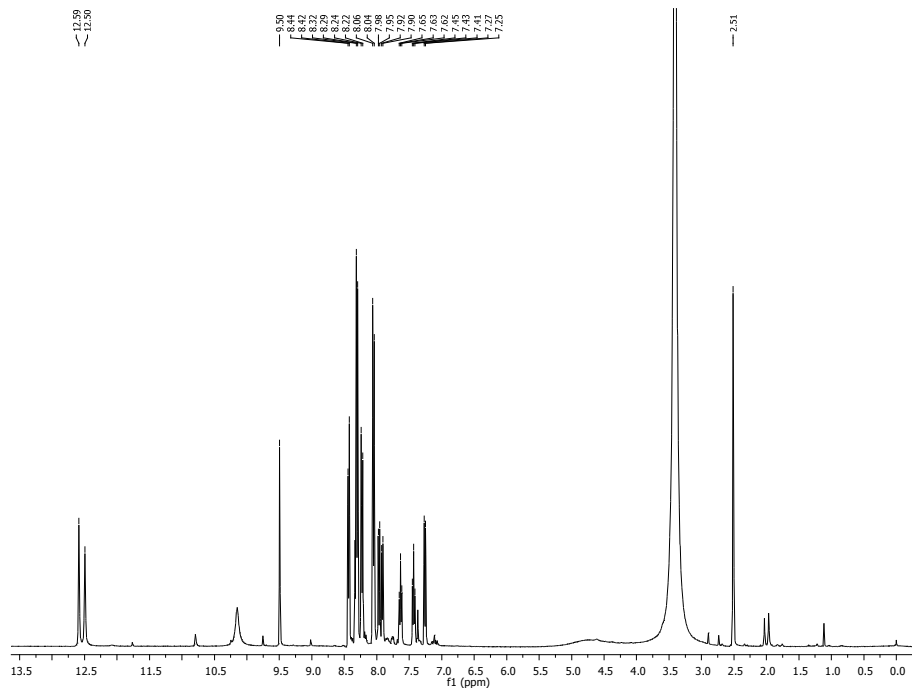
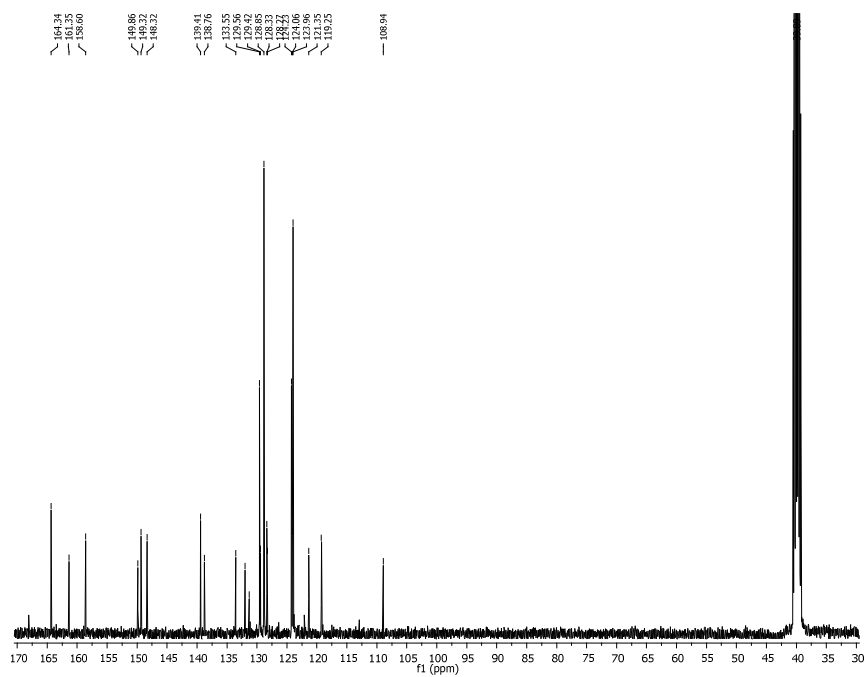


Figure S17. <sup>13</sup>C-NMR spectrum of compound 5a.



**Figure S18.**  $^{13}\text{C}$ -NMR spectrum of compound **6a**.



**Figure S19.**  $^{13}\text{C}$ -NMR spectrum of compound **6a**.

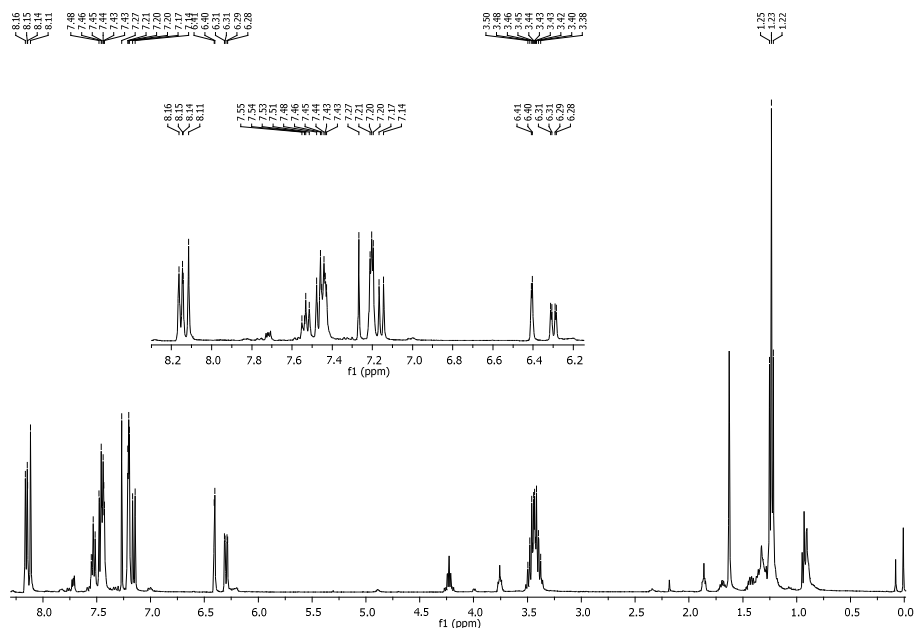


Figure S20. <sup>1</sup>H-NMR spectrum of compound 7a.

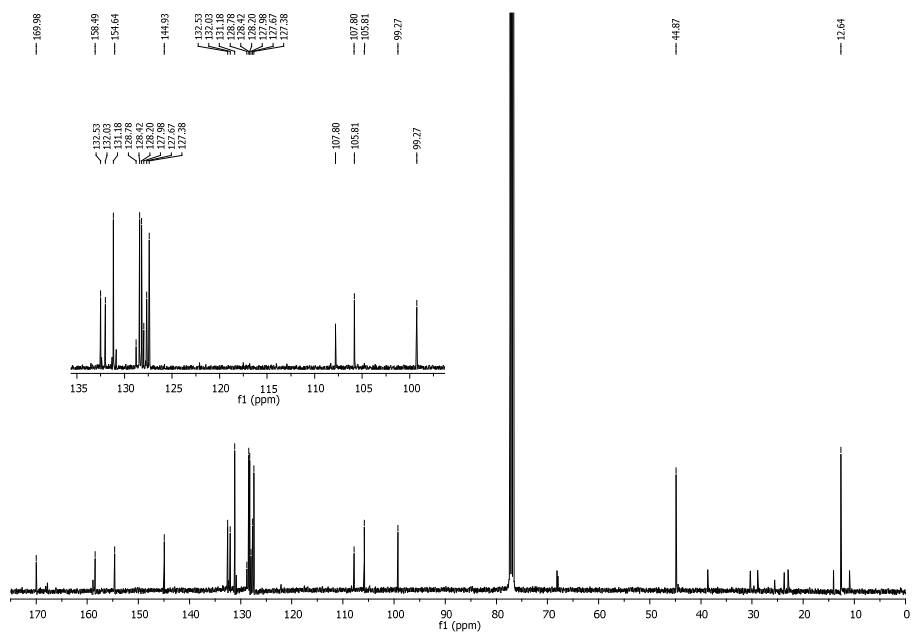


Figure S21. <sup>13</sup>C-NMR spectrum of compound 7a.

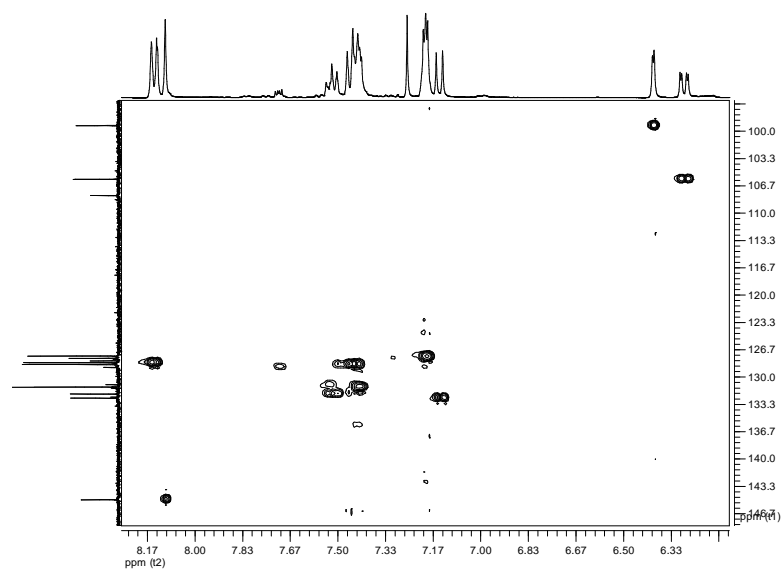


Figure S22.  $^{13}\text{C}$ - $^1\text{H}$  HETCOR spectrum corresponding aromatic region of compound **7a**.

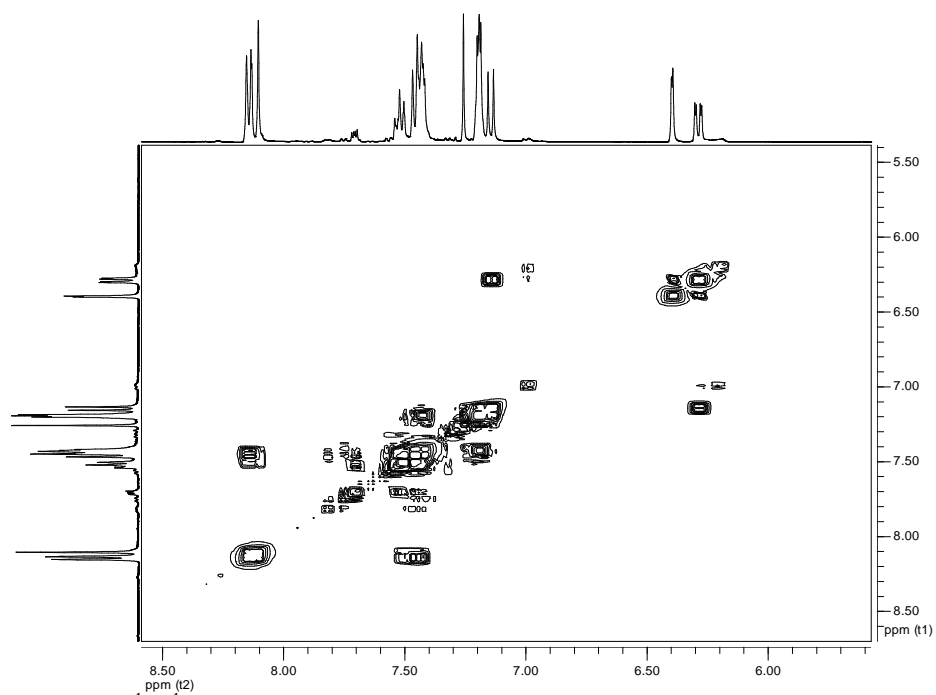


Figure S23.  $^1\text{H}/^1\text{H}$  COSY spectrum corresponding aromatic region of compound **7a**.

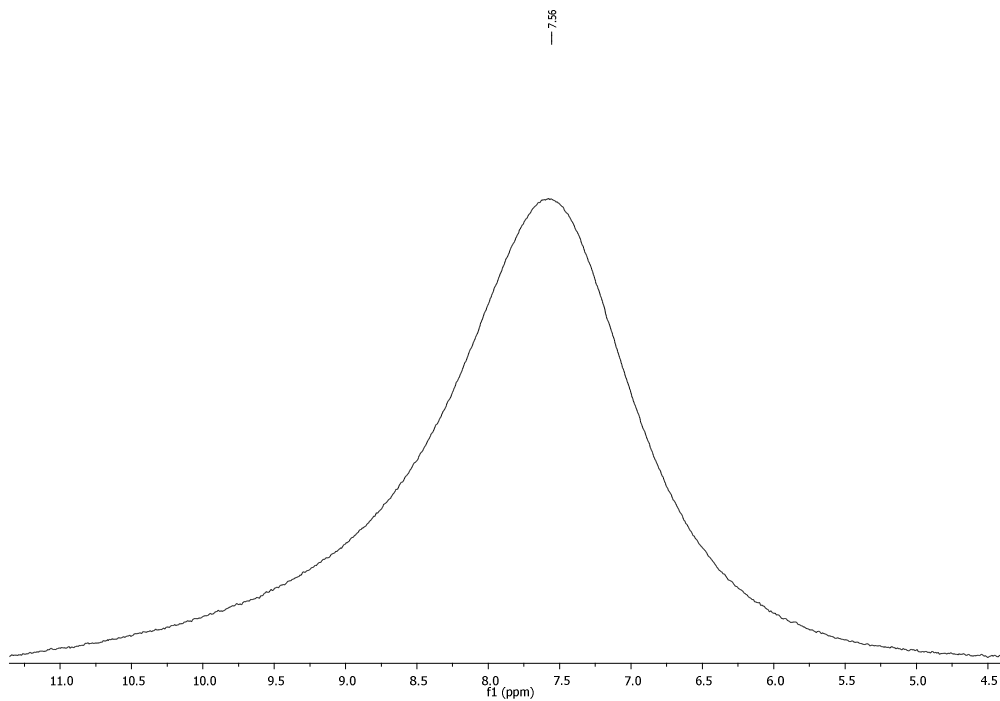


Figure S24.  $^{11}\text{B}$ -NMR spectrum of compound **7a**.

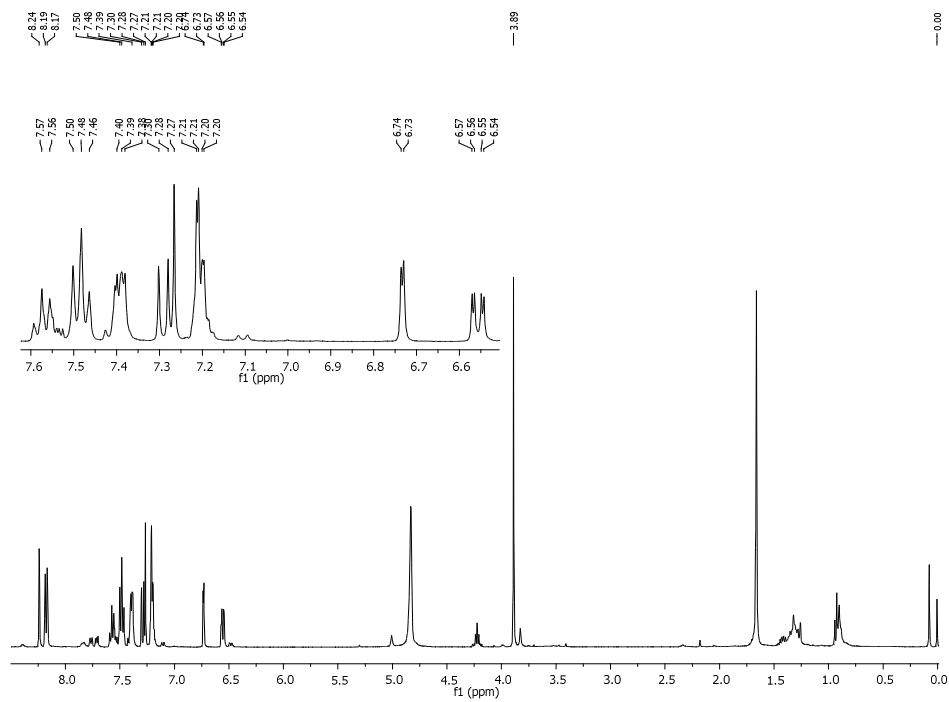


Figure S25.  $^1\text{H}$ -NMR spectrum of compound **8a**.

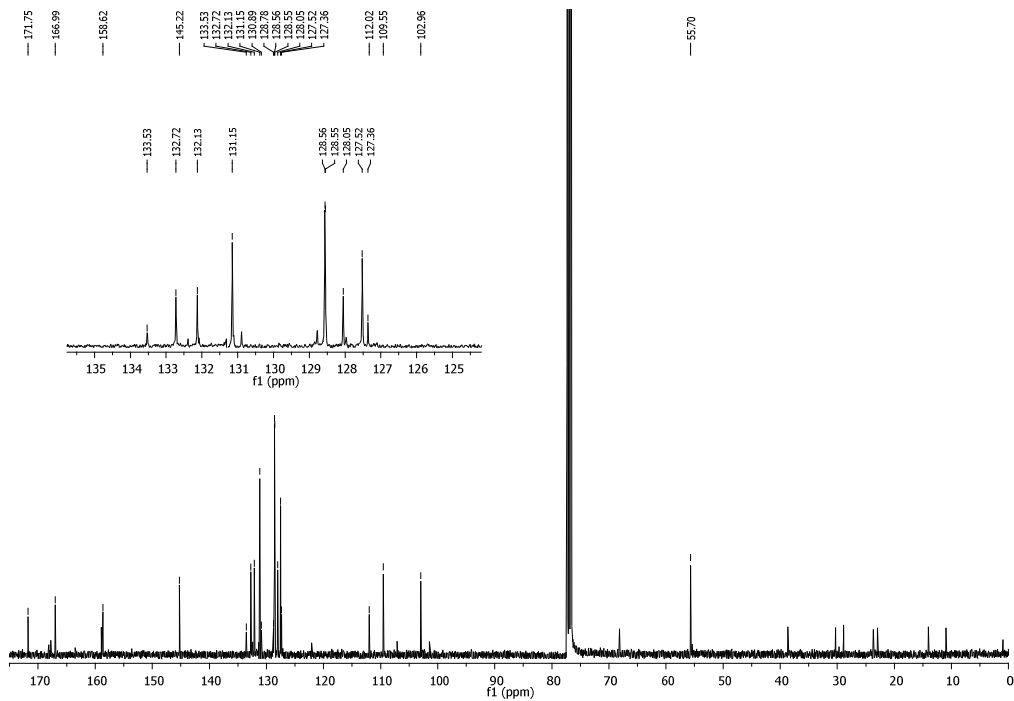


Figure S26.  $^{13}\text{C}$ -NMR spectrum of compound **8a**.

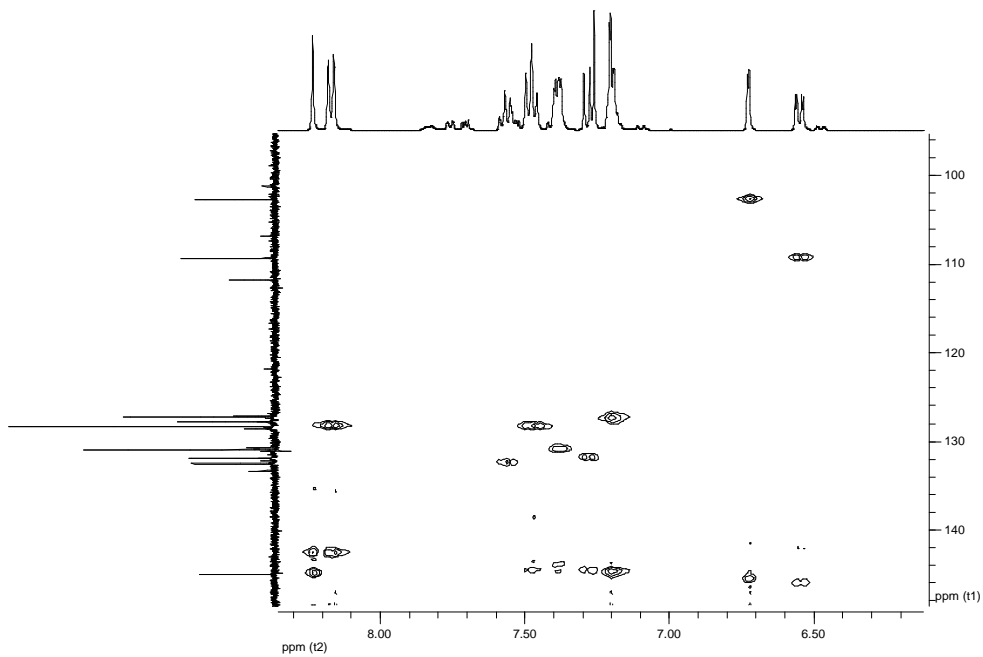
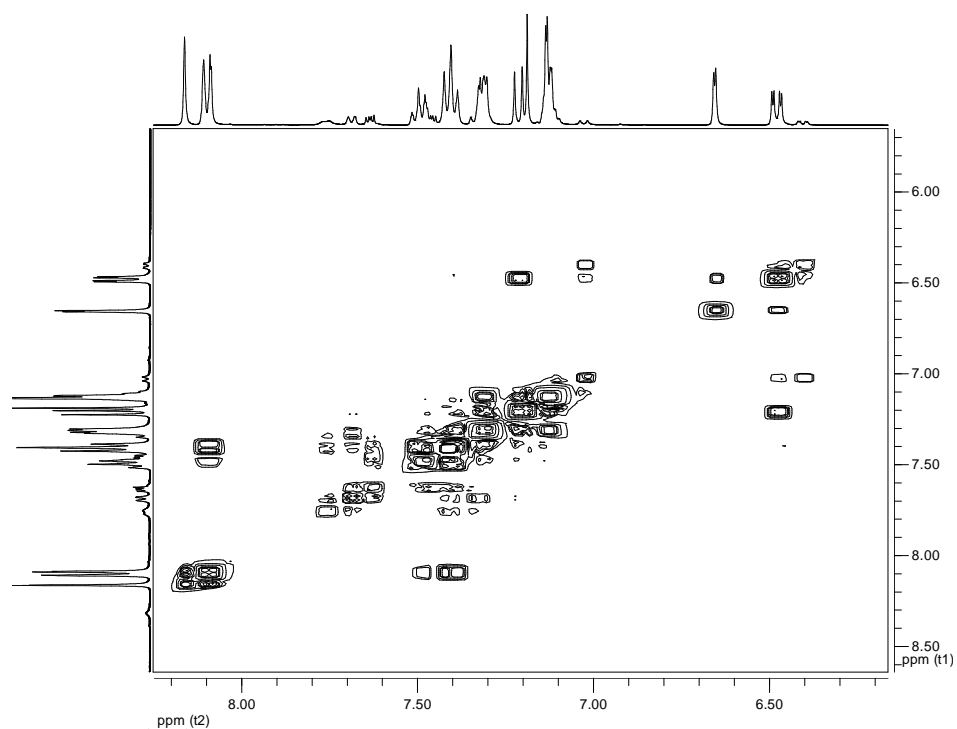
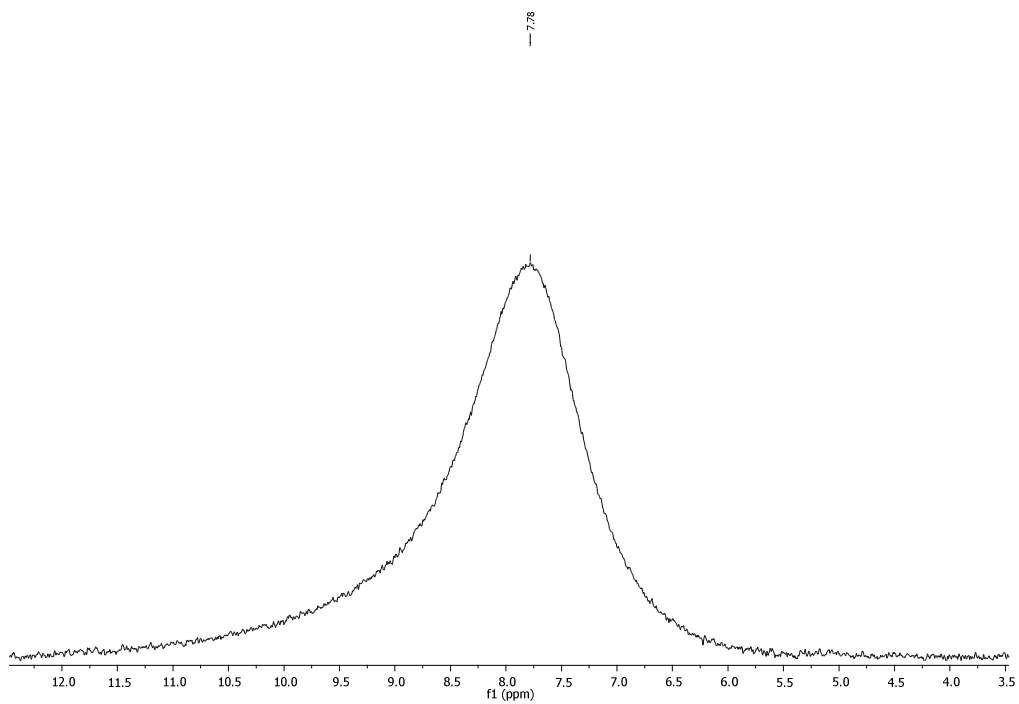


Figure S27.  $^{13}\text{C}$ - $^1\text{H}$  HETCOR spectrum corresponding aromatic region of compound **8a**.



**Figure S28.**  $^1\text{H}/^1\text{H}$  COSY spectrum corresponding aromatic region of compound **8a**.



**Figure S29.**  $^{11}\text{B}$ -NMR spectrum of compound **8a**.

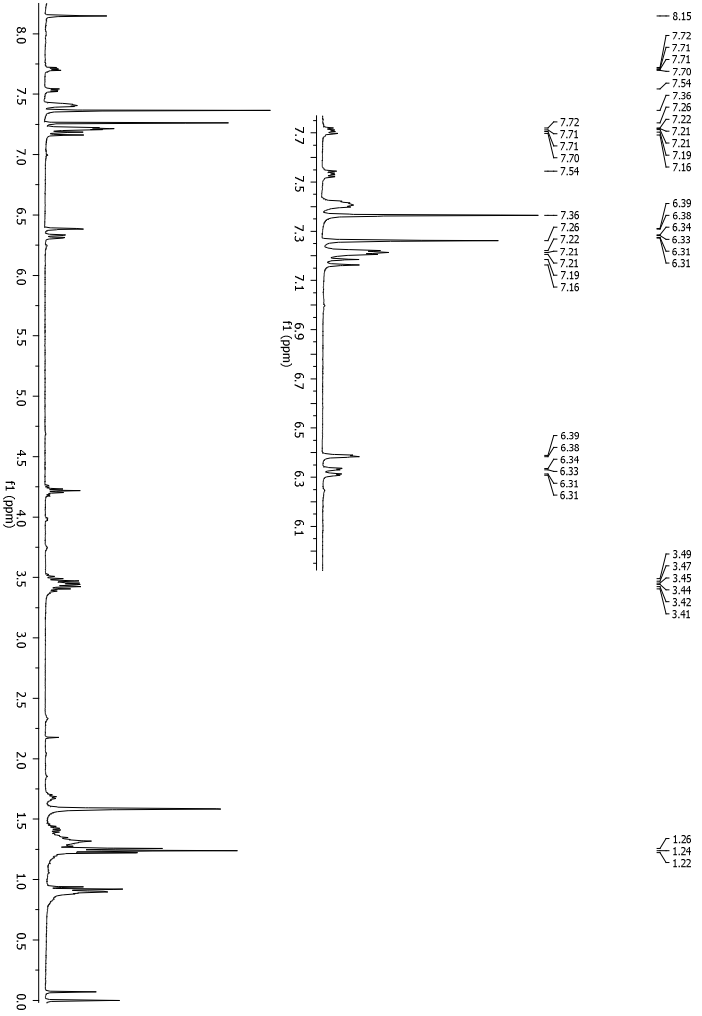


Figure S30. <sup>1</sup>H-NMR spectrum of compound 9a.

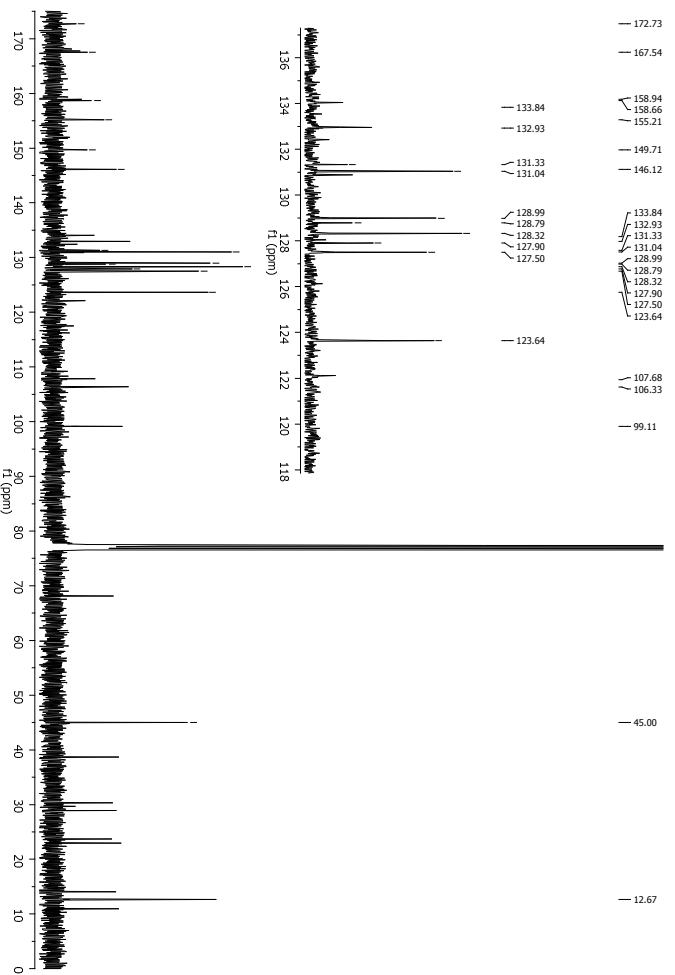


Figure S31. <sup>13</sup>C-NMR spectrum of compound 9a.

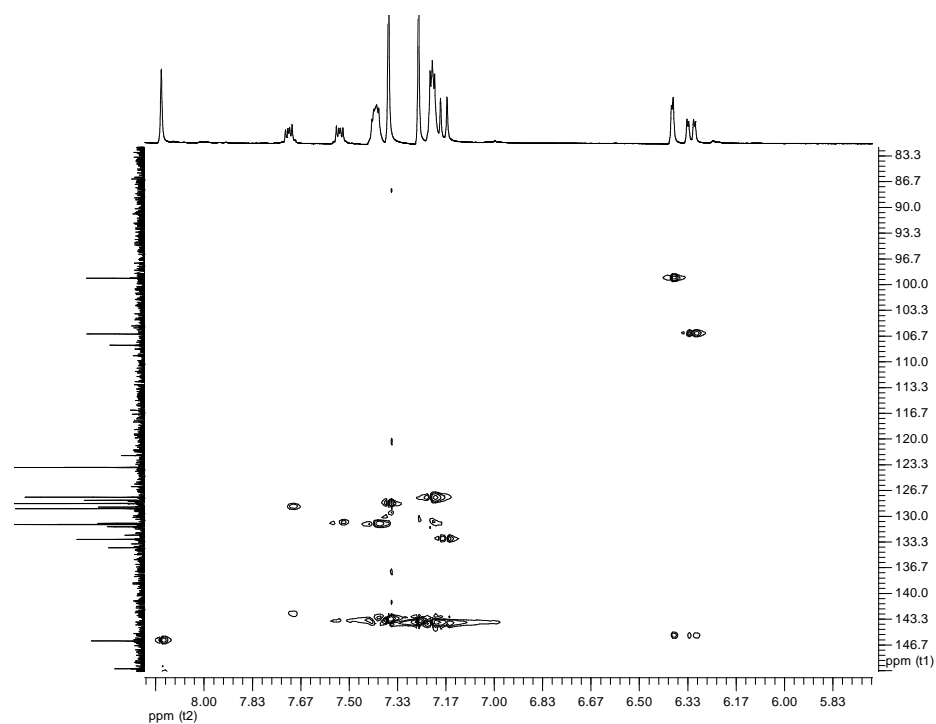


Figure S32.  $^{13}\text{C}$ - $^1\text{H}$  HETCOR spectrum corresponding aromatic region of compound **9a**.

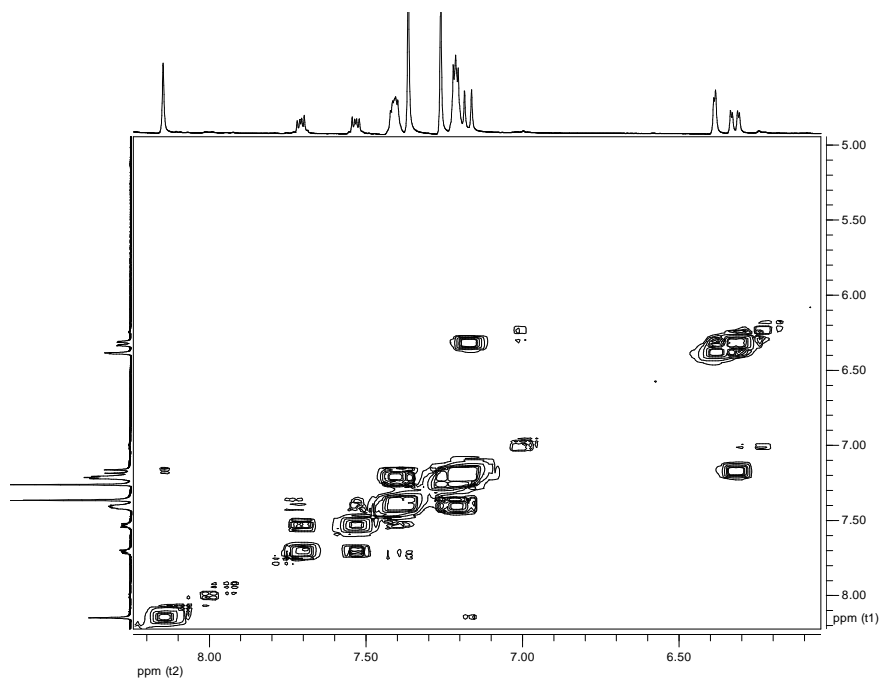


Figure S33.  $^1\text{H}/^1\text{H}$  COSY spectrum corresponding aromatic region of compound **9a**.

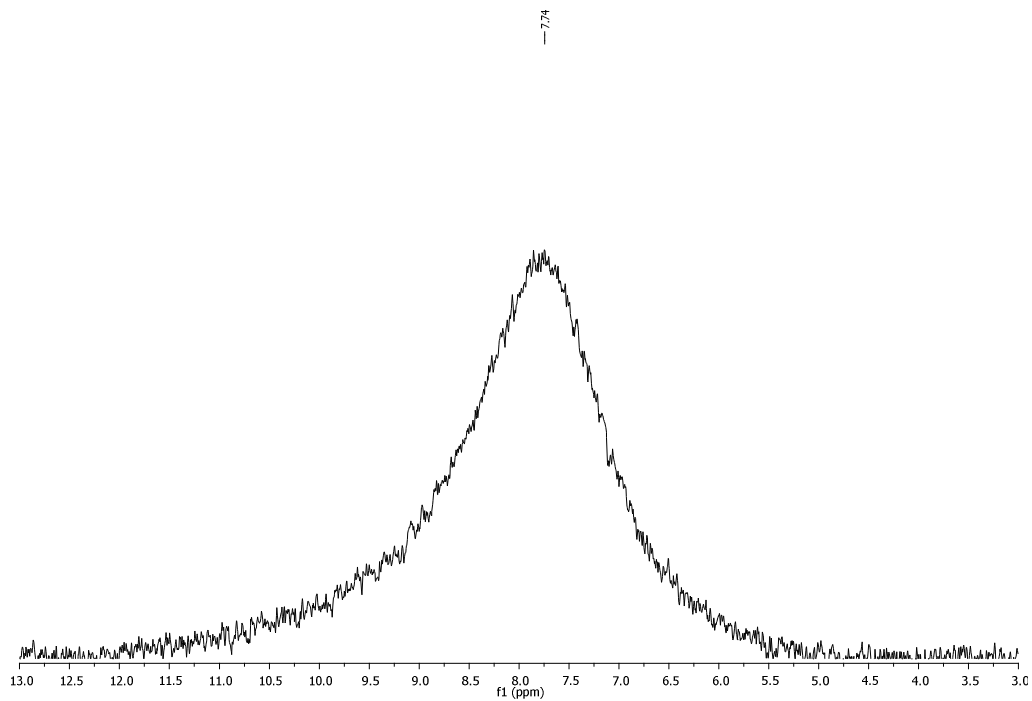


Figure S34.  $^{11}\text{B}$ -NMR spectrum of compound **9a**.

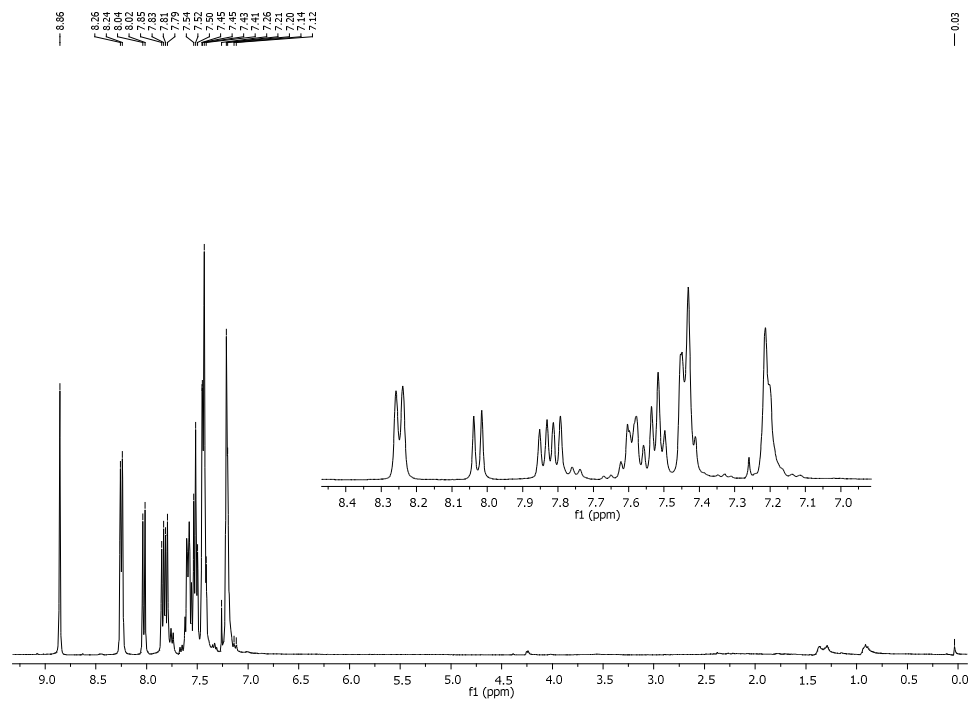
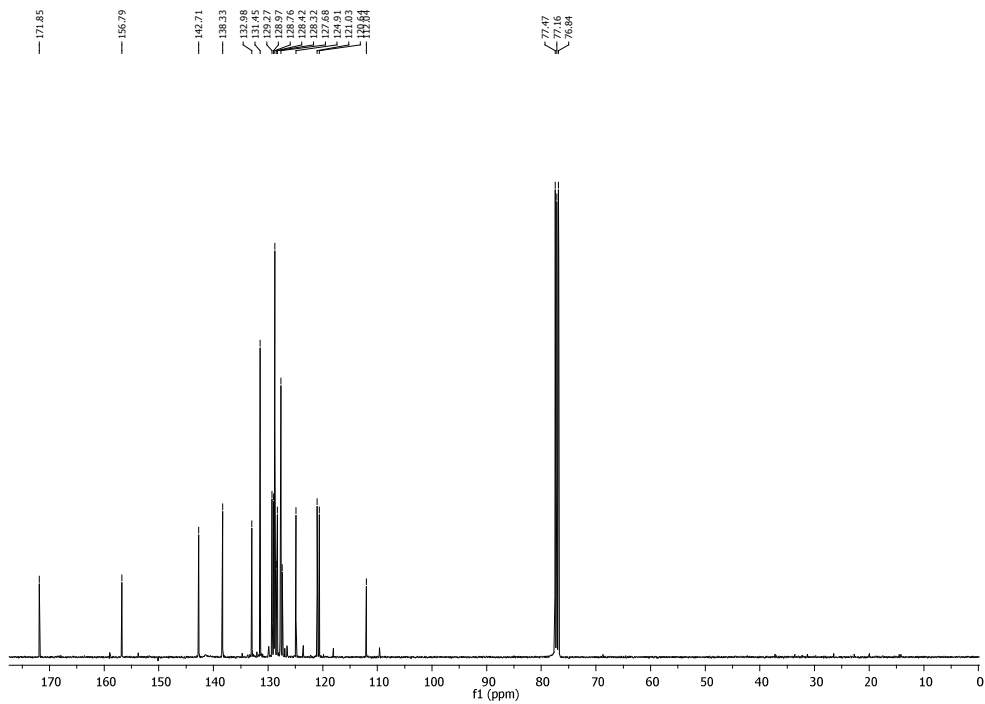
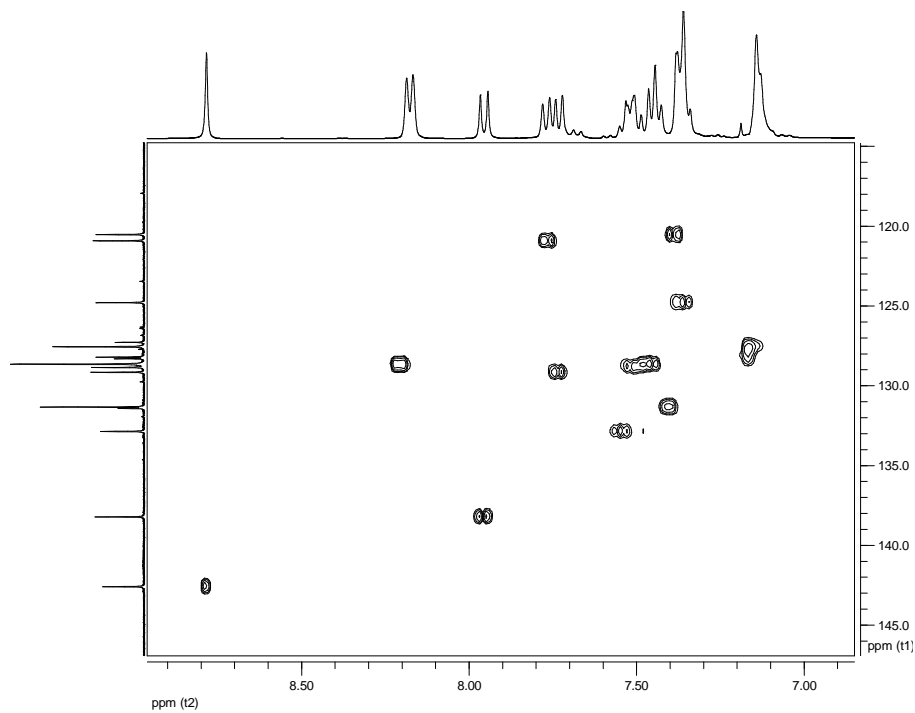


Figure S35.  $^1\text{H}$ -NMR spectrum of compound **11a**.



**Figure S36.**  $^{13}\text{C}$ -NMR spectrum of compound **11a**.



**Figure S37.**  $^{13}\text{C}$ - $^1\text{H}$  HETCOR spectrum corresponding aromatic region of compound **11a**.

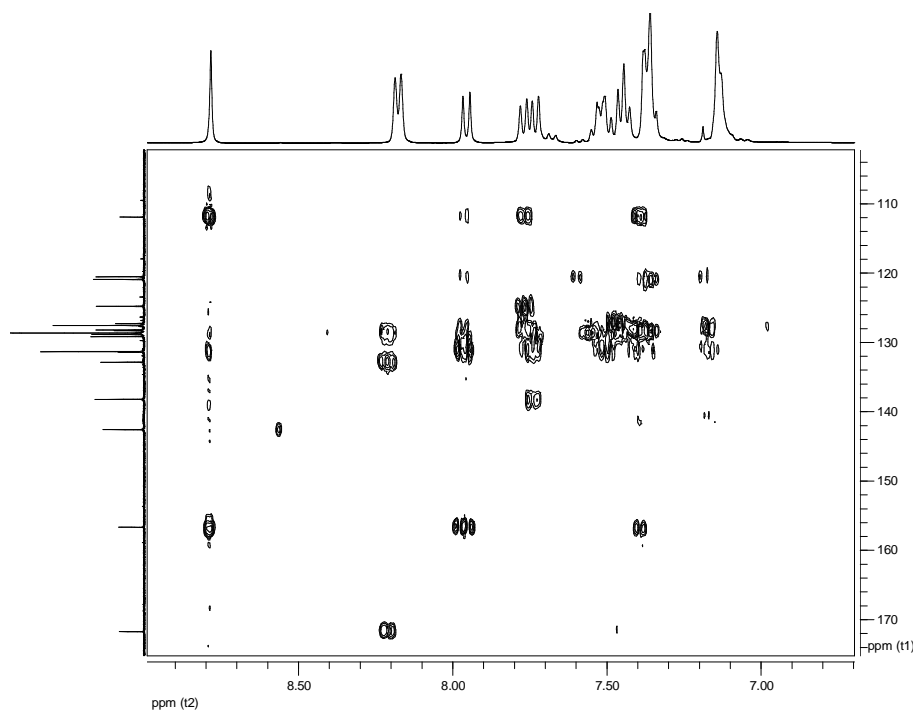


**Figure S38.**  $^1\text{H}/^1\text{H}$  HMBC spectrum corresponding aromatic region of compound **11a**.

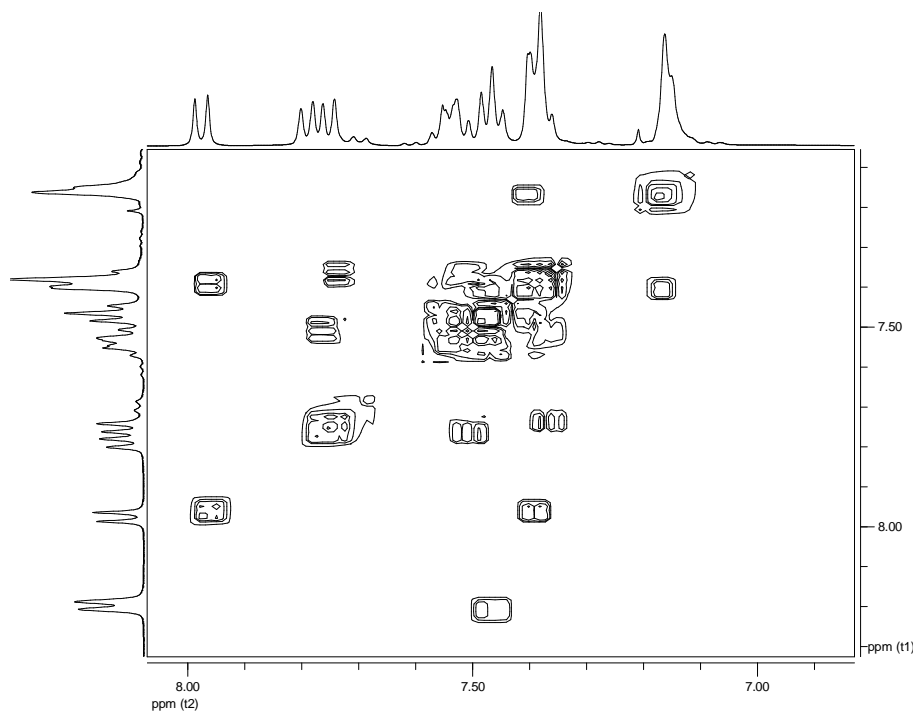


**Figure S39.**  $^1\text{H}/^1\text{H}$  COSY spectrum corresponding aromatic region of compound **11a**.

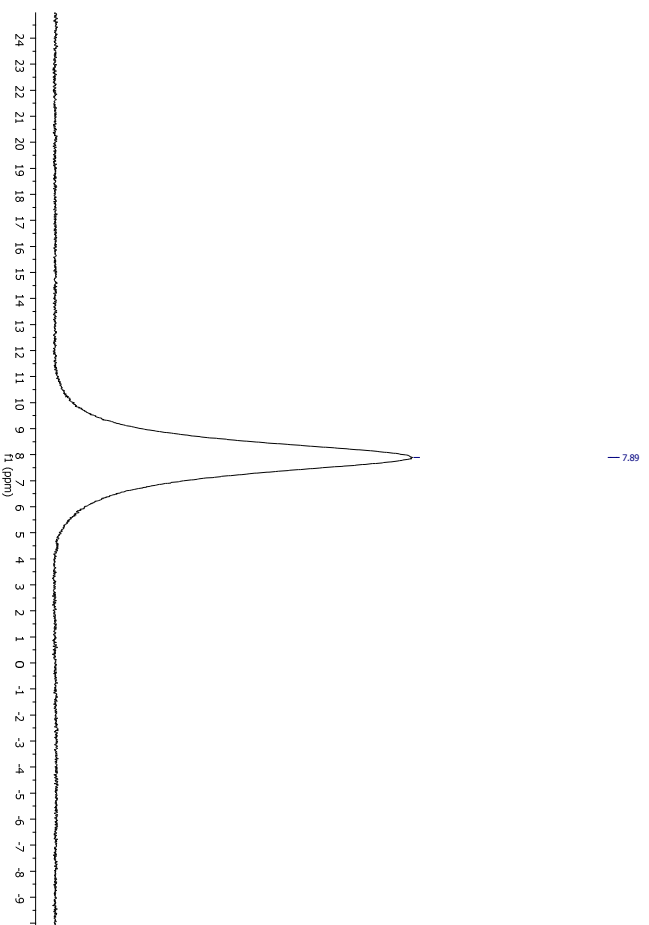


**Figure S40.**  $^{11}\text{B}$ -NMR spectrum of compound 11a.

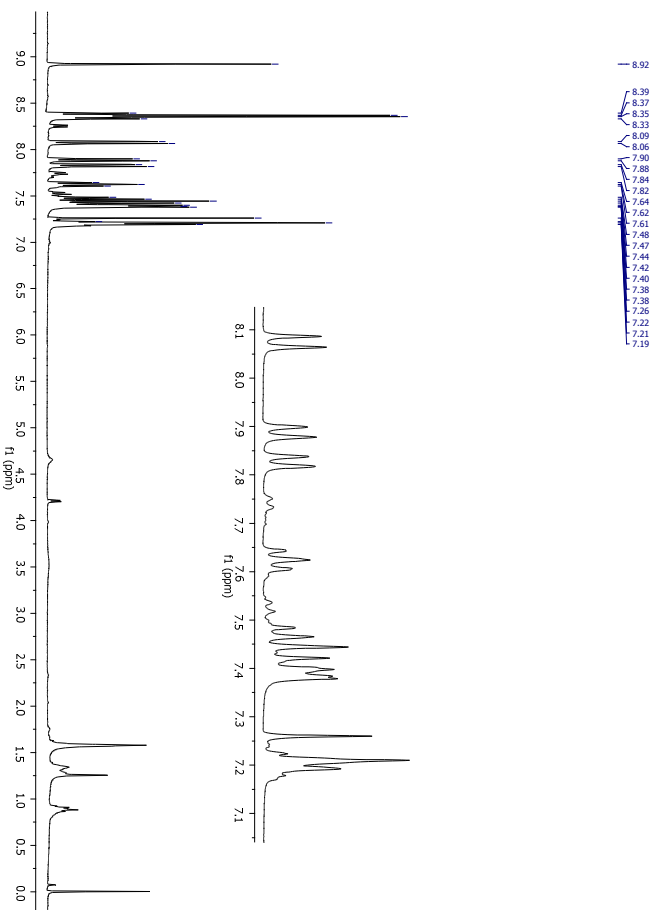


**Figure S41.**  $^1\text{H}$ -NMR spectrum of compound 12a.

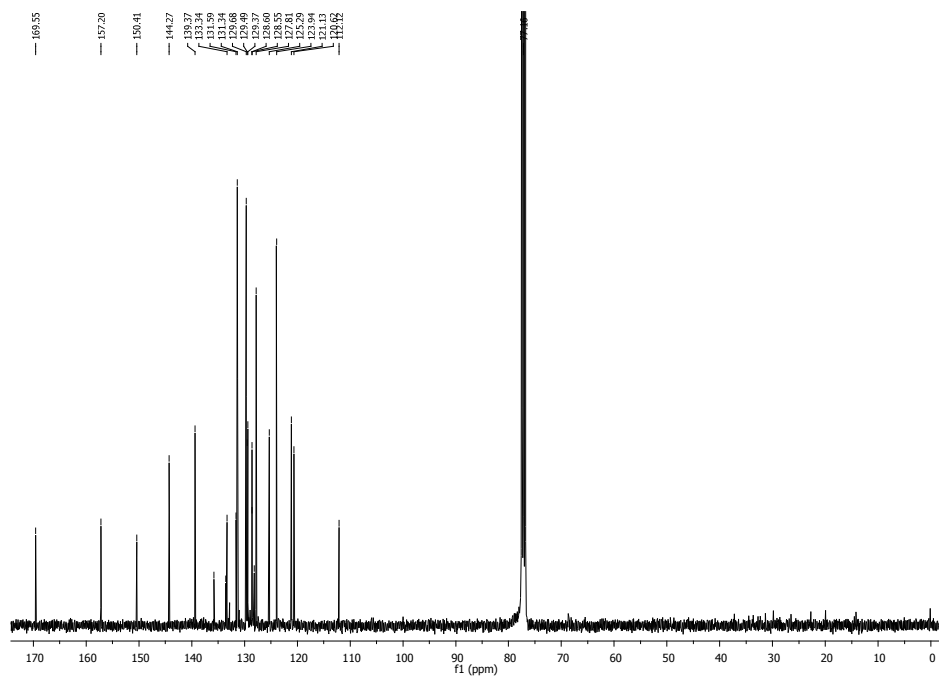


Figure S42.  $^{13}\text{C}$ -NMR spectrum of compound **12a**.

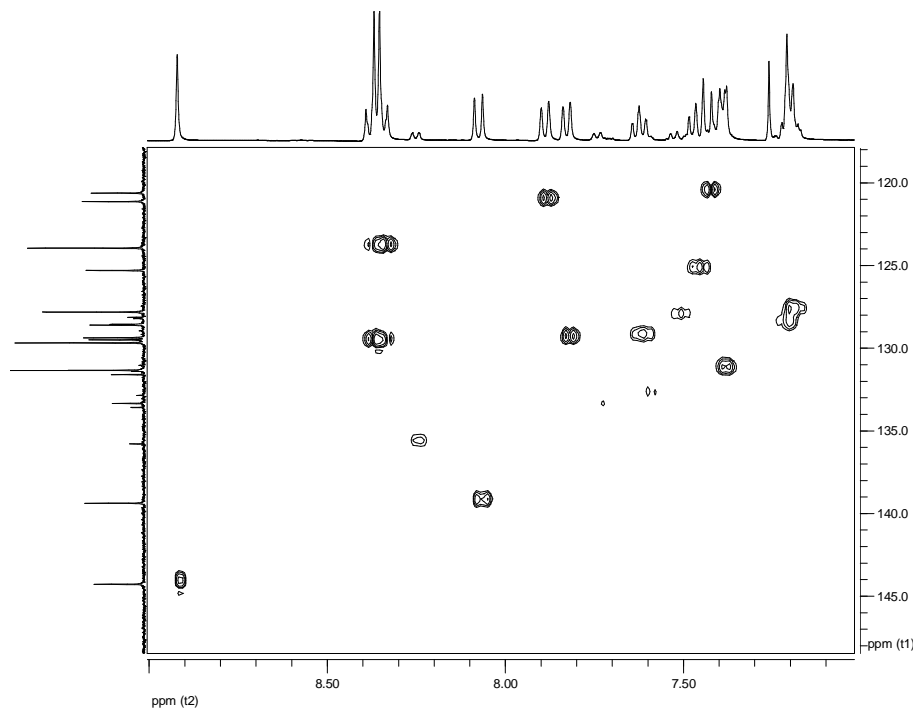
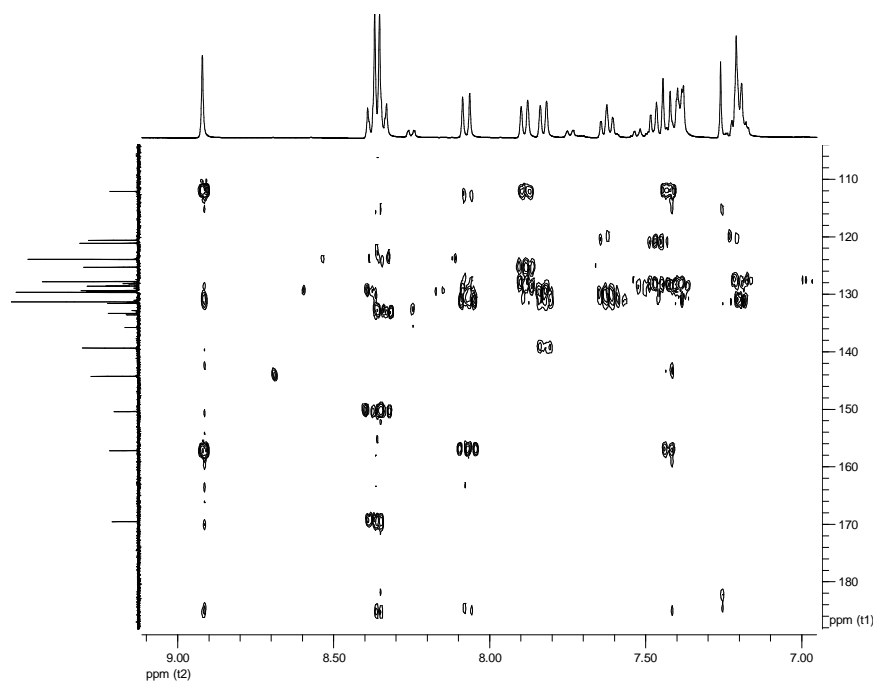
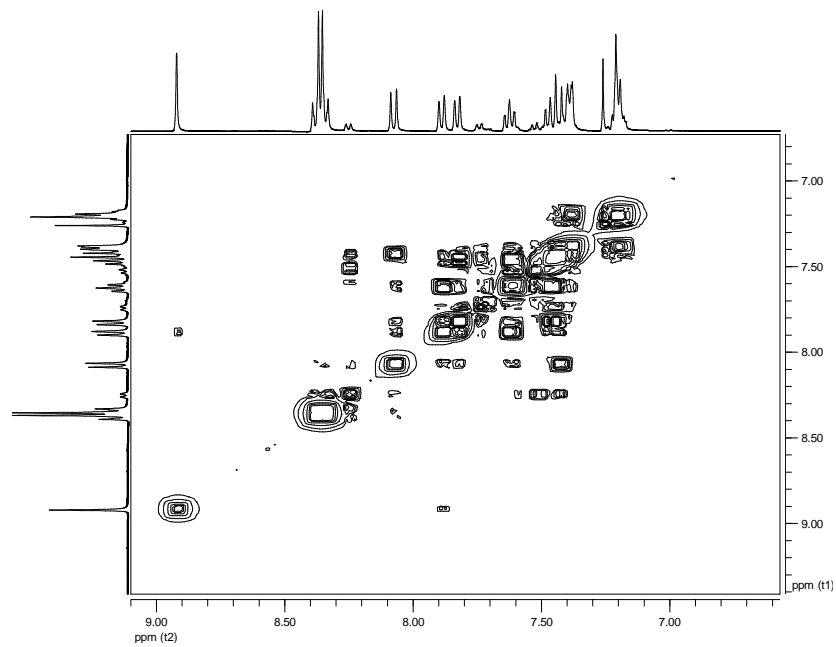


Figure S43.  $^{13}\text{C}$ - $^1\text{H}$  HETCOR spectrum corresponding aromatic region of compound **12a**.



**Figure S44.**  $^1\text{H}/^1\text{H}$  HMBC spectrum corresponding aromatic region of compound **12a**.



**Figure S45.**  $^1\text{H}/^1\text{H}$  COSY spectrum corresponding aromatic region of compound **12a**.

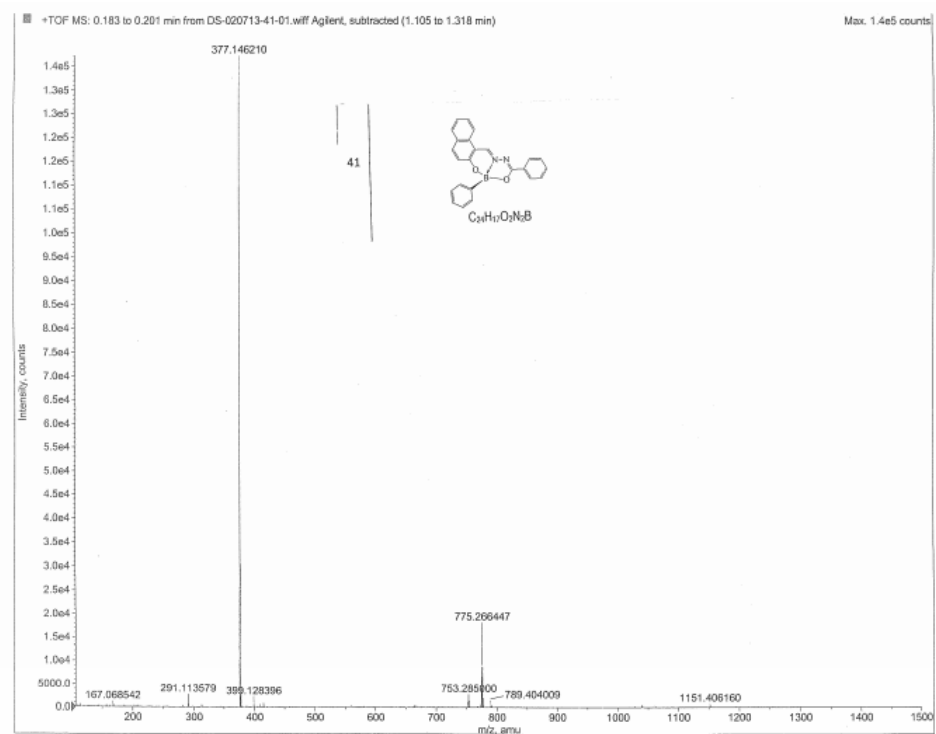


Figure S46. High resolution mass spectrum of compound 11a.

Elemental composition calculator

Target m/z: +377.1462 amu  
Tolerance: +5.0000 ppm  
Result type: Elemental  
Max num of results: 100  
Min DBE: -0.5000 Max DBE: +300.0000  
Electron state: Even  
Num of charges: -1  
Add water: N/A  
Add proton: N/A

	Elements	Min Number	Max Number
1	C	0	60
2	H	0	80
3	O	0	5
4	B	0	2
5	N	0	5

	Formula	Calculated m/z (amu)	mDa Error	PPM Error	DBE
1	C <sub>24</sub> H <sub>18</sub> O <sub>2</sub> N <sub>2</sub> B	377.146681	-0.471896	-1.251230	17.5

Figure S46. High resolution mass spectrum of compound 11a.

Eager Xperience Summarize Results

Date : 21/06/2013 at 14:18:56  
Method Name : NCHS  
Method Filename : N C H S system.mth

Group No : 3	Element %			
Sample Name	Nitrogen	Carbon	Hydrogen	Sulphur
unk46	13.58239174	69.52887726	7.061715603	0
unk46a	13.56980896	69.35482025	7.067774296	0

2 Sample(s) in Group No : 3				
Component Name	Average	Std. Dev.	% Rel. S. D.	Variance
Nitrogen	13.57610035	0.00890	0.0655	0.0001
Carbon	69.44184875	0.12308	0.1772	0.0151
Hydrogen	7.064744949	0.00428	0.0606	0.0000
Sulphur	0	0.00000	0.0000	0.0000

**Figure S47. Elemental analysis for 1a.**

Eager Xperience Summarize Results

Date : 21/06/2013 at 16:16:06  
Method Name : NCHS  
Method Filename : N C H S system.mth

Group No : 7	Element %			
Sample Name	Nitrogen	Carbon	Hydrogen	Sulphur
unk47	9.613542557	63.03879929	5.865962982	0
unk47a	9.417834282	62.34655762	5.786124706	0

2 Sample(s) in Group No : 7				
Component Name	Average	Std. Dev.	% Rel. S. D.	Variance
Nitrogen	9.515688419	0.13839	1.4543	0.0192
Carbon	62.69267845	0.48949	0.7808	0.2396
Hydrogen	5.826043844	0.05645	0.9690	0.0032
Sulphur	0	0.00000	0.0000	0.0000

**Figure S48. Elemental analysis for 2a.**

Eager Xperience Summarize Results

Date : 24/06/2013 at 12:21:17  
Method Name : NCHS  
Method Filename : N C H S system.mth

Group No : 12	Element %			
Sample Name	Nitrogen	Carbon	Hydrogen	Sulphur
unk48	17.46284866	55.0868187	4.022389889	0
unk48a	17.48250771	55.59871292	4.051503658	0

2 Sample(s) in Group No : 12				
Component Name	Average	Std. Dev.	% Rel. S. D.	Variance
Nitrogen	17.47267818	0.01390	0.0796	0.0002
Carbon	55.34276581	0.36196	0.6540	0.1310
Hydrogen	4.036946774	0.02059	0.5100	0.0004
Sulphur	0	0.00000	0.0000	0.0000

**Figure S49. Elemental analysis for 6a.**

Eager Xperience Summarize Results

Date : 21/06/2013 at 14:17:56

Method Name : NCHS

Method Filename : N C H S system.mth

Group No : 2	Element %			
Sample Name	Nitrogen	Carbon	Hydrogen	Sulphur
unk49	10.41042423	72.24578094	6.3202672	0
unk49	10.65014648	72.91390991	6.376935959	0

2 Sample(s) in Group No : 2				
Component Name	Average	Std. Dev.	% Rel. S. D.	Variance
Nitrogen	10.53028536	0.16951	1.6097	0.0287
Carbon	72.57984543	0.47244	0.6509	0.2232
Hydrogen	6.34860158	0.04007	0.6312	0.0016
Sulphur	0	0.00000	0.0000	0.0000

**Figure S50. Elemental analysis for 7a.**

Eager Xperience Summarize Results

Date : 21/06/2013 at 16:15:15

Method Name : NCHS

Method Filename : N C H S system.mth

Group No : 5	Element %			
Sample Name	Nitrogen	Carbon	Hydrogen	Sulphur
unk50	8.062425613	69.73609924	5.061995506	0
unk50a	8.062410355	70.20737457	5.136610985	0
unk50b	8.054373741	70.23638153	5.126435757	0

3 Sample(s) in Group No : 5				
Component Name	Average	Std. Dev.	% Rel. S. D.	Variance
Nitrogen	8.05973657	0.00464	0.0576	0.0000
Carbon	70.05995178	0.28084	0.4009	0.0789
Hydrogen	5.108347416	0.04046	0.7921	0.0016
Sulphur	0	0.00000	0.0000	0.0000

**Figure S51. Elemental analysis for 8a.**

Eager Xperience Summarize Results

Date : 21/06/2013 at 16:16:33  
 Method Name : NCHS  
 Method Filename : N C H S system.mth

Group No : 8	Element %			
Sample Name	Nitrogen	Carbon	Hydrogen	Sulphur
unk51	11.54771614	67.24633789	5.710510731	0
unk51a	11.75971413	67.26586914	5.698055267	0
unk51b	11.57590294	67.15470886	5.693354607	0

3 Sample(s) in Group No : 8

Component Name	Average	Std. Dev.	% Rel. S. D.	Variance
Nitrogen	11.62777774	0.11513	0.9901	0.0133
Carbon	67.2223053	0.05935	0.0883	0.0035
Hydrogen	5.700640202	0.00887	0.1555	0.0001
Sulphur	0	0.00000	0.0000	0.0000

**Figure S52. Elemental analysis for 9a.**

Eager Xperience Summarize Results

Date : 21/06/2013 at 16:15:43  
 Method Name : NCHS  
 Method Filename : N C H S system.mth

Group No : 6	Element %			
Sample Name	Nitrogen	Carbon	Hydrogen	Sulphur
unk52	9.957879066	62.38972092	4.14135313	0
unk52	10.08468246	62.82176208	4.140711784	0

2 Sample(s) in Group No : 6

Component Name	Average	Std. Dev.	% Rel. S. D.	Variance
Nitrogen	10.02128077	0.08966	0.8947	0.0080
Carbon	62.6057415	0.30550	0.4880	0.0933
Hydrogen	4.141032457	0.00045	0.0110	0.0000
Sulphur	0	0.00000	0.0000	0.0000

**Figure S53. Elemental analysis for 10a.**

Eager Xperience Summarize Results

Date : 21/06/2013 at 14:17:10  
 Method Name : NCHS  
 Method Filename : N C H S system.mth

Group No : 1	Element %			
Sample Name	Nitrogen	Carbon	Hydrogen	Sulphur
unk53	7.721977711	76.5302887	4.795921803	0
unk53	7.493245602	76.79264069	4.868200302	0

2 Sample(s) in Group No : 1

Component Name	Average	Std. Dev.	% Rel. S. D.	Variance
Nitrogen	7.607611656	0.16174	2.1260	0.0262
Carbon	76.66146469	0.18551	0.2420	0.0344
Hydrogen	4.832061052	0.05111	1.0577	0.0026
Sulphur	0	0.00000	0.0000	0.0000

**Figure S54. Elemental analysis for 11a.**

Eager Xperience Summarize Results

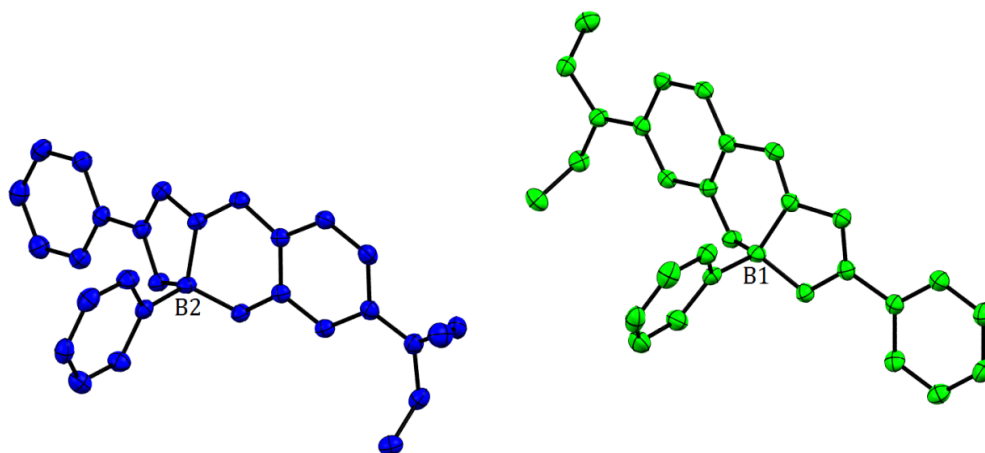
Date : 24/06/2013 at 12:25:20  
Method Name : NCHS  
Method Filename : N C H S system.mth

Group No : 13	Element %			
Sample Name	Nitrogen	Carbon	Hydrogen	Sulphur
unk54	9.696158409	68.52983093	3.921046019	0
unk54a	9.766819954	68.87201691	3.960894823	0

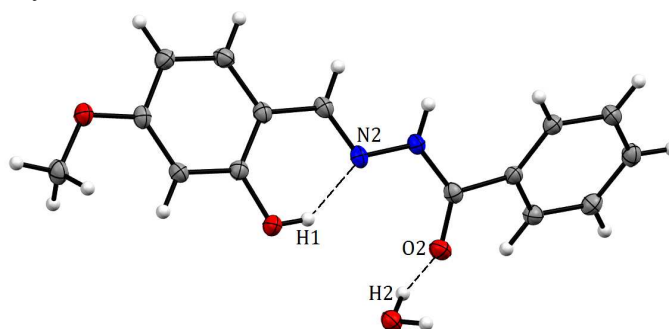
  

2 Sample(s) in Group No : 13				
Component Name	Average	Std. Dev.	% Rel. S. D.	Variance
Nitrogen	9.731489182	0.04997	0.5134	0.0025
Carbon	68.70092392	0.24196	0.3522	0.0585
Hydrogen	3.940970421	0.02818	0.7150	0.0008
Sulphur	0	0.00000	0.0000	0.0000

**Figure S55.** Elemental analysis for **12a**.



**Figure. S56.** X-ray molecular structure of **7a**. The anisotropic displacement parameters are depicted at the 50% probability level. Compound **7a** shows two independent molecules in the asymmetric unit



**Figure. S57.** X-ray molecular structure of **2a**. The anisotropic displacement parameters are depicted at the 50% probability level. Compound **2a**, a molecule of water is present in the asymmetric unit cell. Hydrogen bridge H1...N2 1.958 Å, H2...O2 1.854 Å.

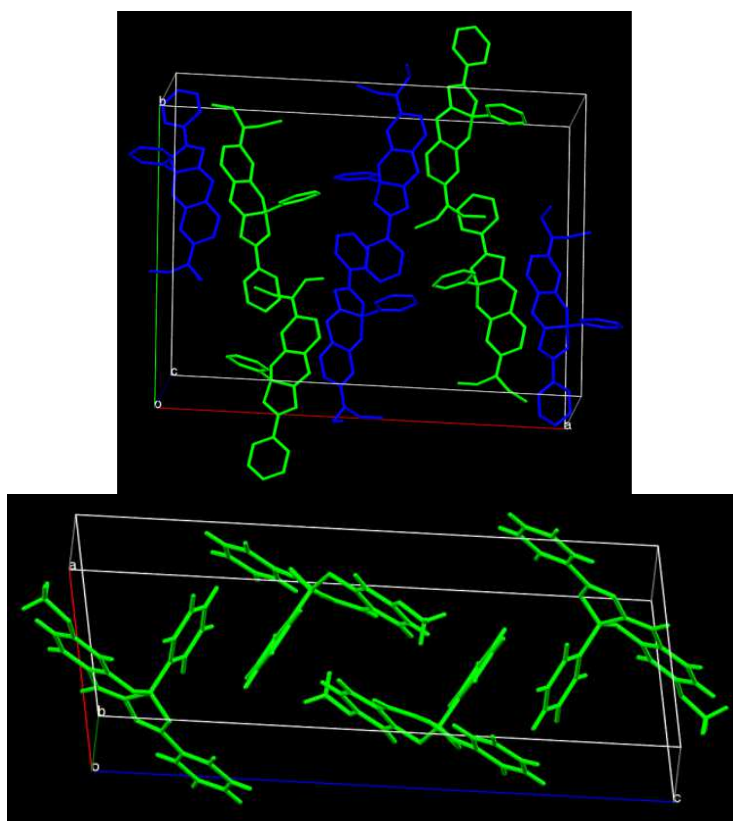


**Figure. S58.** Packing structures of **7a** (top) and **8a** (bottom).

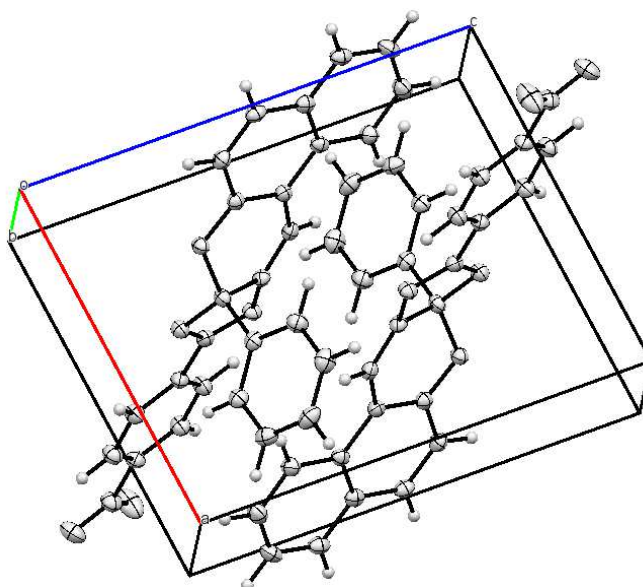


**Figure. S59.** Packing structure of **12a**.

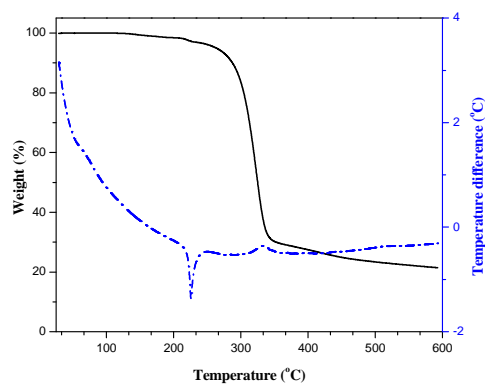


**Fig. S60.** TG and DTA curve of compound **1a**.

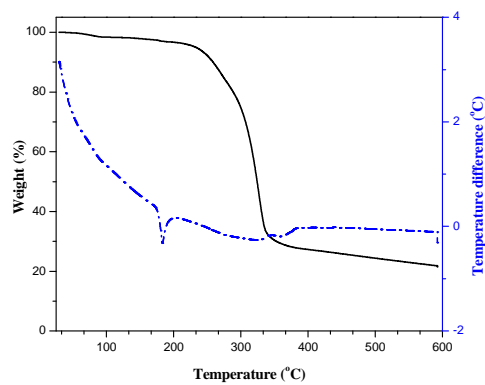


**Fig. 61.** TG and DTA curve of compound **2a**.

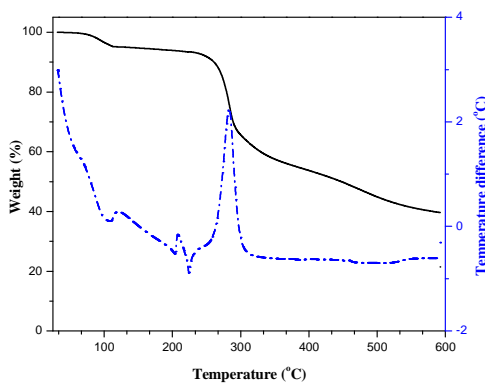


**Fig. S62.** TG and DTA curve of compound **3a**.

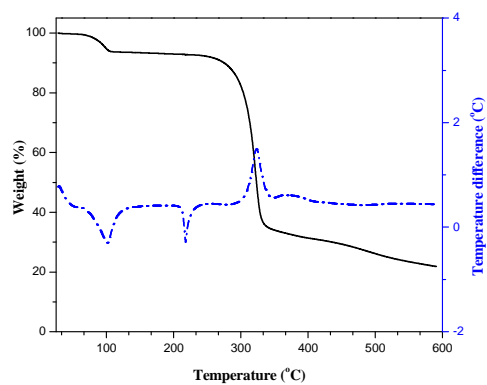


**Fig. S63.** TG and DTA curve of compound **4a**.

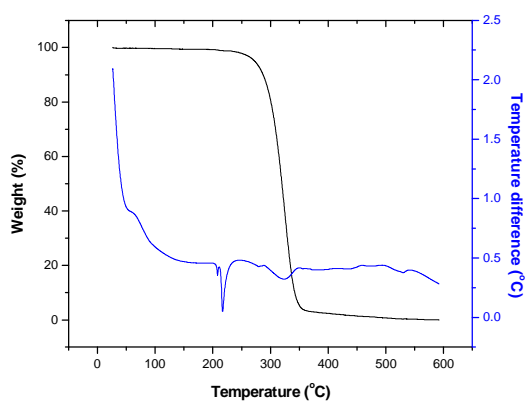


**Fig. S64.** TG and DTA curve of compound **5a**.

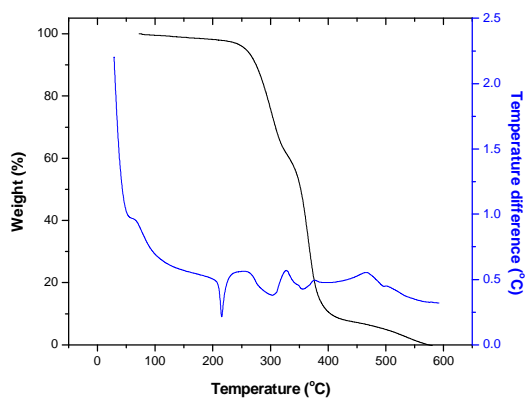


**Fig. S65.** TG and DTA curve of compound **6a**.

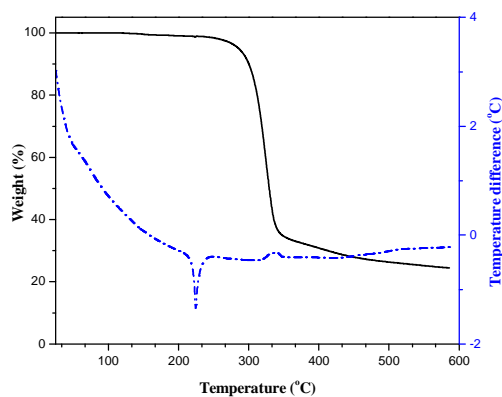


**Fig. S66.** TG and DTA curve of compound **7a**.

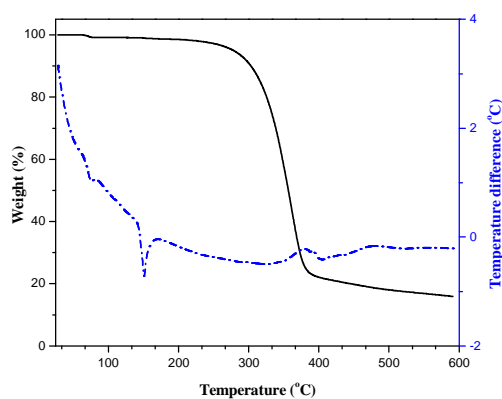


**Fig. S67.** TG and DTA curve of compound **8a**.

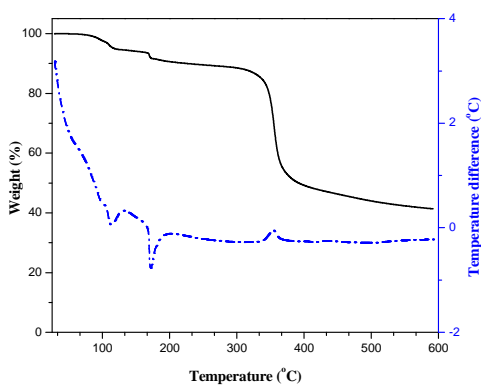


**Fig. S68.** TG and DTA curve of compound **9a**.

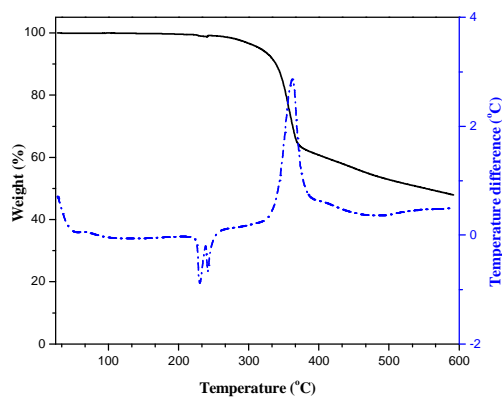


**Fig. S69.** TG and DTA curve of compound **10a**.

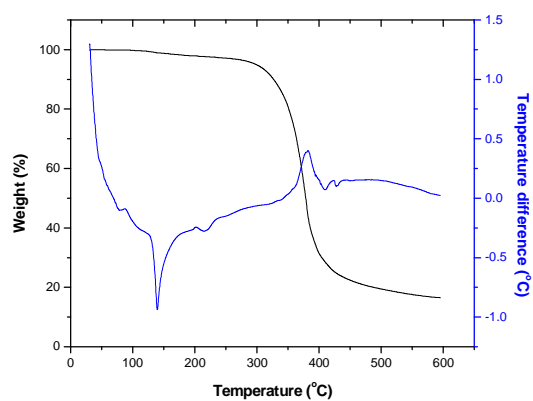


**Fig. S70.** TG and DTA curve of compound **11a**.

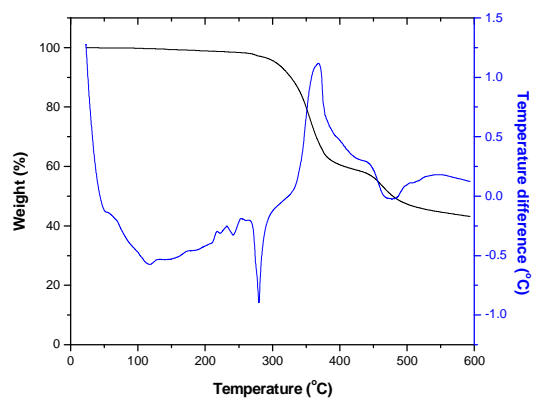


**Fig. S71.** TG and DTA curve of compound **12a**.

# **AUTOBIOGRAPHIC SUMMARY**

**M. en C. RODRIGO ALONSO CHAN NAVARRO**

Candidate for the degree of  
Doctor of Science with Orientation in Materials Chemistry

## **Thesis:**

Synthesis, characterization, determination of luminescent properties of tetracoordinate organoboron compounds derivatives from organic tridentate ligands, and their potential Application in oleds.

Field of study: Materials Chemistry.

Biography: Born in Mérida, Yucatán, México, on April 8<sup>th</sup> of 1981.

## **Education:**

Industrial Chemistry Degree  
Facultad de Ingeniería Química  
Universidad Autónoma de Yucatán

Master of Science with orientation in Organic Chemistry  
Facultad de Química  
Universidad Autónoma de Yucatán

## **Professional experience:**

Academic professor: Universidad Autónoma de Yucatán, Facultad de Ciencias Químicas. Responsible from department of hazardous waste management 2008-2011. Representative from Programa Institucional del Medio Ambiente 2010-2011, Universidad Autónoma de Yucatán, Facultad de Ciencias Químicas. Member of health and safety subcommittee 2010-2011, Universidad Autónoma de Yucatán, Facultad de Ciencias Químicas. Chemical analysis laboratory assistant, CEMEX planta Mérida, Yucatán, México, Quality control department 2004-2005.